การเตรียมไคโทซานที่ดัดแปรด้วย 4-คาร์บอกซีเบนซีนซัลโฟนาไมด์ สำหรับนำส่งอะซีตาโซลาไมด์

นางสาวพฤศจิกา สุวรรณศร

วิทยานิพนธ์นี้เป็นส่วนหนึ่งของการศึกษาตามหลักสูตรปริญญาวิทยาศาสตรมหาบัณฑิต
สาขาวิชาปิโตรเคมีและวิทยาศาสตร์พอลิเมอร์
คณะวิทยาศาสตร์ จุฬาลงกรณ์มหาวิทยาลัย
ปีการศึกษา 2552

PREPARATION OF 4-CARBOXYBENZENESULFONAMIDE MODIFIED CHITOSAN FOR DELIVERY OF ACETAZOLAMIDE

Miss Phruetchika Suvannasara

A Thesis Submitted in Partial Fulfillment of the Requirements
for the Degree of Master of Science Program in Petrochemistry and Polymer Science
Faculty of Science
Chulalongkorn University
Academic Year 2009

Thesis Title	PREPARATION OF 4-CARBOXYBENZENESULFO-NAMIDE MODIFIED CHITOSAN FOR DELIVERY OF ACETAZOLAMIDE
By	Miss Phruetchika Suvannasara
Field of Study	Petrochemistry and Polymer Science
Thesis Principle Advisor	Associate Professor Nongnuj Muangsin, Ph.D.
Thesis Co-advisor	Nalena Praphiraksit, D.V.M., Ph.D.

Accepted by the Faculty of Science, Chulalongkorn University in Partial Fulfillment of the Requirements for the Master's Degree

……Dean of the Faculty of Science
(Professor Supot Hannongbua, Dr.rer.nat.)

THESIS COMMITTEE

…….....Chairman
(Associate Professor Sirirat Kokpol, Ph.D.)

…….....Thesis Advisor
(Associate Professor Nongnuj Muangsin, Ph.D.)

…….....Thesis Co-advisor
(Nalena Praphiraksit, D.V.M., Ph.D.)

…….....Examiner
(Associate Professor Nuanphun Chantarasiri, Ph.D.)

……..... External Examiner
(Assistant Professor Thongdee Leksopee, Ph.D.)

พฤศจิกา สุวรรณศร: การเตรียมไคโทซานที่ดัดแปรด้วย 4-คาร์บอกซีเบนซีนซัลโฟนาไมด์สำหรับนำส่งอะซีตาโซลาไมด์ (PREPARATION OF 4-CARBOXYBENZENESULFONAMIDE MODIFIED CHITOSAN FOR DELIVERY OF ACETAZOLAMIDE) อ. ที่ปรึกษาวิทยานิพนธ์หลัก: รศ. ดร. นงนุช เหมืองสิน, อ. ที่ปรึกษาวิทยานิพนธ์ร่วม: สพญ. ดร. นลินา ประไพรักษ์สิทธิ์, 108 หน้า.

วัตถุประสงค์ของงานวิจัยนี้คือเพื่อดัดแปรไคโทซานด้วย 4-คาร์บอกซีเบนซีนซัลโฟนาไมด์ (4-CBS-CS) ที่อัตราส่วนต่างๆ ให้มีสมบัติเกาะติดเยื่อเมือกที่ดีกว่าไคโทซาน เพื่อเพิ่มโอกาสให้ตัวยับยั้งคาร์บอนิกแอนไฮเดรสซึมผ่านเยื่อบุเมือกเข้าไปถึงเชื้อ *H. pylori* ที่ฝังตัวอยู่ลึกในกระเพาะอาหาร และพิสูจน์เอกลักษณ์ของไคโทซานที่ถูกดัดแปรด้วยเทคนิค ^{1}H-NMR, FT-IR, DSC และ TGA นอกจากนี้ ไคโทซานที่ดัดแปรด้วย 4-CBS-CS (1:0.05) มีสมบัติยึดเกาะเยื่อเมือกและมีความสามารถในการบวมตัวที่ดีมากกว่าไคโทซาน และทนต่อกรดในกระเพาะอาหารได้นานอย่างน้อย 24 ชั่วโมง และไคโทซานดัดแปรที่สังเคราะห์ได้ไม่เป็นพิษต่อเซลล์ปกติและไม่มีฤทธิ์ยับยั้งเซลล์มะเร็ง KB cell, MCF-7, NCI-H187 นอกจากนี้ ยังพบว่าไคโทซานที่ดัดแปรด้วย 4-CBS สามารถยับยั้งเชื้อ *E.coli* และ *S.aureus*

นอกจากนี้ งานวิจัยนี้มุ่งเน้นที่จะตรึงตัวยับยั้งคาร์บอนิกแอนไฮเดรส ซึ่งได้แก่ อะซีตาโซลาไมด์ (ACZ) ลงบนไคโทซานและ 1:0.05 4-CBS-CS ในรูปไมโครสเฟียร์โดยเทคนิคอัลตราโซนิกอะตอมไมเซชัน ไมโครสเฟียร์ของไคโทซานและไคโทซานดัดแปรที่เตรียมได้มีลักษณะเป็นทรงกลมที่มีผิวเรียบมีขนาดอยู่ในช่วง 2-8 ไมโครเมตร เปอร์เซ็นต์การกักเก็บอะซีตาโซลาไมด์ในไมโครสเฟียร์ (%EE) ของ 1:1 ACZ-4-CBS-CS สูงถึง 98% ซึ่งมากกว่าค่า 47% ที่ได้จากอนุภาคไคโทซาน และอะซีตาโซลาไมด์ที่ถูกตรึงด้วยอนุภาค 4-CBS-CS สามารถทยอยการปลดปล่อยได้นานถึง 4 ชั่วโมง

สาขาวิชา ปิโตรเคมีและวิทยาศาสตร์พอลิเมอร์ ลายมือชื่อนิสิต……

ปีการศึกษา 2552 ลายมือชื่อ อ. ที่ปรึกษาวิทยานิพนธ์หลัก……..

ลายมือชื่อ อ. ที่ปรึกษาวิทยานิพนธ์ร่วม……...

5072385923: MAJOR PETROCHEMISTRY AND POLYMER SCIENCE
KEYWORD: 4-CARBOXYBENZENESULFONAMIDE / CHITOSAN / ACETAZOLAMIDE

PHRUETCHIKA SUVANNASARA: PREPARATION OF 4-CARBOXYBENZENESULFONAMIDE MODIFIED CHITOSAN FOR DELIVERY OF ACETAZOLAMIDE. THESIS ADVISOR: ASSOC.PROF. NONGNUJ MUANGSIN, Ph.D., THESIS COADVISOR: NALENA PRAPHAIRAKSIT, D.V.M., Ph.D., 108 pp.

The objective of this research is to modify chitosan (CS) with various ratio of 4-carboxybenzensulfonamide (4-CBS) to improve a mucoadhesive property and thus increases the chance of carbonic anhydrase inhibitor being delivered through the mucosa of the stomach for eradication of *H. pylori*. The 4-CBS-CSs were characterized by ^{1}H-NMR, FT-IR spectroscopy, DSC and TGA analysis. The 4-CBS-CS (1:0.05) has mucoadhesive property and swelling ratio better than CS, and can tolerate in the stomach condition for at least 24 hours in the simulated gastric fluid (pH 1.2) and the phosphate buffer (pH 5.5). The 4-CBS-CSs were non-toxic to Vero cell and inactive against anti-cancer cell lines of epidermoid carcinoma of oral cavity (KB), breast adenocarcinoma (MCF-7) and small cell lung carcinoma (NCI-H187). Moreover, the 4-CBS-CSs can inhibit *Escherichia coli* (*E.coli*) and *Staphylococcus aureus* (*S.aureus*) better than CS.

The application of 4-CBS-CS is focused on the immobilization of acetozalamide (ACZ) onto CS and the 1:0.05 4-CBS-CS in the form of microspheres by electrospray technique. The particle sizes were in the range of 2-8 μm. The percent of ACZ encapsulation efficiency (%EE) of ACZ-4-CBS-CS (1:1) was 98% (47% for 1:1 ACZ-CS microspheres). *In vitro* release profiles of acetazolamide in the SGF showed that 4-CBS-CS can prolong release up to 4 hours.

Field of study: Petrochemistry and Polymer Science..Student's signature:……
Academic year: 2009 Principal Advisor's signature:….
Co-advisor'ssignature:……

ACKNOWLEDGEMENTS

The author thanks many people for kindly providing the knowledge of this study. First, I would like to express gratitude and appreciation to my advisor. Associate Professor Dr. Nongnuj Muangsin and co-advisor, Assistant Professor Dr. Nalena Praphiraksit for invaluable guidance and suggestions throughout this work.

I wish to express my grateful thank to Dr. Krisana Siraleartmukul for her valuable advice. I wish to express my grateful thank to Dr. Sirapan Sukontasing, Dr. Jomkwan Merak and Anamika Kanjanabuntang for assistant about antibacterial test. Furthermore, the author also thank the Center for Petroleum, Petrochemicals and Advanced Materials, Chulalongkorn University, Bangkok 10330, Thailand and the centre of Chitin-Chitosan Biomaterial, Metallurgy and Materials Science Research Institute of Chulalongkorn University for providing the equipment, chemicals, and facilities. I thank the National Nanotechnology Center (NANOTEC) for facilitating the Zetasizer Nano ZS for a particle size measurement.

I would like to extend to Associate Professor Sirirat Kokpol as the chairman, Associate Professor Nuanphun Chantarasiri and Associate Professor Thongdee Leksopee and members of my thesis committee, respectively, for their kind, guidance, helpful discussion and valuable suggestions throughout my study.

Finally, I would like to express my honest thanks to my family especially my parents and friend for their help, cheerful, endless love, understanding and encouragement.

CONTENTS

PAGE

PAGE

PAGE

PAGE

LIST OF TABLES

LIST OF FIGURE

FIGURE PAGE

FIGURE PAGE

LIST OF ABBREVIATIONS

%	Percentage
cm	centimeter
cm^{-1}	Unit of wave number
conc.	concentration
ACZ	acetazolamide
4-CBS	4-carboxybenzenesulfonamide
°C	degree Celsius (centrigrade)
CS	chitosan
DSA	Differential Scanning Calorimeter
EE	entrapment efficiency
FTIR	Fourier Transform Infrared Spectrophotometer
g	gram
kDa	kilodalton
M	concentration in molar
mg	milligram
min	minute
mL	mililiter
MW	molecular weight
NMR	Nuclear Magnetic Resonance spectroscopy
pH	power of hydrogen ion or the negative logarithm (base ten)
ppm	part per million
r^2	correlation coefficient
rpm	round per minute
S.D.	standard deviation
SEM	Scanning Electron Microscope
sub	substitution

S_w	The swelling ratio
TGA	Thermogravimetric Analysis
UV	ultraviolet
v/v	volume/volume
w/w	weight/weight

CHAPTER I

INTRODUCTION

1.1 Introduction

Helicobacter pylori (*H. pylori*) is a gram-negative bacteria that has a unique ability to grow in the stomach which has a high acidic condition, at pH values as low as 1.4 [1]. It plays a major role in pathogenesis of peptic ulcer disease, chronic gastritis, gastric mucosa-associated lymphoid tissue, lymphoid tissue lymphoma, and gastric cancer [2].

Amoxicillin is a semi-synthetic antibiotic that is effective for treating *H.pylori* infection [3]. However, none of using antibiotics alone achieve a significant eradication rate. Therefore, combinations of proton pump inhibitors (PPIs) and antibiotic drugs have been studied [4]. The PPI is antisecretory agent which increase the pH in the stomach and then protect a degradation of an antibiotic drug. Example of a combination of one PPI and one antibiotic drug is the combination of omeprazole and clarithromycin [4]. Alternatively, a therapy consisting of one PPI and two antibiotic drugs was recommended, for example, the combination of acetazolamide, amoxicillin and clarithromycin [5]. However, PPIs have some side effects such as flatulence, diarrhea, and vomiting [6], which are not suitable for infant or elderly patients.

Recent studies suggested that carbonic anhydrase inhibitors (CAIs) can reduce the ability of *H.pylori* to survive in an acid environment in the stomach [7]. Because when the *H. pylori* get into the human body, it immobilizes in the stomach and produces at least two enzymes; urease [1] and carbonic anhydrase [8] coated on itself to protect it from the gastric acid.

Acetazolamide is a carbonic anhydrase inhibitor used for glaucoma, epilepsy, benign intracranial hypertension and altitude sickness [9]. Nishimori et al. reported a study of inhibition profile with a panel of sulfonamides/sulfamates as CAIs against β-carbonic anhydrase (hpβCA) of *H.pylori* [10]. Therefore, in this work focused on the

possibility to use acetazolamide combining with an antibiotic drug to eradicate *H.pylori* in the stomach.

However, most of enzyme inhibitors do not remain concentrated on the target sites. They are often diluted in various body fluids and subsequently absorbed from mucosal tissues leading to systemic toxic side effects [11]. The immobilization of enzyme inhibitors to polymer is an alternatively approach to keep these enzyme inhibitors concentrated and slowly release to a target organ.

Many enzyme inhibitors controlled release systems have been reported, for example, Bernkop-Schnurch et al. [12] gave an overview of chemically modified chitosans to immobilize enzyme inhibitors which still displayed enzyme inhibitory properties.

Wang et al. [13] have developed the targeted delivery system using semitelechelic poly (N-2-(hydroxypropyl)methacrylamide) (ST-PHPMA) as a carrier for cathapsin K.

Bernkop-Shnurch et al. [14] have prepared the mucoadhesive chitosan for protecting embedded therapeutic peptides or proteins from trypsinic degradation by using trypsin inhibitor. The drug system was lower toxic than using enzyme inhibitors alone.

Therefore, in order to reduce the side effects of CAIs, carbonic anhydrase inhibitors can be immobilized onto polymer. Ray et al. [15] has purified human erythrocyte carbonic anhydrase B and immobilized it in polyacrylamide gel in order to study heat resistant and sulphanilamide actions and Crumbliss et al. [16] reported the imobilization of bovine carbonic anhydrase on porous silica beads and graphite The enzyme activity were also studied.

Nowaday, mucoadhesive polymers become more interesting for transmucosal routes such as nasal, pulmonary, and oral routes due to several advantages, for example, increasing the localization at target site, a prolonged residence time at the site of drug absorption and intensified contact with the mucosa increasing the drug concentration gradient. Numerous polymers adhere to mucosal tissues, for instance, chitosan [17], thiolated polymers such as chitosan-thioglycolic acid conjugates [18], chitosan-poly (lactide-co-glycolide) [19] and carboxymethyl cellulose (CMC) [20].

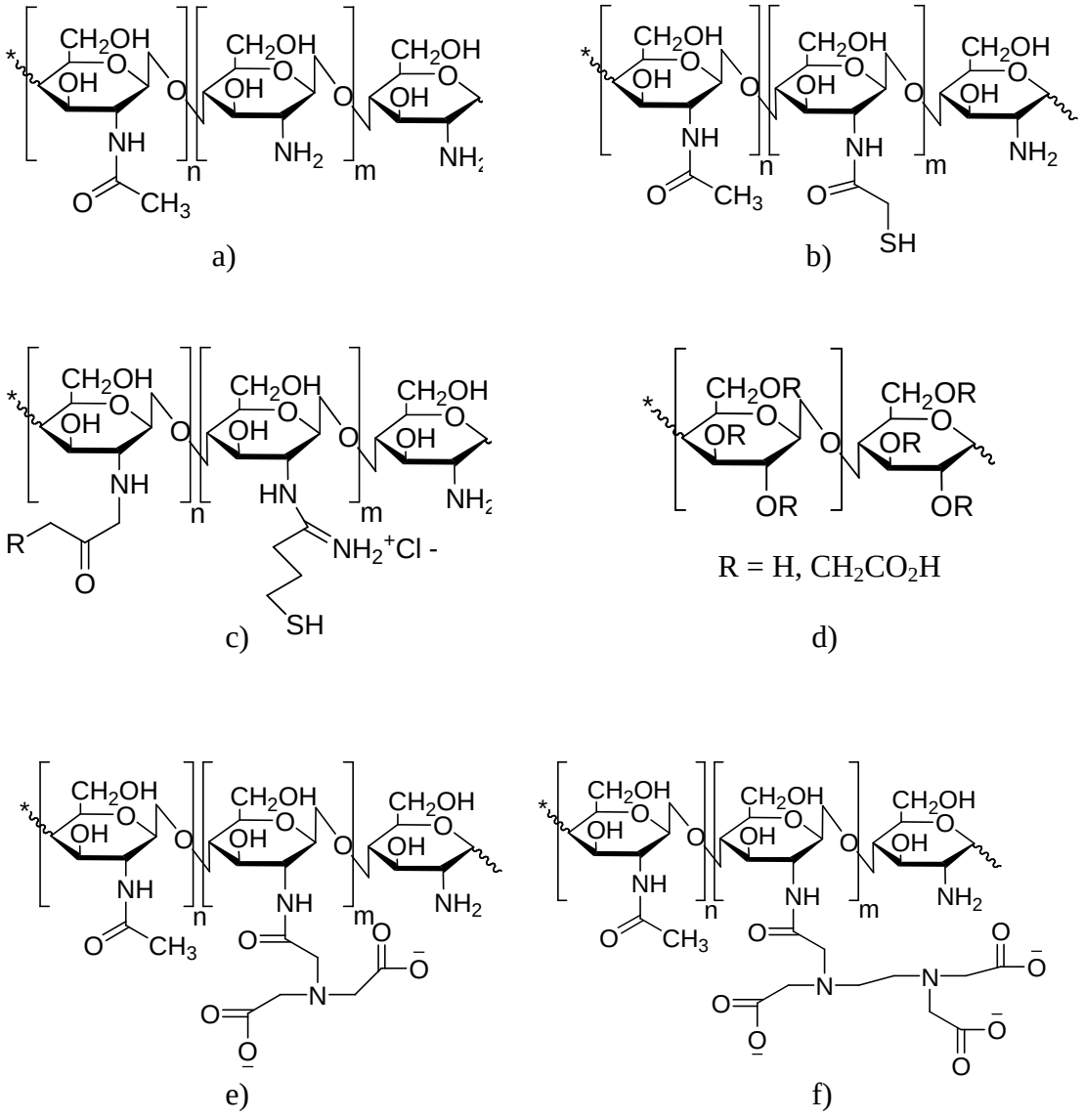

Figure 1.1 Chemical structures of a) chitosan, b) chitosan-thioglycolic acid conjugates, c) chitosan-poly (lactide-co-glycolide) d) carboxymethyl cellulose (CMC), e) chitosan-nitrilotriacetic acid conjugates and f) chitosan-EDTA conjugates

Chitosan or poly [β-(1→4)-2-amino-2-deoxy-D-glucopyranose], a natural biopolyaminosaccharide, is obtained by alkaline deacetylation of chitin that is found widely in nature. It has been widely used for developing drug systems because of its excellent mucoadhesive properties [17].

Kotadiya et al. [21] have prepared clarithromycin loaded chitosan based mucoadhesive microspheres for providing prolonged contact time for antibiotics drug delivery.

Yamamoto et al. [22] have prepared the surface modified PLGA chitosan nanospheres by the emulsion solvent diffusion method for mucoadhesive pulmonary delivery of elcatonin.

Bernkop-Schnurch et al. [23] have reported the chitosan-ethylenediaminetetraacetic acid (EDTA) conjugates. The effect of the ratio of chitosan to EDTA, for example, viscosity and mucoadhesive properties were investigated.

Tikhonov et al. [24] have immobilized the nitrilotriacetic acid as complexing agent onto chitosan. The product is water soluble, hence it may possibly to be useful as chromatography supports, enzyme immobilization and water treatment.

Yuan et al. [25] synthesized cholesterol hydrophobically modified chitosan via diafiltration method for entrapment of cyclosporine A to delivery at ocular surface.

Therefore, the objective of this work is to develop a mucoadhesive chitosan with a good swelling property, resistance in an acidic condition for delivery drug especially at the gastrointestinal tract to eradicate *H.pylori*. This can be achieved by modification of chitosan with 4-carboxybenzenesulfonamide using a carbodiimide (EDAC) as a coupling agent via a coupling reaction. Furthermore, the immobilization of acetazolamide onto chitosan and 4-carboxybenzenesulfonamide-chitosan were fabricated into the form of microspheres using electrospray technique.

1.2 The objectives of research

1) To prepare mucoadhesive chitosan (CS) covalently attachment of 4-carboxybenzensulfonamide (4-CBS) onto CS.

2) To immobilize carbonic anhydrase inhibitor, namely acetazolamine (ACZ) onto CS and the 4-CBS-CS conjugates.

3) To study sustain release profiles of ACZ in the stimulated gastrointestinal tract condition.

1.3 The scope of research

The scope of this research was carried out by stepwise methodology as follow:

1) Review literatures for related research work.
2) Preparation of 4-CBS-CS conjugates using carbodiimide (EDAC) as a coupling agent.
3) Evaluation the optimum conditions to obtain the maximum mucoadhesive properties of the 4-CBS-CS conjugates by varying proportions of 4-CBS to CS, the ratio of 4-CBS to EDAC, reaction time and reaction temperature.
4) Characterization of the physico-chemical properties of the 4-CBS-CS conjugates, by for example, ^{1}H-NMR, FT-IR, DSC and TGA.
5) Determination of
    a. degree of substitution by UV-Vis spectroscopy technique.
    b. mucoadhesive properties of mucin-conjugate polymers in the simulated gastric fluid at pH 1.2 and 5.5.
    c. swelling properties water and the simulated gastric fluid at pH 1.2 and the simulated intestinal fluid phosphate buffer pH 7.4.
    d. Toxicity and ability of conjugate polymers to against positive and negative gram bacteria.
6) Immobilize acetazolamide (ACZ) onto 4-CBS-CS conjugates.
    a. Determination of the optimum preparation conditions for ACZ loaded 4-CBS-CS conjugates
    b. Characterization of the physico-chemical properties of ACZ immobilized onto 4-CBS-chitosan conjugates by FT-IR, DSC, and SEM.

c. Study the release behavior of the ACZ form microspheres as prepared by electrospray ionizing technique in the simulated gastric fluid pH 1.2 and the simulated intestinal fluid phosphate buffer pH 7.4 using UV-Vis Spectroscopy.

7) Immobilize acetazolamide (ACZ) onto CS.
8) Comparison the immolization efficiency of ACZ onto 4-CBS-CS conjugates with CS.
9) Summarize the results.

Part I: Flow chart for synthesis of 4-CBS-CS conjugates

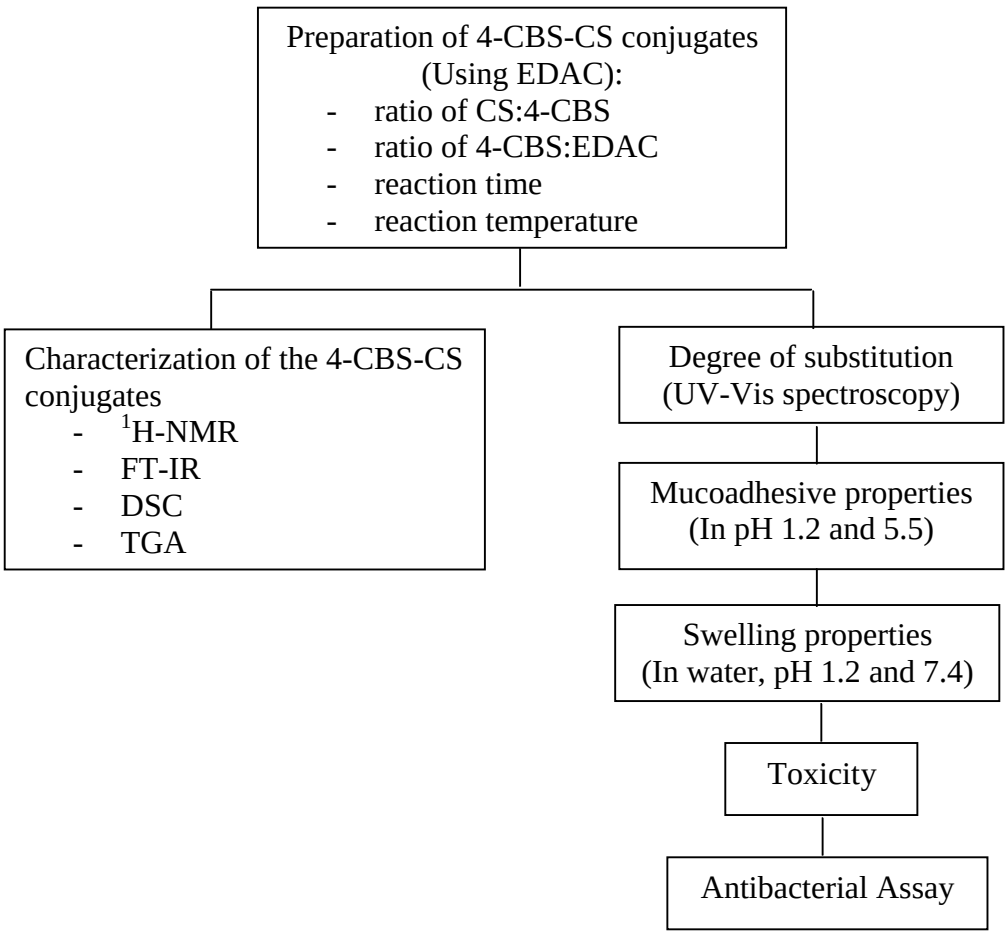

Part II: Phamaceutical application: Immobilization of ACZ

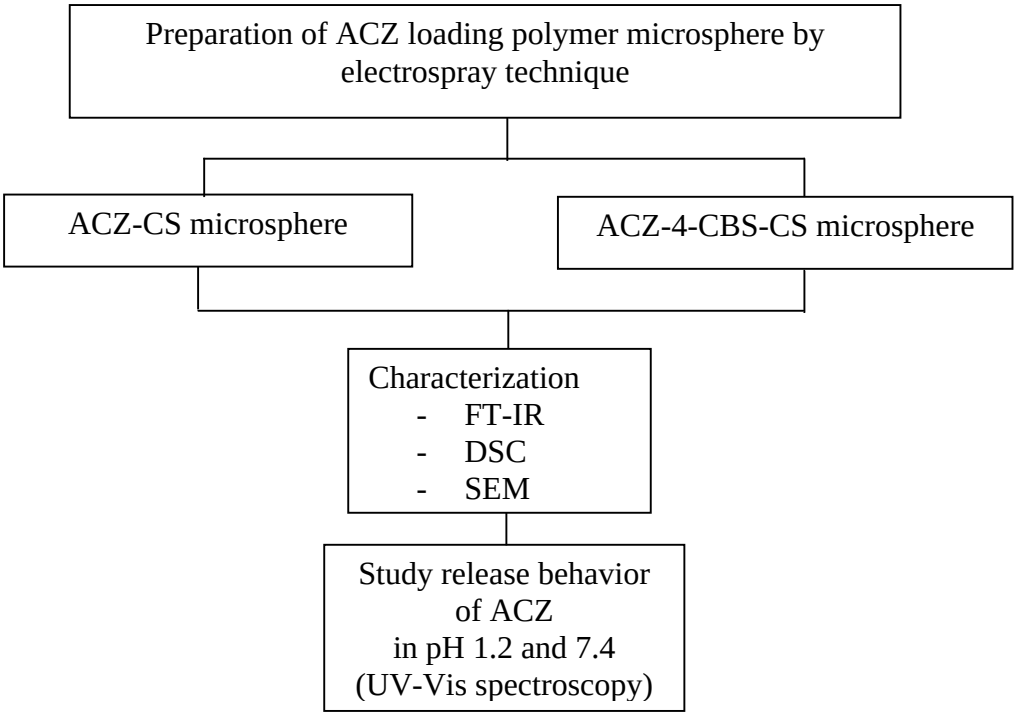

Figure 1.2 The scope of research

CHAPTER II

BACKGROUND AND LITERATURE REVIEWS

2. Background and literature reviews

2.1 *Helicobacter pylori*

Helicobacter pylori (*H.pylori*) is a gram-negative and microaerophilic bacterium that unique ability to grow in the stomach presenting highly acidic conditions, at pH values as low as 1.4 [1]. Due to this bacterium get into human body, it immobilizes in stomach and produces at least two enzymes, urease and carbonic anhydrase [8] coated on itself to protect it from gastric acid. It plays a major role in pathogenesis of peptic ulcer disease, chronic gastritis, gastric mucosa-associated lymphoid tissue, lymphoid tissue lymphoma, and gastric cancer [26].

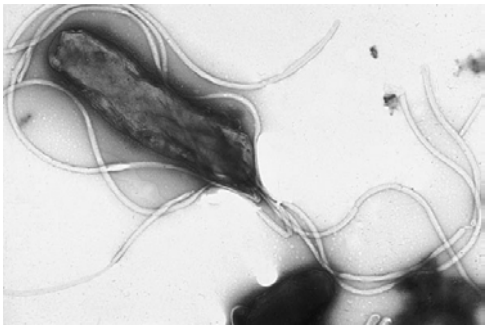

Figure 2.1 *Helicobacter pylori* (*H.pylori*) [4]

2.1.1 Causes of infection and Symptoms

H.pylori is a bacterium which probably spread by consuming food or water contaminated with fecal matter. A clean and hygienic environment can help decrease the risk of *H.pylori* infection.

Most individuals with peptic ulcer disease, chronic gastritis, gastric mucosa-associated lymphoid tissue and lymphoid tissue lymphoma have not symptoms.

However, some people have symptoms, for example, pain or discomfort, bloating, feeling full after eating a small amount of food, lack of appetite, nausea or vomiting, dark or tar-colored stools and ulcers that bleed. The abnormal changes from *H.pylori* infection can lead to certain forms of gastric cancer.

2.1.2 Treatment of infection

Patients with a history of peptic ulcer disease, chronic gastritis, gastric mucosa-associated lymphoid tissue and lymphoid tissue lymphoma associated with *H.pylori* infection should be given treatment in order to reduce the risk of gastric cancer. Amoxicillin is semi-synthetic antibiotic that effective for *H.pylori* infection treatment [3]. A number of researchers have prepared new controlled release tablets of amoxicillin with desired release profile and less degradation rate of amoxicillin [3]. *H.pylori* infection should be treated with antibiotics but none of ones that achieve a significant eradication rate when used alone. Proton pump inhibitors (PPIs) were antisecretory agents for adjuvant therapy to increase the stomach pH and protect antibiotic degraded. The recommended therapy consists of a PPI and two antibiotic, mainly amoxicillin and clarithromycin [5]. Variations of the therapy have been developed such as using a different proton pump inhibitor, as with pantoprazole or rabeprazole, or using metronidazole instead of amoxicillin in those allergic to penicilline [4]. However, side effects of PPIs are flatulence, diarrhea, and vomiting. Another problem is when the disease get into human body, it immobilizes in stomach and produces at least two enzymes, urease [1] and carbonic anhydrase [8] coated on itself to protect it from gastric acid. This result is antibiotic can not reacts with disease. Recent studies suggest that carbonic anhydrase inhibiton reduces the ability of *H.pylori* to survive in an acid environment as present in the stomach [7].

2.2 Enzyme inhibitor

Enzyme inhibitors are molecules which can bind with enzyme so as to decrease their activity. Since blocking an activity of enzyme can kill a pathogen or correct a metabolic imbalance. The binding of an inhibitor can stop the entering of

enzyme in active site region of substrate. Inhibitor binding is either reversible or irreversible. Irreversible inhibitors as usually covalently react with the enzyme and change it chemically. In contrast, reversible inhibitors bind to enzyme with non-covalent interactions and can be easily removed by dilution or dialysis. Many drug molecules are enzyme inhibitors, so their discovery and improvement is an active area of research in biochemistry and pharmacology. The medicinal enzyme inhibitors as high specificity and potency ensure that a drug will have a few side effects and low toxicity.

2.2.1 Carbonic anhydrase inhibitors

Carbonic anhydrase or carbonate dehydrates is a family of metalloenzymes which the most active site contains a zinc ion. The zinc ion is coordinated by three histidine side chain and water. The water position accepts a proton that can leaves hydroxide attached to zinc. Carbonic anhydrase can catalyze the rapid conversion of carbon dioxide to bicarbonate and protons which reaction rate is one of the fastest of all enzymes. The active site contains a pocket of carbon dioxide which it close to hydroxide group. The electron rich of hydroxide attacked with carbon dioxide, forming bicarbonate.

$$CO_2 + H_2O \xrightarrow{\text{carbonic anhydrase}} HCO_3^- + H^+$$

The reverse reaction is also relatively slow.

$$HCO_3^- + H^+ \longrightarrow H_2CO_3 \longrightarrow CO_2 + H_2O$$

Carbonic anhydrase occurs five type, for example, α, β, γ, δ and ε-carbonic anhydrase. Carbonic anhydrase inhibitors such as acetazolamide, ethoxzolamide methazolamide, dorzolamide, topiramate and sulpiride, which can inhibit carbonic anhydrase, are a class of pharmaceuticals that suppress the activity of carbonic anhydrase. Their clinical use has been established as antiglucoma agents,

antiepileptics, diuretics, mountain sickness, gastric and duodenal ulcers, neurological disorders and osteoporosis.

Recent studies suggest that carbonic anhydrase inhibiton reduces the ability of *H.pylori* to survive in an acid environment as present in the stomach. The reserchers investigated the molecular cloning of some of some of the 15 presently known human carbonic anhydrase (hCA) isoforms [10], as well as screening analyses for inhibitory/activatory effects of a variety of compounds on most of them, showing that various such isozymes (e.g., hCA I, II, IV, VA, VB, VI,VII, IX, XII, XIII, and XIV) constitute valid targets for the development of novel antiglaucoma, antitumor, antiobesity or anticovulsant drugs [31]. Nishimori and et.al clone DNA of β-carbonic anhydrase of *H.pylori* (hpβCA) and study inhibition profile of sulfonamides/sulfamates against hpβCA [10]. However, enzyme inhibitors do not remain concentrated on polymer drug carrier systems. They are diluted in various body fluids and subsequently absorbed from mucosal tissues leading to systemic toxic side effects [11]. The immobilization of enzyme inhibitors to polymer keeps these drug agents concentrated and slow release to target organ. Bernkop-Schnurch et al. give an overview of chemically modified chitosan (CS) displaying enzyme inhibitory properties [12].

2.2.1.1 Acetazolamide

Acetazolamide is the most famous sulfonamide inhibitor of carbonic anhydrase used to treat glaucoma, epileptic seizures, benign intracranial hypertension (pseudotumor cerebri), altitude sickness, cystinuria, dural ectasia and as a generic drug and is also used as a diuretic. Acetazolamide can be recrystallize so as to obtain a material for direct compression [27]. Duarte et.al. were study the possibility of preparing ophthalmic drug delivery systems using supercritical anti-solvent technology, using eudragit and acetazolamide as drug carrier and model drug respectively [6].

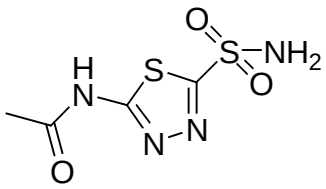

Figure 2.2 Chemical structure of acetazolamide

1) Physicochemical properties

Physical : Crystalline white solid and odorless

IUPAC name : N-(5-sulfamoyl-1,3,4-thiadiazol-2-yl)acetamide

Trade name : Diamox

Empirical formula : $C_4H_6N_4O_3S_2$

Molecular weight : 222.245 g/mole

Melting point : 258.5 °C

2) Side effect of acetazolamide

The using acetazolamide has many common side effects include numbness and tingling in the fingers and toes, and taste alterations, especially for carbonated drinks. Some may also experience blurred vision but this usually disappears shortly after stopping the medication. Acetazolamide also increases the risk of developing calcium oxalate and calcium phosphate kidney stones. Everyone will experience more frequent urination as a result of using acetazolamide. One should drink more fluids than usual to prevent dehydration and headaches. Acetazolamide prolongs the effects of amphetamines and related drugs.

2.2.1.2 4-carboxybenzenesulfonamide

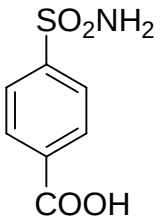

Figure 2.3 Chemical structure of 4-carboxybenzenesulfonamide

Physical	: White powder
IUPAC name	: 4-sulfamoylbenzoic acid
Empirical formula	: $C_7H_7NO_4S$
Molecular weight	: 201.20 g/mole

2.3 Mucoadhesion

Mucoadhesion is the ability of macromolecules such as proteins and peptides to adhere at mucosal membranes which are the moist surfaces lining the walls of various body cavities.

Mucoadhesive drug delivery systems, designed to adhere to mucosal surface, become interesting nowadays for transmucosal routes such as pulmonary, nasal, and oral routes due to their several advantages such as:

1) Prolong residence time of the dosage form on mucosal tissue for increasing drug absorption and drug's bioavailability.

2) High concentration gradient drug at the site of adhesion-absorption membrane which will create a driving force for the paracellular passive uptake.

3) Immediate absorption from the bioadhesive drug delivery system without previous dilution and possible degration in luminal fluids of body [12].

4) Enhancement of topical action of certain drugs such as antibiotic against certain bacteria that colonize the stomach such as *H.pylori* [28]. Better stability and longer residence time allow more of antibiotic to penetrate through the gastric mucus layer to act on *H.pylori*.

2.3.1 Mucoadhesive polymers

Numerous polymers adhere to mucosal tissues. These include synthetic polymers, for instance, poly(acrylic acid) (PAA) [29], hydroxypropyl methylcellulose, poly(methylacrylate) derivatives and thiolated polymers [30], as well as naturally occurring polymers such as hyaluronic acid [31] and CS [17]. Among these various possible bioadhesive polymeric hydrogels, PAA has been considered as a good mucoadhesive. However, due to a high transition temperature and higher interfacial free energy, PAA does not wet the mucosal surface to the optimal level, causing loose interdiffusion of the polymer. Therefore, PAA is copolymerized with polyethylene glycol (PEG) or poly(vinyl pyrrolidone) (PVP) to improve these properties. It is important to realise that balanced adhesive and cohesive properties for a polymer is essential for its application in a transmucosal drug delivery systems, especially for the removable devices.

2.3.2 Interaction of mucoadhesion

Mucoadhesion involves different kinds of interaction forces between mucoadhesive materials and the mucus surface; these include electrostatic attraction, hydrogen bonding, Van der Waals forces, mechanical interpenetration and entanglement. Their mucoadhesive properties can be explained due to the interaction with glycoproteins of the mucus mainly based on non-covalent bonds such as ionic interactions, hydrogen bonds and van der Waal’s forces [32].

Many methods have been used to evaluate these interactions. Viscometric measurement for mucin/polymer dispersions were preformed using a Brookfield viscometer and an Oswald viscometer used to measure mucoadhesive properties of polymer [33]. The researcher found that the mucoadhesive property of thiolated

polymers is chemical modification which is well-established mucoadhesive polymers [18]. The researcher were study the mucoadhesive properties of various polymer in two different test systems [34].

2.3.3 CS as a mucoadhesive polymer

CS mucoadhesion has been widely studied, the basis for these properties remains unclear. Electrostatic interactions of cationic CS with negatively charged mucin have been reported as the main driving force for its strong mucosal adhesion. Interactions with mucin appear to be both electrostatic, via NH_3^+ groups on the CS with either COO^- or SO_3^- groups on the mucin carbohydrate side chains and/or hydrophobic, via – CH_3 groups on acetylated CS residues with
– CH_3 groups on mucin side chains (depending on the degree of acetylation of the CS, local solvent conditions, for example, pH, ionic strength, and the degree of sulphonation and sialic acid content of the mucin).

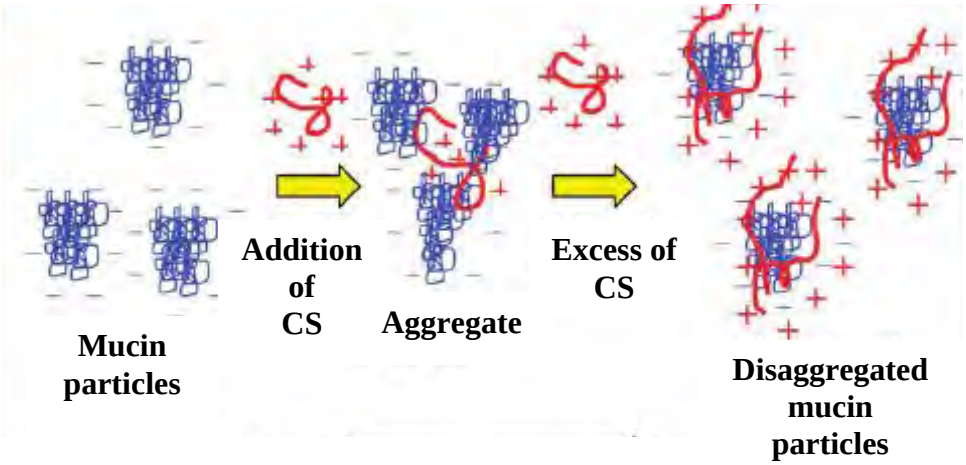

Figure 2.4 Diagram depicting aggregation/disaggregation of pig gastric mucin in the presence of mucin [17]

2.4 CS

CS, a natural cationic biopolyaminosaccharide, was discovered by Rouget in 1859 and gave a name by Hoppe-Seyler in 1894 [35]. It is produced commercially by deacetylation of chitin in strong alkaline solution, which is noticeably present in outer skeletons of arthropods in particular, for example, in the epidermis of crustaceans such as crabs and shrimp shells, lobsters, prawns and cell walls of some fungi such as *aspergillus* and *mucor*. In plants, chitin is present in hyphae or spores of molds. The degree of deacetylation (%DA) can be determined by NMR spectroscopy, and the % DA in commercial CS is in the range 60-100 %. It was reported that CS is a potentially useful pharmaceutical material owing to its good biocompatibility and low toxicity.

2.4.1 Structure of CS

CS $(C_6H_{11}O_4N)_n$, a natural linear biopolyaminosaccharide composed of randomly distributed β-(1-4)-linked 2-acetamido-2-deoxy-D-glucopyranose and 2-amino-2-deoxy-D-glucopyranose (Figure 2.5). A fraction of the repeating units in the CS backbone contains hydroxyl groups (–OH) and amine pendent groups ($–NH_2$) while the rest contains acetamide group (–NHCO) in its place. Both reactive primary amine and hydroxyl group can be used to chemically alter its properties under mild reaction conditions. The polymer differs from chitin in that a majority of the N-acetyl groups in CS are hydrolyzed. The degree of hydrolysis (deacetylation) can be controlled by time, temperature and concentration of alkaline treatment of chitin [34], so has significant effect on the solubility and rheological properties of polymer.

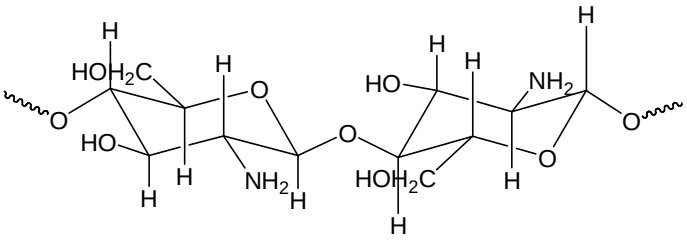

Figure 2.5 Chemical structure of CS

2.4.2 Physico-chemical properties of CS

CS is the large polysaccharide, which is various different the degree of deacetylation and high molecular weight. It is very important effect on the biological properties.

CS is a cationic polysaccharide which is a weak base with pK_a value of the D-glucosamine residue of about 6.2-7.0. Therefore, is insoluble at neutral and alkaline pH values. However, make salts with inorganic and organic acids such as acetic acid, hydrochloric, glutamic acid, and lactic acid making it soluble in water. Because of in acidic medium, the amine groups of CS can undergo protonation, positively charged polysaccharide. Furthermore, the solubility of CS is depending on the degree of deacetylation and pH of solution.

The viscosities of CS are depending on concentration and temperature Increasing the degree of deacetylatin increases the viscosity. As the CS concentration increases and temperature decreases, the viscosity increases. Because the hydrogen bonding in CS chains due to the presence of amine and hydroxyl groups causes the high viscosity of CS solutions.

2.4.3 Pharmaceutical CS uses

Due to its low-toxicity, biocompatibility with human body tissue, CS have displayed their effectiveness for all forms of dressings-artificial skin, corneal bandages and suture thread in surgery-as well as for implants or gum cicatrization in bone repair or dental surgery.

Lastly, CS is an excellent medium for carrying and slow release of medicinal active principles in plants, animals and man. If degree of deacetylation and molecular weight can be controlled, it would be good advantage for developing size of CS for drug delivery system [36].

2.5 Carbodiimide

Carbodiimide is a consisting of the formula N=C=N. Carbodiimide hydrolyze to form ureas or thioureas, which makes them rarely found in nature [37]. It was often used to activate carboxylic acids in order to produce the amide or ester functional group. Additives, such as N-hydroxybenzotriazole or N-hydroxysuccinimide, are often added to increase yields and decrease side reactions.

2.5.1 EDAC

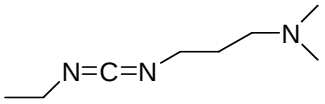

Figure 2.6 Chemical structure of EADC

EDAC (also EDC or EDCI, acronyms for 1-ethyl-3-(3-dimethylaminopropyl) carbodiimide hydrochloride) is a water soluble carbodiimide which is typically employed in the 4.0-6.0 pH range. It is generally used as a carboxyl activating agent for coupling of primary amines to yield amide bonds. Common uses for this carbodiimide include peptide synthesis, protein crosslinking to nucleic acids and preparation of immunoconjugates. Additionally, EDC can also be used to activate phosphate groups. EDAC is often used in combination with N-hydroxysuccinimide (NHS) or sulfo-NHS to increase coupling efficiency or create a stable amine-reactive product.

EDAC also used in organic chemistry to couple a carboxylic acid to alcohol using DMAP as a catalyst.

2.5.2 The formation of amide group of 4-CBS-CS conjugates by using EDAC

The formation of an amide of 4-CBS-CS conjugates using EDAC is straightforward, but with several side effect complicating the subject. The carboxylic acid will react with the carbodiimide to produce the key intermediate: the O-acylisourea, which can viewed as a carboxylic ester with an activated leaving group. The O-acylisourea will react with amines group of CS to give the desired amide group of 4-CBS-CS conjugates and urea.

Furthermore, the side reaction of the O-acylisourea can produce both desired and undesired products. The O-acylisourea can react with an addition carboxylic acid to give acid anhydride. The main undesired reaction pathway involves the rearrangement of the O-acylisourea to the stable N-acylurea . The use of solvents with low-dielectric constants such as dichloromethane or chloroform can minimize this side reaction.

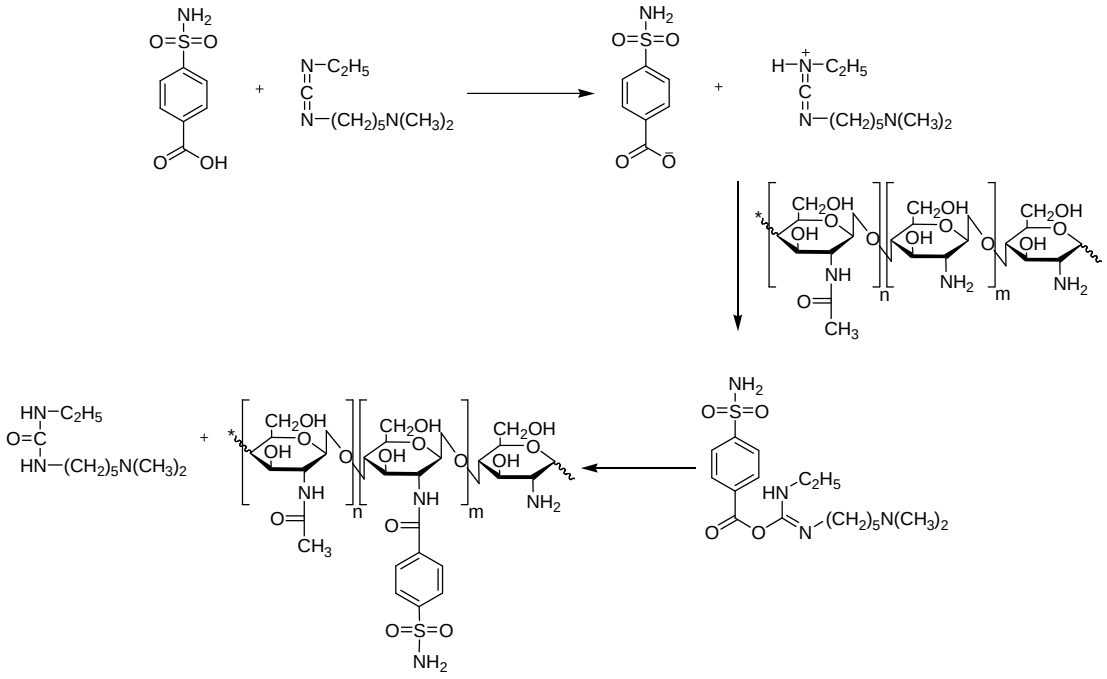

Figure 2.7 EDAC as coupling reagent for the formation of 4-CBS-CS conjugates

2.6 Controlled drug release system

The pharmaceutical field has used controlled release widely in oral medication since the early 1950s. Enteric coating of such dosage forms as tablets with pH-sensitive materials has been and remains very common. Similarly, encapsulated pellet or beads have been used, as have sparingly soluble salts, complexed systems, and porous insoluble tablets containing dispersed drug.

2.6.1 Advantage of controlled release

Controlled release system provides numerous advantages over conventional dosage form, for example, able to control the rate of drug delivery, the target area of administration and maintain therapeutic levels of drug with narrow fluctuations (Figure 2.8) [38]. Thus the toxicity and undesired of drug, which is fasten release was reduced. The serum concentration of drug released from controlled release dosage form fluctuates within the therapeutic range over a long period of time. That makes it possible to reduce the frequency of drug administration and improvement in treatment efficiency.

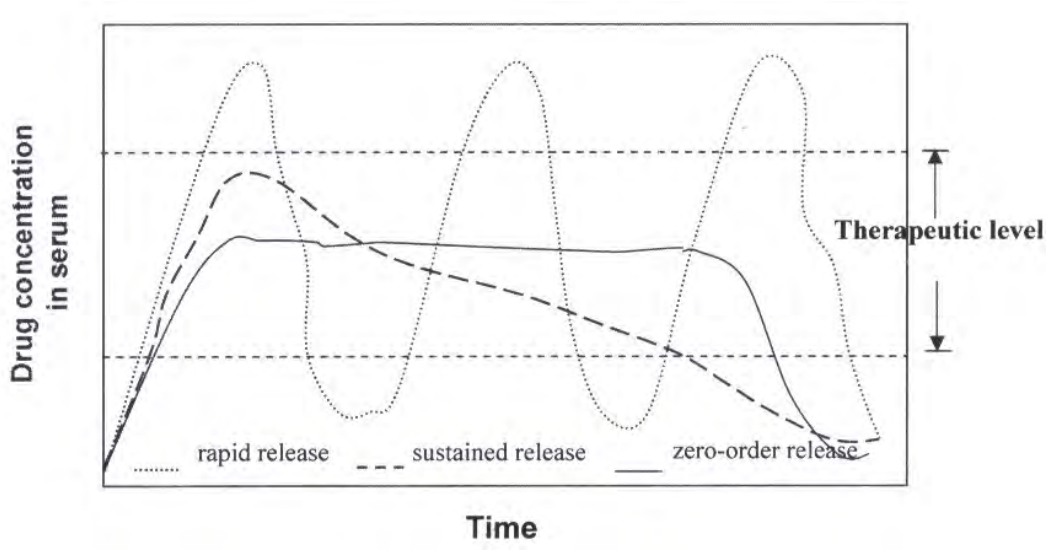

Figure 2.8 Hypothetical serum drug concentrations of various oral dosage form [48].

2.6.2 Type of CS based drug delivery systems

The pharmaceutical application of CS particulate systems is interesting as potential drug carrier for many target areas [39]. For example, colon, mucosal, cancer, gene, topical and ocular delivery. In addition CS can be good coating material.

Table 2.1 Summary of CS-based drug delivery systems prepared by different methods for various kinds of drugs [39]

Type of system	Method of preparation	Drug
Tablet	matrix coating	diclofenac sodium, pentoxyphylline, salicylic acid, theophylline propranolol HCl
Capsules	capsule shell	insulin, 5-amino salicylic acid
Microspheres/ Microparticles	emulsion cross-linking	theophylline, cisplatin, pentazocine, phenobarbitone, theophylline, insulin, 5-fluorouracil, diclofenac sodium, griseofulvin, aspirin, diphtheria toxoid, pamidronate, suberoylbisphosphonate, mitoxantrone, progesterone

Type of system	Method of preparation	Drug
Microspheres/ Microparticles	coacervation/ precipitation	prednisolone, interleukin-2, propranolol-HCl
	spray-drying	cimetidine, famotidine, nizatidine, vitamin D-2, diolofenac sodium, ketoprofen, metoclopramide-HCl, bovine serum albumin, ampicillin, cetylpyridinuim chloride, oxtetracycline, betamethasone
	ionic gelation	felodipine
	sieving method	clozapine
Nanoparticles	emulsion-droplet coalescence	gadopentetic acid
	coacervation/ precipitation	DNA, doxorubicin
	ionic gelation	insulin, ricin, bovin serum albumin, cyclosporine A
	reverse micellar method	doxorubicin
Beads	coacervation/ precipitation	adriamycin, nifedipine, bovine serum albumin, salbutamol sulfate, lidocaine HCl, riboflavin

Type of system	Method of preparation	Drug
Films	solution casting	isosorbide dinitrate, chlorhexidine gluconate, trypsin, granulocyte-macrophage colony-stimulating factor, acyclovir, riboflavine, testosterone, progesterone, beta-oestradiol
Gel	Cross-linking	chlorpheniramine maleate, aspirin, theophylline, caffeine, lidocaine-HCl, hydrocortisone acetate, 5-fluorouracil

2.6.3 Methods of preparation of micro/nanoparticles of CS [39]

The various methods were used to prepare CS particle. It is important for the control of particle size which is affected to drug loading and efficiency of encapsulation.

The major types of method of preparation of micro/nanoparticle of CS, as follow:

(1) Emulsion cross-linking
(2) Coacervaion/preparation
(3) Spray-drying
(4) Emulsion-droplet coalescence method
(5) Ionic gelation
(6) Reverse micellar method
(7) Sieving method
(8) Electrospray ionization method

The choice of method for achieving in a particular application depends on the nature of the active molecule as well as the type of delivery device.

2.7 Electrospray ionization technigue

Electrospray ionization is a situ method to produce ions by using high voltage electrostatic systems, which employs electricity to disperse a liquid. High voltage is applied to a liquid supplied through an emitter. The positive electrode of the electrostatic system was connected to the needle assembly, whereas a negative electrode, hollow in the middle, was placed vertically in the midpoint between the needle tip (positive electrode) and the receiving beaker. When a strong electrical field is applied, it stretches the liquid meniscus at the capillary tip until it deforms and breaks off.

The advantage of electrospray ionization

(1) Droplets size is smaller than conventional mechanical atomisers, and can be smaller than 1 μm.

(2) Size distribution of the droplets is narrow

(3) Charged droplets are self-dispersing in the space, that results in absence of droplet agglomeration and coagulation

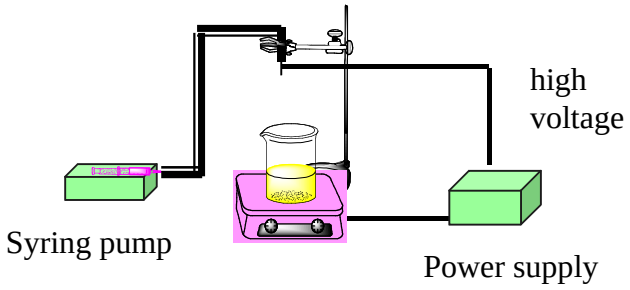

Figure 2.9 Electrospray ionization apparatus

CHAPTER III

EXPERIMENTAL

3.1 Materials

The following materials were obtained from commercial suppliers.

- Acetazolamide (ACZ) 99% minimum (Sigma-aldrich, USA) using without purification
- Chitosan (CS), food grade, Lot No. 497613, M.w. 500,000-1,000,000 KDa, Deacetylation 95 % (Bonafides, Thailand)
- Ammonia solution (NH_3OH) 30%, AR grade (Sigma-aldrich)
- 4-carboxybenzenesulfonamide (4-CBS) 97 %, AR grade (Sigma-Aldrich,USA)
- Ethanol 95 %, commercial grade (EtOH) (Merck, Germany)
- 1-ethyl-3-(3-dimethylaminopropyl) carbodiimide hydrochloride (EDAC)
- Hydrochloric acid fuming (HCl) 37 %, AR grade (Merck, Germany)
- Lactic acid (Union chemicals, Thailand)
- Mucin from porcine stomach (type 2), (Sigma-Aldrich,USA)
- Potassium dihydrogen phosphate, (KH_2PO_4) AR grade (Merck, Germany)
- Potassium bromide, (KBr), AR grade (Merck, Germany)
- Sodium chloride (NaCl), AR grade (Merck, Germany)
- Sodium hydrogen phosphate, (Na_2HPO_4), AR grade (Merck, Germany)
- Sodium hydroxide (NaOH), AR grade (Merck, Germany)
- Sodium tripolyphosphate, ($Na_5P_3O_{10}$), AR grade (Sigma-Aldrich, USA)
- Cellulose dialysis membrane with $\overline{M}_w$ cut off at 3,500 Da (Spectrum Laboratories Inc.)

3.2 Instruments

The instruments used in this study are listed in Table 3.1

Table 3.1 Instruments

Instrument	Manufacture	Model
Analytical balance	Mettle	AT 200
Diaphragm vacuum pump	Becthai	ME 2
Differential scanning colorimeter	Netzsch	DSC 7
Digital camera	Sony	T 70
Freez dryer	Labconco	Freeze 6
FT-IR spectrometer	PerkinElmer	Spectrum RX I
High voltage	Ormond beach	GAMMA
Horizotal shaking water-bath	Lab-line instrument	3575-1
Micropipette	Mettler Toledo	Volumate
NMR spectrometer	Varian	400 Hz
PH-meter	Metrohm	744
Scanning electron microscope	Phillips	XL30CP
Syring pump	Pennyful	kdScience
Thermogravimetric analysis	NETZSCH 409	STA 409
UV-VIS spectrometer	PerkinElmer	Lambda 800
Viscometer	Tamsom	TV 4000
Ultrasonic bath	Ney Ultrasonik	28 H

3.3 Methods

Part I: Flow chart for synthesis of 4-CBS-CS conjugates

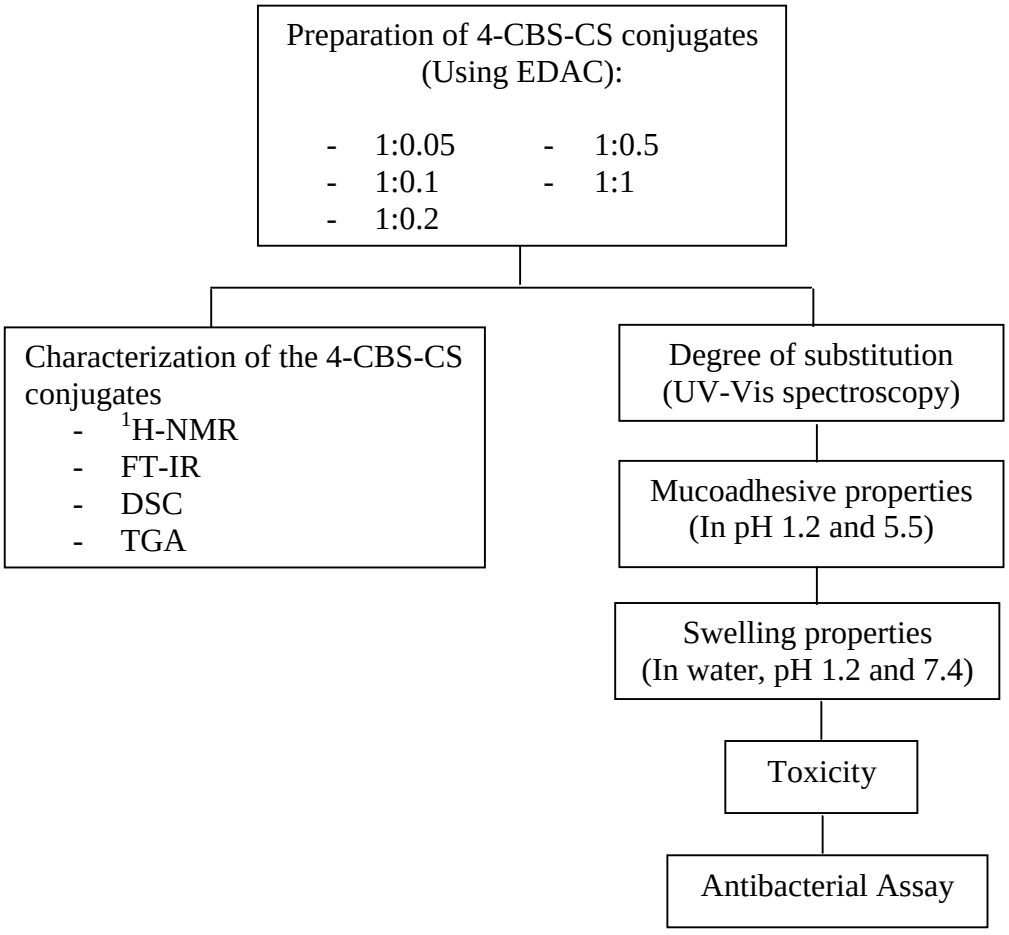

Part II: Phamaceutical application: Immobilization of ACZ

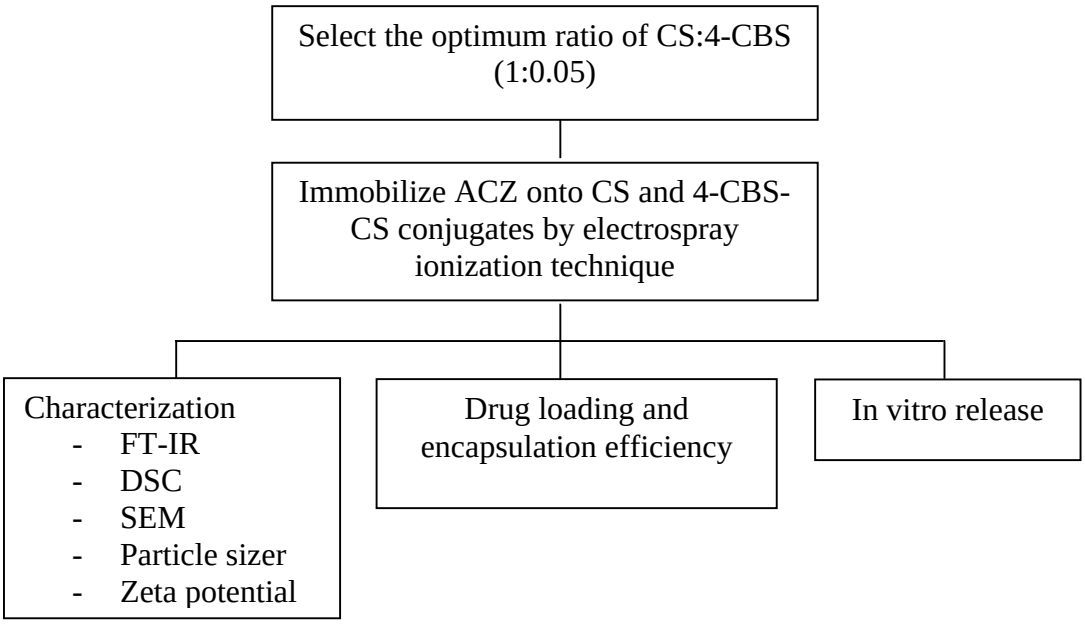

Figure 3.1 Scope of the experiment

3.3.1 Synthesis of 4-carboxybenzenesulfonamide-chitosan (4-CBS-CS) conjugates

1 g of CS was dissolved in 100 ml of 1% (v/v) lactic acid at room temperature overnight to give a 1% (w/v) CS solution. Different ratios of 4-CBS, were added into 1% (w/v) CS solution. Next, EDAC as the coupling agent was added with the constant mole ratio of 1.2:1 of EDAC to 4-CBS and then refluxed for 6 hours. EDAC was removed by adding 1 N HCl. Then the 4-CBS-CS conjugate was precipitated by adding 1 N NaOH. Afterward, the precipitated 4-CBS-CS conjugate was filtered, washed with distilled water until neutral and air-dried. The resulted conjugate polymer was post-treatmented by dissolving in 1% (v/v) lactic acid before used.

Effect of weight ratio of CS to 4-CBS

The 4-CBS-CS conjugates were prepared by the above mentioned method with various weight ratio of CS to 4-CBS, e.g. 1:0.05, 1:0.1, 1:0.2, 1:0.5 and 1:1.

The appropriate ratio of CS to 4-CBS was selected with the criteria of the maximum mucoadhesion properties.

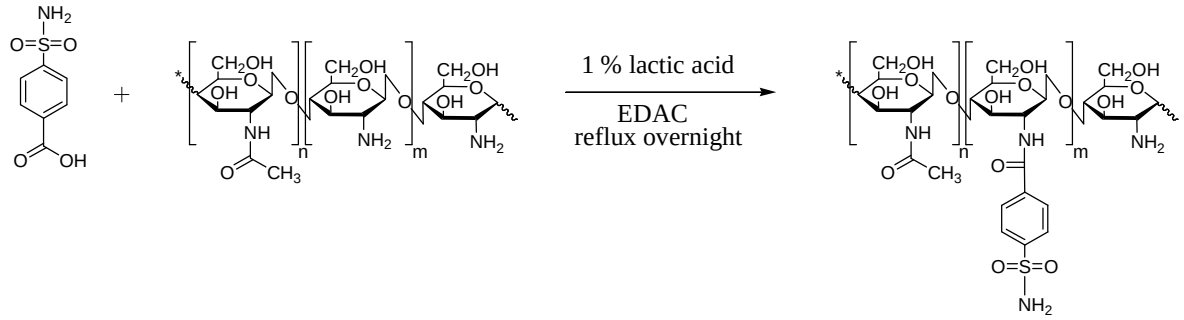

Figure 3.2 Reaction scheme of 4-CBS-CS conjugates

3.3.2 Characterization of 4-CBS-CS conjugates

3.3.2.1 ^{1}H Nuclear magnetic resonance spectroscopy (^{1}H NMR)

For the characterizations of 4-CBS-CS conjugates, 4 mg of compounds were prepared by dissolved in 2% d_4 acetic acid (CH_3COOD) in deuterium oxide (D_2O). ^{1}H NMR spectra were recorded on Varian Mercury NMR spectrometer operated at 400 MHz (Varian Company, CA, USA).

3.3.2.2 Fourier transform infrared spectroscopy (FT-IR)

Infrared spectroscopy was used to confirm the functional groups of substances and 4-CBS-CS conjugates by observing the positions and intensities of IR peaks.

The obtained 4-CBS-CS conjugates used for the FT-IR analysis first was dried and ground into a powder form. The dried 4-CBS-CS flims was mixed with potassium bromide (KBr) (1:100) to the power in agate mortar and pestle. The mixture was then transferred to a hydraulic pressing machine and pressed into a disc. Analysis was performed on an FT-IR spectrometer (Perkin Elmer Spectrum RX-1 FT-IR system). The sample was scanned from wavenumbers of 400 to 4400 cm^{-1}.

3.3.2.3 Thermal analysis

3.3.2.3.1 Differential scanning calorimetry (DSC)

Approximately 3-6 mg of 4-CBS-CS conjugates flims were weighed in the aluminum pan, then crimped with the sealed pan for determinations. And empty pan, sealed in the same way as the sample, was used as a reference. DSC was obtained with Netzsch DSC 204 under nitrogen atmosphere. The temperature range is 25-320 °C and heating rate of 10 °C /min.

3.2.3.3.2 Thermogravimetric analysis (TGA)

The mass of the samples was generally in the range of 3-6 mg. The aluminium oxide pan was placed in the balance system equipment. The mass of the aluminium oxide pan was continuously recorded as a function of temperature. TGA was obtained with Netzsch 409 and Mettler Star SW 9.01 in under nitrogen atmosphere. The temperature range is 24-800 °C and heating rate of 10 °C /min.

3.3.3 Determination of CS substitution degree by UV-Vis absorption spectroscopy

3.3.3.1 Calibration curve of 4-CBS

The standard stock 4-CBS solution was prepared in 1% (v/v) lactic acid. 4-CBS 10 mg was accurately weighed and dissolved with 1% (v/v) lactic acid into 100 ml volumetric flask and adjusted to volume (100 ppm). The stock 4-CBS solution was diluted to 1, 10, 20, 30 and 40 ppm with 1% (v/v) lactic acid in volumetric flask. The absorbance of standard solution was determined by UV-VIS spectrophotometer at 228 nm. The 1% (v/v) lactic acid was used as a reference solution. The absorbance and calibration curve of 4-CBS in 1% (v/v) lactic acid was shown in appendix A, Table A1 and Figure A1.

3.3.3.2 The degree of substitution of 4-CBS on CS

Sulfonamide groups were appeared in 4-CBS. After reaction finished, amide groups of CS were substituted by 4-CBS. The substitution of 4-CBS onto CS was determined using UV-Vis spectrophotometer (Perkin-Elmer, Lamda 800). The absorption peak of sulfonamide functional groups were displayed at 234 nm.

The calibration was performed using standard stock solutions of 4-CBS in 1% (v/v) lactic acid. Stock solutions of 4-CBS-CS conjugates at 1:0.05, 1:0.1, 1:0.2, 1:0.5 and 1:1 ratios were prepared in 1% (v/v) lactic acid at 200 ppm and measured absorption peak. A slight shift of absorption wavelength to 228 nm was observed for the conjugates. The concentration of sulfonamide groups in the conjugates were determined by rearranging calibration curve equation of 4-CBS when know absorbance values of the conjugates. The concentration (mg/l) was used to calculate the degree of 4-CBS substitution on CS according to the following equation.

$$\%\ sub = \frac{W_i}{W_o} \times 100\%$$

where W_i is a weight of 4-CBS in 4-CBS-CS conjugates calculated from the calibration curve of 4-CBS and W_o is a weight of 4-CBS-CS conjugates were prepared. Experiment was carried out three times.

3.3.4 Determination mucoadhesive of 4-CBS-CS conjugates

Mucoadhesive properties of 4-CBS-CS conjugates were determined based on the viscometric changes of porcine gastric mucin and selected polymers in stimulated buffers of pH 1.2 and 5.5. The viscosities of 0.1% (w/v) of each polymers, 15% (w/v) mucin and 15% (w/v) mucin-0.1% polymer mixtures in stimulated buffers at pH 1.2 or 5.5 were performed at 37°C on an Oswald viscometer (Tamson, TV 4000) using the procedure decribed by Hassan and Gallo, 1989 [33]. Briefly, dried mucin was hydrated with 0.1 N hydrochloric acid (pH 1.2) or 0.1 N acetate buffer (pH 5.5) by gentle stirring for 3 hours at 25°C to yield a dispersion of 20% (w/v). CS was dissolved in 10% lactic acid to yield a stock 4% (w/v) CS solution. Then a stock 4% (w/v) CS solution was diluted by 0.1 N hydrochloric acid (pH 1.2) or 0.1 N acetate buffer (pH 5.5) to yield a 0.1% (w/v) CS solution. 4-CBS-CS conjugates were dissolved in 0.1 N hydrochloric acid (pH 1.2) or 0.1 N acetate buffer (pH 5.5) to yield a 0.1% (w/v) 4-CBS-CS conjugates solution. The viscosities of 15% (w/v) mucin-0.1% polymer mixtures were performed in either 0.1 N hydrochloric acid or 0.1 N acetate buffer (pH 5.5) for 15 mins.

The viscosity coefficient was determined by the equation as follows:

$$\eta t = \eta m + \eta p + \eta b$$

where η_t is the viscosity coefficient of system, and η_m and η_p are the individual viscosity coefficients of mucin and polymer, respectively. η_b is the viscosity component due to mucoadhesive. Experiments were carried out three times. The results are average values with standard deviations.

3.3.5 Swelling of CS and 4-CBS-CS conjugates

The swelling of CS and 4-CBS-CS conjugates flims were studied by observing the change of diameter of the films. The dried flims were cut into a circular shape with a diameter of 6.0 mm and placed in water, the simulated gastric fluid pH 1.2 and simulated intestinal fluid pH 7.4 at room temperature.

The swelling ratios were measured at particular predetermined time points after immersed in the solutions.

The swelling ratios were expressed by measuring the change diameters of flims using a micrometer scale. The swelling ratio of each flim was determined by this equation [40].

$$Sw\,(\%) \quad = \quad \frac{Dt}{Do}$$

where D_t was the film diameter at time t and D_0 was the initial film diameter. Experiment was carried out in triplicates.

3.3.6 Cytotoxic activity of 4-CBS-CS conjugates

The obtained the ratio of CS:4-CBS at 1:0.05 as 4-CBS-CS conjugates were studied in cytotoxicity against various types of primate cell line (vero) and cancer cell lines.

3.3.6.1 Cytotoxicity against primate cell line (Vero)

The GFP-expressing Vero cell line was generated in-house by stable transfecting the African green monkey kidney cell line (Vero, ATCC CCL-81), with pEGFP-N1 plasmid (Clontech).The cell line is maintained in minimal essential medium supplemented with 10% heat-inactivated fetal bovine serum, 2 mM L-glutamine, 1 mM sodium pyruvate, 1.5 g/L sodium bicarbonate and 0,8 mg/ml geneticin, at 37^{o}C in a humidified incubator with 5% CO_2.

The assay is carried out by adding 45 μl of cell suspension at $3.3x10^4$ cells/ml to each well of 384-well plates containing of 5 μl of test compounds previously diluted in 0.5% DMSO and then incubating for 4 days in 37°C in 5% CO_2 incubator. Fluorescence signals are measured by using SpectraMax M5 multi-detection microplate reader (Molecular Devices, USA) in the bottom reading mode with excitation and emission wavelength of 485 nm and 535 nm. Fluorescence signal at day 4 is subtracted with background fluorescence at day 0. The percentage of cytotoxicity is calculated by the following equation.

$$\% \text{ inhibition} = [1-(FU_T/ FU_C) *100$$

Whereas FU_T and FU_C are the fluorescence units from treated and untreated conditions, respectively.

IC_{50} values are derived from dose-response curves, using 6 concentrations of 2-fold serially diluted samples, by the SOFTMax Pro Software (Molecular Devices, USA). Ellipticine and 0.5%DMSO are used as a positive and negative control, respectively. [41]

3.3.6.2 Cancer cell growth inhibition

Cytotoxicity test were performed based on the resazurin microplate assay (REMA) which was describe by Brien (2000) [42]. Three cancer cell lines were used for this assay; KB cell line (epidermoid carcinoma of oral cavity), MCF-7 cell line (breast adenocarcinoma) and NCL-H187 (small cell lung carcinoma). The growth cell are harvested and diluted to $7x10^4$ cells/ml for KB and $9x10^4$ cells/ml for MCF-7 and NCL-H187, in fresh medium. Then 5 μg of test sample diluted in 5% DMSO, and 45 μl of cell suspension are added to 384-well plates, incubated at 37°C in 5% CO_2 incubator. After the incubation period (3 days for KB and MCF-7, and 5 days for NCL-H187), 12.5μl of 62.5 μg/ml resazurin solution is added to each well, and the plates are then incubated at 37°C for 4hr. Fluorescence signal is measured using SpectraMax M5 multi-detection microplate reader (Molecular Devices, USA) at the

excitation and emission wavelength of 530 nm and 590 nm. Percent inhibition of cell growth is calculated by the following equation:

$$\% \text{ inhibition} = [1-(FU_T/ FU_C) *100$$

Whereas FU_T and FU_C are mean fluorescent unit from treated and untreated conditions, respectively.

The response curves are plotted from 6 concentrations of 2-fold serially diluted test compounds and the sample concentrations that inhibit cell growth by 50% (IC_{50}) can be derived using the SOFTMax Pro Software (Molecular Devices, USA).

3.3.7 Inhibition of 4-CBS-CS conjugates against bacteria

Antibacterial activity of the ratio of CS: 4-CBS (1:0.05) against *E.coli* (Gram-negative) and *S. aureus* (Gram-positive) was evaluated by using agar well diffusion method. The *E. coli* and *S. aureus* were obtained from Department of Medical Sciences (Thailand). Firstly, a representative bacteria single colony was picked off, placed in nutrient broth (peptone 5 g, beef extract 3 g, agar 17 g in distilled water 1000 ml; pH 7.0-7.2) and incubated at 37 C° for 24 hours. Then the obtained fresh culture where bacterial cells grew luxuriantly was ready for antibacterial test. Lastly, 2.5 mg 4-CBS-CS conjugates were dissolved in 1% lactic acid 1 ml. A volume of 20 μl solution of microbe suspension and 20 μl solution of 4-CBS-CS conjugates were orderly added into the petri dishes. All the petri dishes were incubated at 37 C° for 24 hours and take out of photograph. The experiments were repeated for three times.

3.3.8 Immobilize ACZ onto CS and 4-CBS-CS conjugates

3.3.8.1 ACZ loading in CS and 4-CBS-CS conjugates

The particles of 4-CBS-CS conjugates were prepared by electrospray ionizing technique by using a high-voltage electrostatic system. 1 g 4-CBS-CS

conjugates were dissolved in 100 ml of l% (v/v) lactic acid to yield a 1% (w/v) 4-CBS-CS conjugates solution. The 4-CBS-CS conjugates solution was dropped into an ACZ solution for the fabrication of 4-CBS-CS microspheres. The ACZ solution was obtained by mixing 15 ml of 0.1 N ammonia solution and 25 ml of 10% (w/v) sodium tripolyphosphate. Control 4-CBS-CS solution was prepared in the same method as mentioned above.

The positive electrode of the electrostatic system was connected to the needle. A negative electrode, hollow in the middle, was placed vertically in the midpoint between the needle tip (positive electrode) and the receiving beaker, filled with sodium tripolyphosphate/ammonia solution solution in order to form microsphere particles. The pump flow rate was maintained at 2.5 ml/hours, using a type 26 gauge needle, applied voltage is 10 kV and the distance between the needle tip and the negative electrode is 10 centimeters.

3.3.8.2 Characterization ACZ immobilized onto CS and 4-CBS-CS conjugates

3.3.8.2.1 Scanning electron microscope (SEM)

The surface, shape and size morphology of CS, 4-CBS-CS conjugates, ACZ immobilized CS and ACZ immobilized onto 4-CBS-CS conjugates particles were observed via scanning electron microscope (Philips, XL30CP). In preparation of SEM examination, the samples were dropped on metal grids and coated by gold under vacuum before observation. The photographed were taken at different magnifications.

3.3.8.2.2 Particle size measurement

The size measurement of CS, 4-CBS-CS conjugates, ACZ immobilized CS and ACZ immobilized onto 4-CBS-CS conjugates particles were performed on a particle sizer using He-Ne laser with 4.0 mW power at a 532 nm wavelength. Size calculation was based on DLS method as a software protocol. The

scattering light was collected at an angle of 90º through fiber optics and converted to an electrical signal by an avalanche photodiode array (APDs). All samples were sonicated and run in triplicate with the number of runs set to 5 and run duration set to 10 seconds**.**

In addition, the mean particle size of CS, 4-CBS-CS conjugates, ACZ immobilized CS and ACZ immobilized onto 4-CBS-CS conjugates was also determined from the scanning electron micrographs, in which the diameters of 100 randomly selected particles were measured by digital software. The averaged particle size determined by SEM was reported as the size of 'dry' particles.

3.3.8.2.3 Zetapotential

Zeta potential of CS, 4-CBS-CS conjugates, and ACZ immobilized onto CS and 4-CBS-CS conjugates particles were determined using particle sizer. The analysis was performed at a scattering angle of 90^{o}. All samples were sonicated and run in triplicate with the number of runs set to 5 and run duration set to 10 seconds**.**

3.3.8.2.4 Fourier transformed infrared spectroscopy (FT-IR)

The obtained CS, 4-CBS-CS conjugates, and ACZ immobilized onto CS and 4-CBS-CS conjugates particles were used for the FT-IR analysis first was dried and ground into a powder form. The dried sample particles were mixed with potassium bromide (KBr) (1:100) to the power in agate mortar and pestle. The mixture was then transferred to a hydraulic pressing machine and pressed into a disc. Analysis was performed on an FT-IR spectrometer (Perkin Elmer Spectrum RX-1 FT-IR system). The sample was scanned from wavenumbers of 400 to 4400 cm^{-1}.

3.3.8.2.5 Differential scanning calorimetry (DSC)

Approximately 3-6 mg of CS, 4-CBS-CS conjugates, ACZ immobilized CS and ACZ immobilized onto 4-CBS-CS conjugates particles were weighed in the aluminum pan, then crimped with the sealed pan for determinations. And empty pan, sealed in the same way as the sample, was used as a reference. DSC was obtained with NETZSCH DSC 204 under nitrogen atmosphere. The temperature range is 25-320 C° and heating rate of 10 K/min.

3.3.8.3 Study the drug behavior of the particles as prepared by electrospray ionizing technique

3.3.8.3.1 Calibration curve of ACZ

The standard stock ACZ solution was prepared in simulated gastric fluid pH 1.2 and simulated intestinal fluid pH 7.4. ACZ 10 mg was accurately weighed and dissolved in simulated gastric fluid pH 1.2 and simulated intestinal fluid pH 7.4 into 100 ml volumetric flask and adjusted to volume (100 ppm).

The stock ACZ solution was diluted to 1, 10, 20, 30 and 40 ppm with simulated gastric fluid pH 1.2 and simulated intestinal fluid pH 7.4 in volumetric flask.

The absorbance of standard solution was determined by UV-VIS spectrophotometer at 266 and 267 nm, respectively. The simulated gastric fluid pH 1.2 and simulated intestinal fluid pH 7.4 were used as a reference solution. The absorbance and calibration curve of ACZ in simulated gastric fluid pH 1.2 and simulated intestinal fluid pH 7.4 were shown in appendix B and Figure B1 and B2, respectively.

3.3.8.3.2 Encapsulation efficiency

The dried ACZ immobilized onto CS and 4-CBS-CS conjugates particles (2.5 mg) were immersed in 50 ml of simulated gastric fluid pH 1.2 and simulated intestinal fluid pH 7.4. The mixture was stirred at room temperature for 24 hours. After stirring, total drug content entrapped inside the CS and 4-CBS-CS conjugates particles were released in the solution. The solution was collected and determined by UV-VIS spectrophotometer at 266 and 267 nm, respectively.

The actual ACZ content was calculated from calibaration curve of ACZ in simulated gastric fluid pH 1.2 and simulated intestinal fluid pH 7.4.

The encapsulation efficiency was calculated according to the following equation. All experiments were repeated for three times.

$$EE(\%) = \frac{Actual\ drug\ content}{Theoretical\ drug\ content} \times 100\%$$

3.3.8.3.3 *In vitro* drug release

The ACZ release from CS and 4-CBS-CS conjugates particles were studied in simulated gastric fluid pH 1.2 and simulated intestinal fluid pH 7.4 by dialysis bag diffusion technique [54]. The accurately weighed quantities of 2.5 mg particles were enclosed in a dialysis bag with a molecular weight cutoff of 3500 Da and immersed into 10 ml of simulated gastric fluid pH 1.2 and simulated intestinal fluid pH 7.4 in a flask. The flask was placed in a shaken water bath at speed of 50 rounds per minutes and incubated at 37±1 °C.

The 1 ml of medium solution was kept at 0, 5, 10, 20, 30, 45 minutes and 1, 1.5, 2, 3, 4, 6, 8 and 24 hours, respectively and 1 ml of refreshed simulated gastric fluid pH 1.2 and simulated intestinal fluid pH 7.4 was replaced immediately after each sampling.

The release rate of ACZ was determinated by UV-VIS spectrophotometer measured at 266 and 267 nm for in simulated gastric fluid pH 1.2 and simulated intestinal fluid pH 7.4, respectively. All experiments were performed in

triplicates. The amount of ACZ released was calculated by interpolation from a calibration curves containing increasing concentrations of ACZ. The percentages of cumulative ACZ release were calculated from this equation.

$$\%Cumulative\ release = \frac{Amount\ of\ ACZ\ from\ release}{Amount\ of\ ACZ\ before\ release}$$

3.3.9 Statistical analysis

All measurements were performed in triplicate in each experiment. Results are presented as means ± SD. Statistical analysis was performed by one-way ANOVA using Microsoft Excel (Microsoft Corporation) with $P < 0.05$ considered to indicate statistical significance.

CHAPTER IV

RESULT AND DISCUSSION

4.1 Synthesis of 4-CBS-CS conjugates

The covalent attachment of 4-CBS to CS was achieved by the coupling reaction of the primary amine groups (-NH_2) of CS and the carboxylic acid groups (-COOH) of 4-CBS according to the reaction scheme as shown in Figure 4.1. The reaction conditions were investigated and listed in Table 4.1.

The carboxylic acid moieties of 4-CBS were activated by EDAC as a coupling agent to form an *o*-acylurea derivative as an intermediate product. Then, the *o*-acylurea reacts with the primary amine groups of CS to form the amide 4-CBS-CS conjugates.

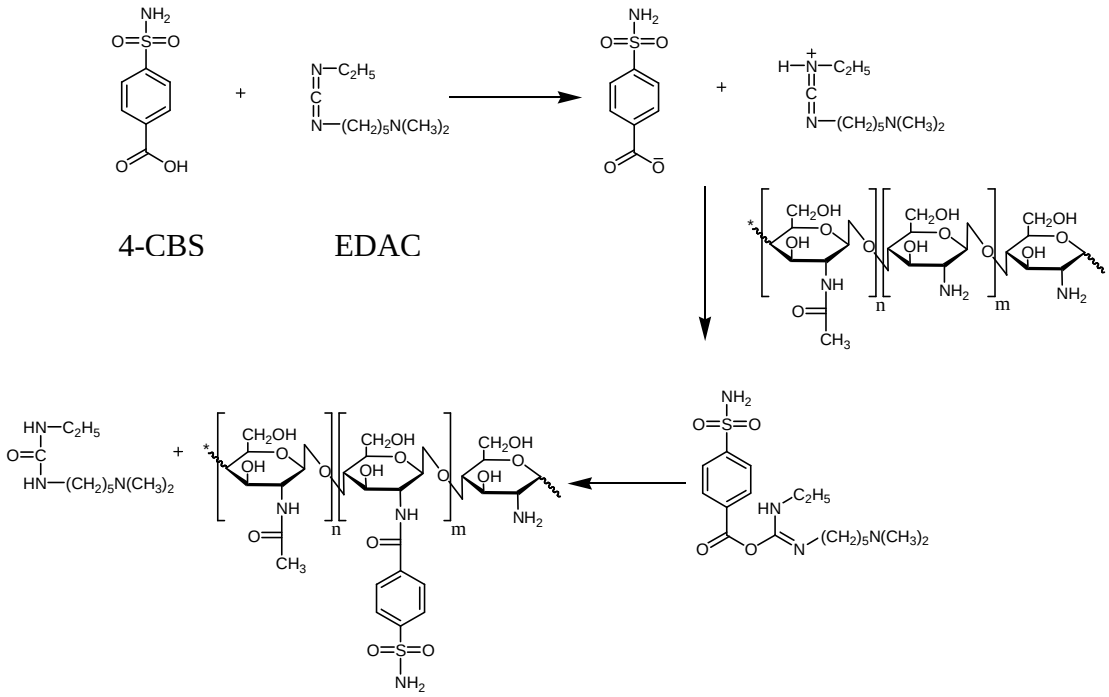

Figure 4.1 Reaction scheme of the covalent attachment of 4-CBS to CS using EDAC as a coupling reagent

Table 4.1 Formulations, weight ratios (w/w) of CS to 4-CBS, degree of substitution (%) and the component of mucoadhesion (cps) of 4-CBS-CS conjugates

Formulation	Weight ratio of CS:4-CBS (w/w)	Degree of substitution (%)[a]	The component of mucoadhesion (η_b)[b]	
			pH 1.2	pH 5.5
F1 (CS)	1:0	-	12.50 ± 1.87	70.73 ± 1.20
F2	1:0.05	1.92 ± 0.02	28.32 ± 3.49	17.35 ± 0.51
F3	1:0.1	5.98 ± 0.02	25.04 ± 3.05	11.44 ± 1.39
F4	1:0.2	10.06 ± 0.02	15.85 ± 2.56	9.35 ± 2.32
F5	1:0.5	17.91 ± 0.81	7.62 ± 0.86	4.23 ± 2.16
F6	1:1	21.42 ± 0.08	9.10 ± 2.26	17.38 ± 0.39

[a] By UV-Vis absorption spectroscopy

[b] By Oswald viscometer

The resulted products, 4-CBS-CS conjugates, appeared as white, odorless fibrous polymer. It is easily dissolved in lactic acid solution and formed as high viscosity pale yellow gel. The obtained 4-CBS-CS conjugates were characterized by ^{1}H-NMR, FT-IR, DSC and TGA.

4.2 Characterization of 4-CBS-CS conjugates

4.2.1 ^{1}H Nuclear Magnetic Resonance Spectroscopy (^{1}H NMR)

The chemical structures of CS, 4-CBS and the 4-CBS-CS conjugates with the different mass ratio were characterized by ^{1}H NMR as shown in Figure 4.2.

The ^{1}H NMR spectrum of CS was shown in Figure 4.2 (a), the signal at 1.77 ppm (s, 3H) was assigned to acetyl proton. A singlet at 2.89 ppm (s, 2H) was attributed to H_2. The signals due to the hydrogen atoms (H_3 – H_6) in the CS ring were observed around 3.43 – 3.48 ppm

The ^{1}H NMR spectrum of 4-CBS was shown in Figure 4.2 (b), the signal at 8.06 ppm (dd, 2H, *J*=8.0 Hz) and 7.89 (dd, 2H, *J*=8.4 Hz) were assigned to H_b+H_c and H_d+H_e, respectively.

The representative ^{1}H NMR spectra of 1:1 4-CBS:CS showed the characteristic peaks of both CS and 4-CBS segments, confirming the formation of 4-CBS-CS conjugates. The proton chemical shifts of sulfonamide residue at 7.66 ppm (dd, 2H, *J*=8.0 Hz) and 7.83 (dd, 2H, *J*=8.0 Hz) were assigned to H_b+H_c and H_d+H_e, respectively. Both *N*-acetyl-D-glucosamine unit and D-glucosamine unit were shown the attributed multiplet peaks region of anomeric carbons (H_3-H_6) from 3.40 to 3.59 ppm. The chemical shift at 1.74 ppm (s, 3H) was assigned to the acetyl proton. These results confirmed that the 4-CBS:CS conjugates were successfully prepared. The ^{1}H-NMR spectrum of another ratio of 4-CBS:CS conjugates are similar to that of the 1:1 ratio.

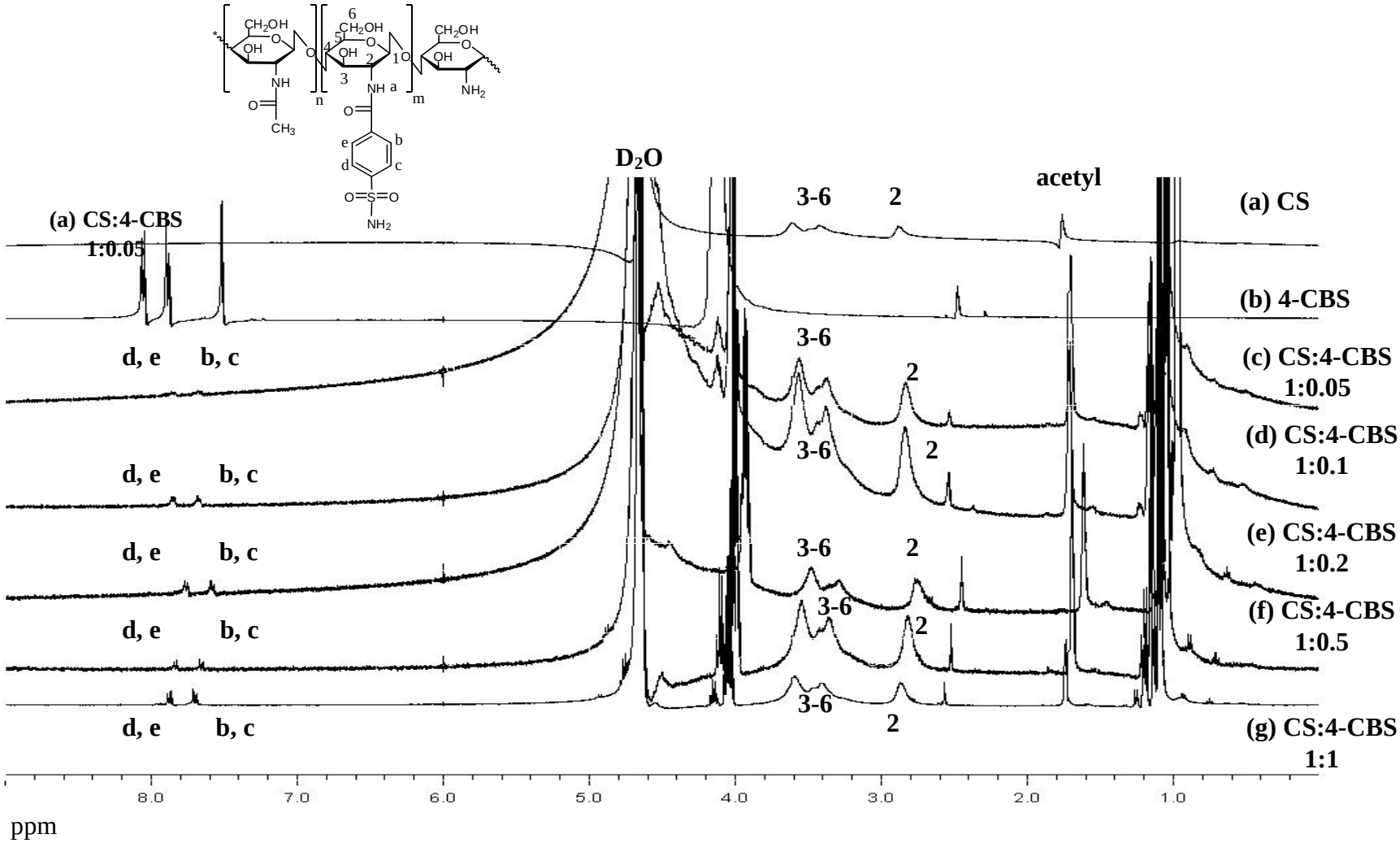

Figure 4.2 ^{1}H NMR spectrum of (a) CS, (b) 4-CBS, and the CS:4-CBS ratio of (c) 1:0.05, (d) 1:0.1, (e) 1:0.2, (f) 1:0.5 and (g) 1:1

Positions	(a) CS		(b) 4-CBS-CS conjugates (1:1)		(c) 4-CBS	
	NMR peak	δ (ppm)	NMR peak	δ (ppm)	NMR peak	δ (ppm)
CH_3-acetyl	s	1.76	s	1.74	-	-
CH_2	s	2.89	s	2.87	-	-
CH_3-CH_6	m	3.43-3.48	m	3.40-3.59	-	-
H_b-H_c	-	-	dd, *J*= 8.0, 8.0 Hz	7.66	-	-
H_d-H_e	-	-	dd, *J*= 7.8, 7.8 Hz	7.83	-	-
H_b-H_c	-	-	-	-	dd, *J*= 8.0, 8.0 Hz	8.06
H_d-H_e	-	-	-	-	dd, *J*= 8.4,8.4 Hz	7.89

4.2.2 Fourier transformed infrared spectroscopy (FT-IR)

FT-IR spectroscopy was used to determine the functional groups of the CS, 4-CBS and 4-CBS-CS conjugates were shown in Figure 4.3.

The FT-IR spectrum of CS was displayed in Figure 4.3 (a). The broad absorption band around at 3446 cm^{-1} was shown the stretching vibration of O-H and N-H bonds. The IR absorption at 2928 cm^{-1} was assigned to $–CH_3$ stretching which indicate that the CS not fully deacetylated. The characteristic of CS peaks were observed at 1659 and 1623 cm^{-1}, corresponding to C=O stretching of amide and N–H bending of amine, respectively.

The FT-IR spectrum of 4-CBS was displayed in Figure 4.3 (b). The 4-CBS spectrum was shown the signals at 3366 and 3263 cm^{-1} related to N–H stretching of primary amine. The presence of absorption at 1695 cm^{-1} was shown C=O stretching of carboxyl groups. The characteristic of 4-CBS peaks were observed at 1342 and 1161 cm^{-1} were attributed to S=O stretching of sulfonyl groups.

The FT-IR spectra of 4-CBS-CS conjugates with different ratio of the polymer were shown in Figure 4.3 (c)-(g). The spectrum of 1:0.05 CS:4-CBS (Figure 4.3(c)) showed the absorption peak at 1723 cm^{-1} corresponding to the C=O stretching of the modified CS. A peak showed at 1627 cm^{-1} was attributed to N–H bending of unmodified CS. These results confirmed that the 4-CBS-CS conjugates were successfully prepared. The FT-IR spectra of the another ratio of CS:4-CBS conjugates are similar to that the 1:0.05 ratio. The spectrum of 1:1 4-CBS-CS (Figure 4.3 (g)), showed the characteristic C=O stretching of unmodified CS unit at 1648 cm^{-1} and C=O stretching of modified unit at 1726 cm^{-1}, possibly indicating that there were still remained the unreacted CS in the product.

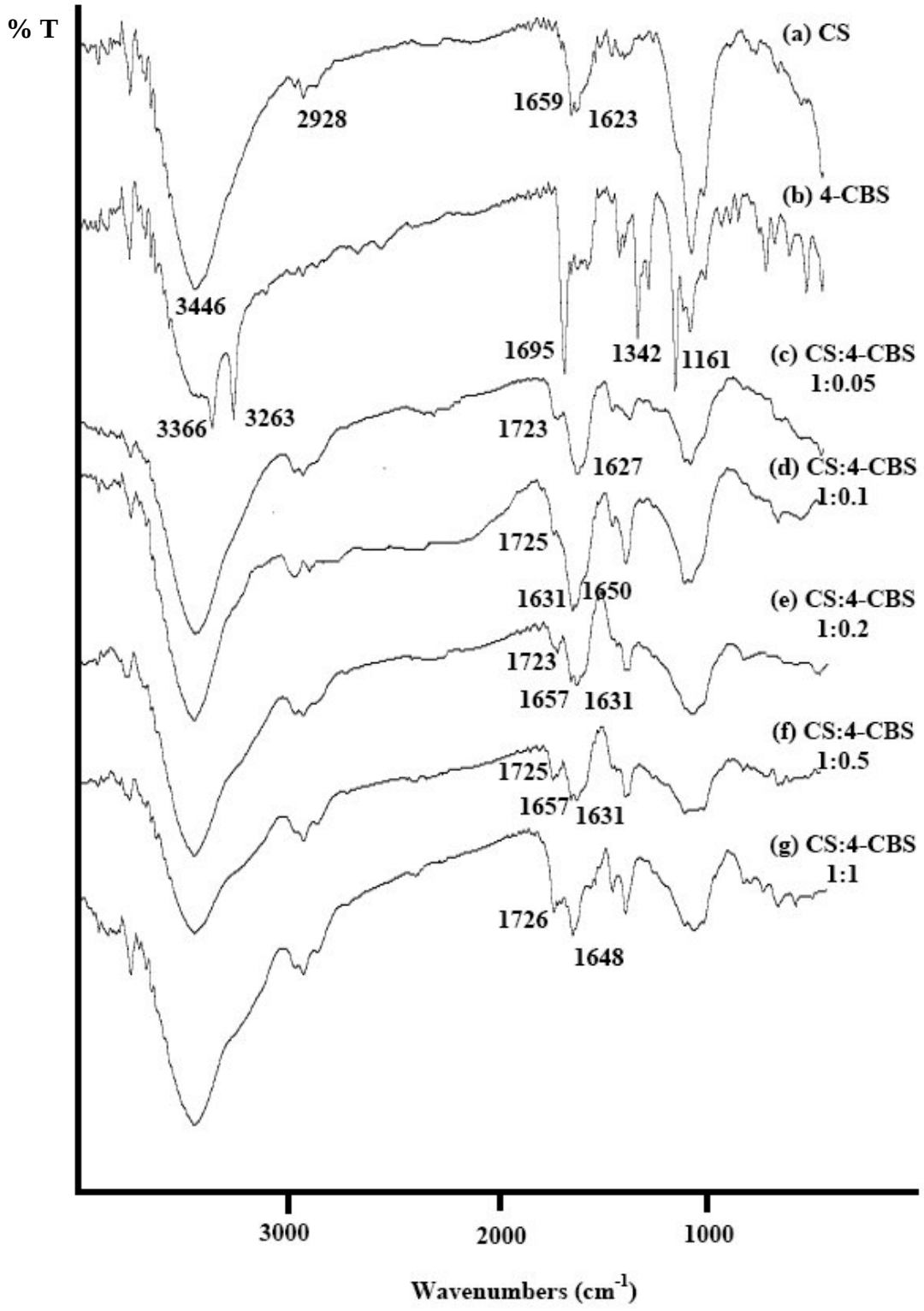

Figure 4.3 IR spectra of (a) CS, (b) 4-CBS and the CS:4-CBS ratio of (c) 1:0.05, (d) 1:0.1, (e) 1:0.2, (f) 1:0.5 and (g) 1:1

4.2.3 Differential scanning calorimetry (DSC)

The DSC thermograms of the CS, 4-CBS and the various ratios of 4-CBS-CS conjugates were shown in Figure.4.4.

The CS thermogram revealed the melting broad peak onset at 108.6^{o}C, Figure 4.4 (a), which represented the melting temperature. Whereas, the exothermic peak was shown at about 300^{o}C may be related to the decomposition of amine units.

The DSC thermogram of 4-CBS, Figure 4.4 (b), showed the melting peak at 284.5^{o}C, indicating the melting temperature of 4-CBS. The exothermic peak was shown at 290.0^{o}C, which is a decomposition temperature of 4-CBS.

The DSC thermograms of the CS:4-CBS conjugates were displayed in Figure 4.4 (c)-(g). The thermogram of 1:0.05 CS:4-CBS (Figure 4.4 (c)) was shown the first melting peak occurred at 171.8^{o}C which is different from the melting peaks obtained from the pure CS (108.6^{o}C) and 4-CBS (284.5^{o}C). The melting peak of 1:0.05 CS:4-CBS was shifted to higher temperature from CS because of chemical interactions between the amine groups of CS and the carboxyl groups of 4-CBS. The second melting peak of the 1:0.05 CS:4-CBS was occurred at higher temperature (278.8^{o}C), representing the melting temperature of an unreacted 4-CBS remained in the 4-CBS-CS product. The DSC thermograms of the another ratio of CS:4-CBS conjugates are similar to the one of the 1:0.05 ratio.

Therefore, the results confirmed that the chemical reactions of CS and 4-CBS resulted in new chemical bonds and hence new modified CS, contributing to the shifting of melting temperature.

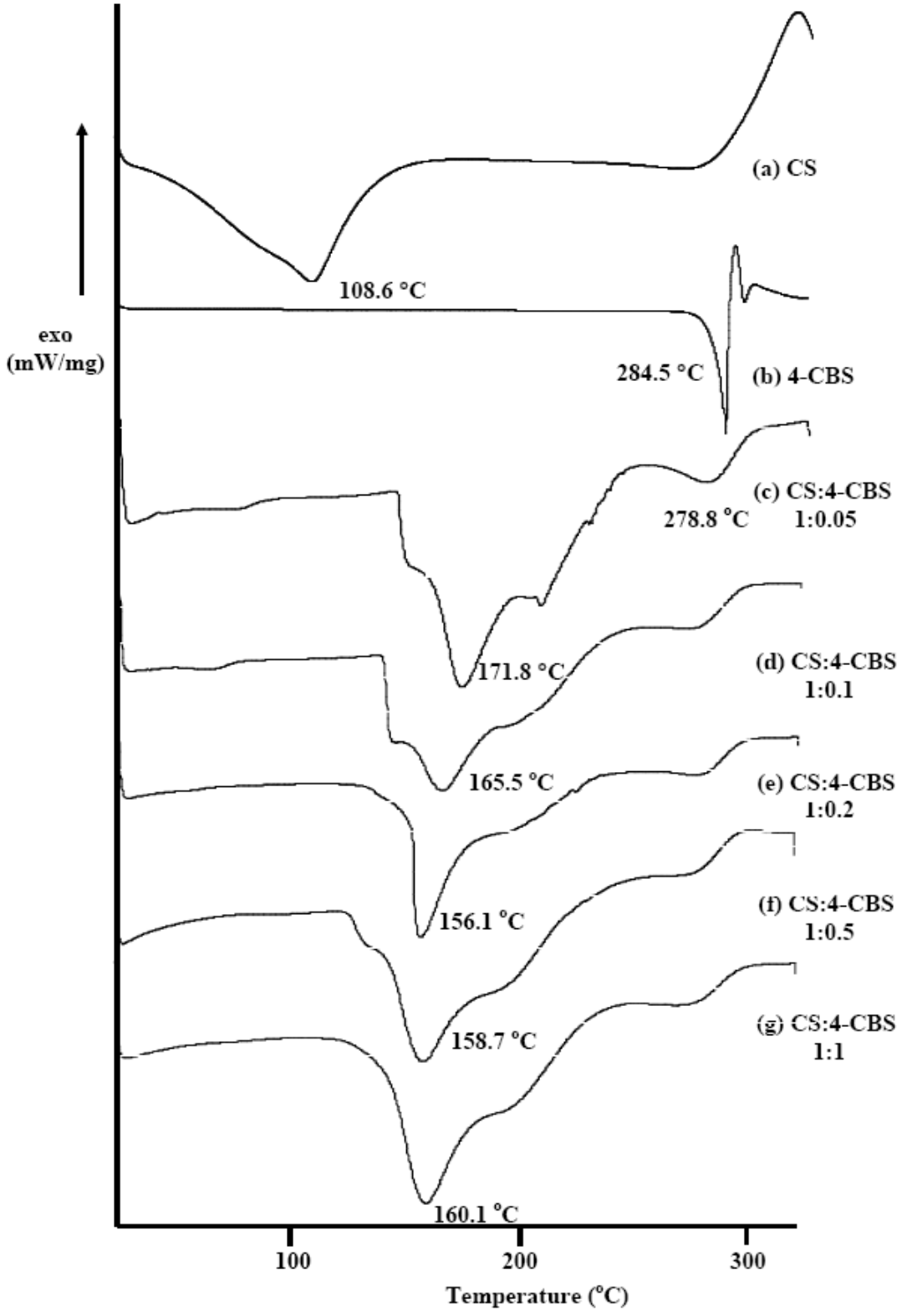

Figure 4.4 DSC thermograms of (a) CS, (b) 4-CBS and CS:4-CBS ratio of (c) 1:0.05, (d) 1:0.1, (e) 1:0.2, (f) 1:0.5 and (g) 1:1

4.2.4 Thermogravimetric analysis (TGA)

The TGA thermograms of the CS, 4-CBS and the various ratios of 4-CBS-CS conjugates were shown in Figure 4.5 and Table 4.3.

In the CS thermogram, Figure 4.4 (a), was revealed a 11.1 % weight loss of water (28.8^{o}C to 177.2^{o}C). Whereas the degradation temperature of CS onset at 274.3^{o}C with the additional derivative thermogravimetric (DTG) peak at 302.1°C, and showed 52.7 % weight loss..

The degradation of 4-CBS was presented, at the onset temperature of 339.3^{o}C with the additional peak of the DTG at 372.0 °C and has 69.6 % weight loss.

The TGA curve of the 4-CBS-CS conjugates showed the in 3 degradation stages. The first stage, the thermogram of 1:0.05 CS:4-CBS was shown an onset temperature at 80.3°C with 10.2 % weight loss of water. The second stage, onset at 162.5^{o}C with 17.9 % weight loss of lactic acid-CS by product. The third stage is dued to the degradation of 4-CBS-CS conjugates. The degradation started at 270.1^{o}C (onset) with the DTG peak at 288.7^{o}C, and presented 43.0 % weight loss. Furthermore, the weight loss temperature in the stage 3 of the 4-CBS-CS increase from 43.0 % to 46.3 % when increasing the content of 4-CBS onto CS polymeric chain. This might be attributed to chemical bonding between the amine groups (-NH_2) of CS and the carboxyl groups (-COOH) of 4-CBS. The TGA thermograms of another ratios of CS:4-CBS conjugates are similar to the one of the 1:0.05 ratio. The results were also consistent with the degree of substitution of 4-CBS onto CS (explained in the next section).

Table 4.3 Thermogravimetric analysis of CS, 4-CBS and the different ratio of CS-4-CBS conjugates

Composition	Temperature range (°C)	Weight loss (%)	DTG peak (°C)
CS	28.8-177.2 158.2-600.0	11.1 52.8	95.0 302.1
4-CBS	125-600	69.6	372.0
1:0.05 CS:4-CBS	30.2-124.3 124.2-223.1 223.3-432.4	10.2 17.9 43.0	80.3 178.4 288.7
1:0.1 CS:4-CBS	37.5-133.3 134.2-231.3 231.6-406.1	10.0 19.4 40.2	85.6 191.3 282.4
1:0.2 CS:4-CBS	33.5-123.3 123.2-232.1 232.4-408.7	9.3 25.5 37.7	79.3 188.5 284.2
1:0.5 CS:4-CBS	31.8-120.3 120.2-220.5 220.2-447.5	9.0 21.1 42.7	72.5 182.3 280.7
1:1 CS:4-CBS	37.8-138.6 138.4-219.3 219.2-419.1	9.4 15.2 46.3	84.2 186.3 270.4

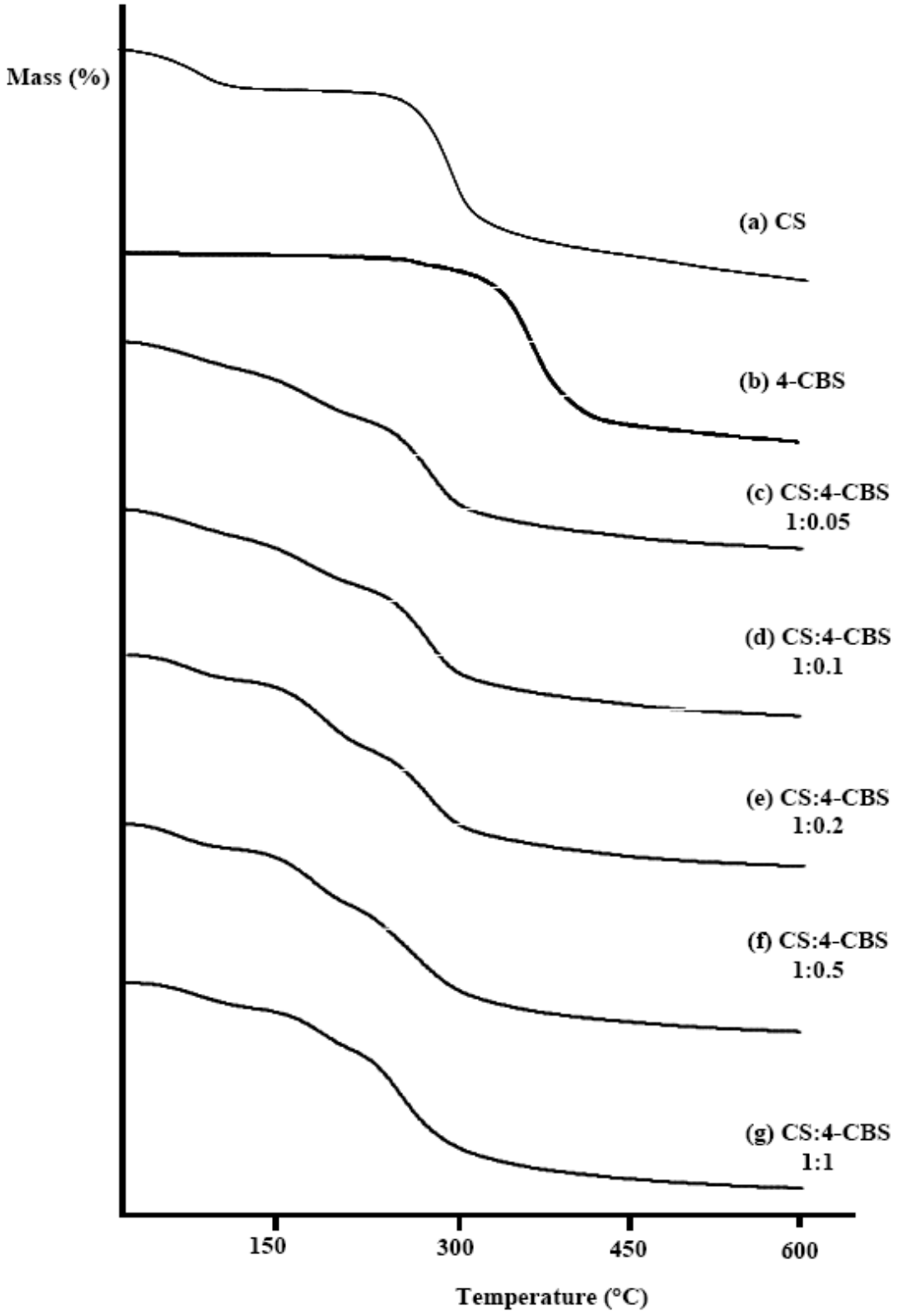

Figure 4.5 TGA thermograms of (a) CS, (b) 4-CBS and CS:4-CBS ratio of (c) 1:0.05, (d) 1:0.1, (e) 1:0.2, (f) 1:0.5 and (g) 1:1

4.3 Determination of chitosan substitution degree by UV-Vis absorption spectroscopy

The degree of substitution of 4-CBS was analysed by UV-Vis spectrophotometer and shown in Figure 4.6 and Table 4.1. Calibration standard curve was displayed linear relationship between the concentrations of 1-30 ppm of 4-CBS in 1% (v/v) lactic acid aqueous solution and gave the maximum absorbance at 234 nm. Calibration standard equation is $y = 0.0822x - 0.0649$, $r^2 = 0.9958$.

The concentration of 4-CBS in 4-CBS-CS conjugates can be obtained by rearranging equation of 4-CBS standard calibration curve shown above when know absorbance values. A slightly shift of absorption wavelength from 234 to 228 nm was observed for the conjugates.

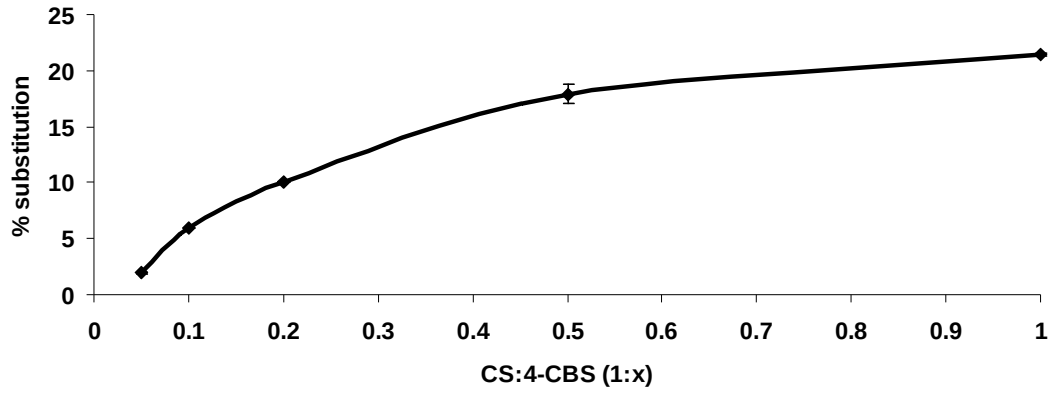

Figure 4.6 Degree of substitution of 4-CBS-CS conjugates at different ratio of CS:4-CBS

The results showed that the degree of substitution of 4-CBS onto CS were in the range of 1.9 to 21.4 % for the CS:4-CBS of 1:0.05 to 1:1. The degree of substitution of 4-CBS-CS conjugates increased with increasing of 4-CBS contents in the 4-CBS-CS conjugates, relative with sulfonamide groups increased.

4.4 Determination mucoadhesive of 4-CBS-CS conjugates

The viscosity of 4-CBS-CS conjugates is an important factor to mucoadhesive properties. Because the mucoadhesion has advantage, for example, increasing the localization at target site, a prolonged residence time at the site of drug absorption and intensified contact with the mucosa increasing the drug concentration gradient. Tobyn et al. reported that increasing the molecular mass of polymer leading to the higher internal cohesive of the molecule that consequently increases the mucoadhesion. Therefore, in this work, the mucoadhesion of the difference ratios of CS to 4-CBS with mucin were investigated under the stimulated gastric fluid (pH 1.2) and the phosphate buffer pH 5.5 (skin pH). Mucoadhesive property is the action of ionic interactions between polymer and mucin. When ionic interactions of polymer and mucin increased, the mixture viscosity was increased and exhibited good mucoadhesive properties. Therefore, the component of mucoadhesion was related to the mucoadhesive force between the interesting polymer and mucin as mentioned in the experimental section.

The component of mucoadhesion of CS and the 4-CBS-CS conjugates under the stimulated gastric fluid (pH 1.2) and the phosphate buffer pH 5.5 (skin pH) were shown in Figure 4.7 and Table 4.1.

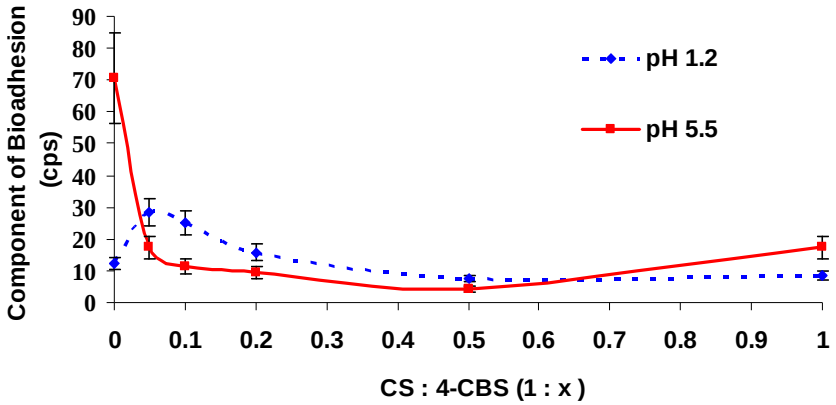

Figure 4.7 The component of mucoadhesion (cps) of 4-CBS-CS conjugates in pH 1.2 and 5.5

Mucoadhesive property of CS and the 4-CBS-CS conjugates in simulated gastric fluid pH 1.2

At pH 1.2, CS showed the component of mucoadhesion at 12.50 cps. The 1:0.05 CS:4-CBS showed the highest component of mucoadhesion at 28.32 cps. However, when there were more 4-CBS content onto CS polymeric chain, the component of mucoadhesion were lower expect to CS and 1:0.05 CS:4-CBS.

This is probably due to the carboxylic acid groups from terminal sialic acid will be unionized at low pH, so the force of interaction is not solely due to ionic interactions. The interactions of polymer with mucin appear to be both electrostatic and hydrophobic interactions. For electrostatic effect, the NH_3^+ groups on polymer interact with either the COO^- or SO_3^- groups on the mucin carbohydrate side chain. For the hydrophobic effect, the $-CH_3$ groups on polymer residue interact with the $-CH_3$ groups on the mucin side chains. At the ratio of 1:0.05 CS:4-CBS, the degree of substitution of 4-CBS was minimum, the remained $-NH_3^+$ groups of CS were maximum, so that the component of mucoadhesion were maximum. At the higher ratios of 1:0.1 and 1:0.2 of CS:4-CBS, they had higher components of mucoadhesion than that of the CS but less than the 1:0.05 ratio. This was consistent with the degree of substitutions, when the degree of substitution of 4-CBS increased, the $-NH_3^+$ groups of polymer were decreased. So that when increase the CS:4-CBS ratio to 1:0.5 and 1:1, the component of mucoadhesion were decreased. This also implied that the mucoadhesive forces between the 4-CBS-CS and mucin at the higher ratios of 4-CBS will be dominated by hydrophobic interactions.

From these results suggested that the most suitable mucoadhesion 4-CBS-CS polymer using for mucoadhesive drug delivery system in the stomach condition is 1:0.05 CS:4-CBS.

Mucoadhesive property of CS and the 4-CBS-CS conjugates in phosphate buffer pH 5.5 (skin pH)

At phosphate pH 5.5, CS showed the component of mucoadhesion at 70.73 cps. All ratios of CS:4-CBS showed the component of mucoadhesion in the range about 17.35 to 4.32 cps which were lower than that of CS.

The mucoadhesive property of CS in pH 5.5 was higher than that of in pH 1.2, because the sialic acid of mucin was in the anion form, hence more ionic attractions with CS, resulted in more mucoadhesive force. However, the modified CS with 4-CBS exhibited lower mucoadhesive properties than that of the native CS because the $-NH_3^+$ groups of CS were decreased.

This may indicated that the 4-CBS-CS was more suitable as a mucoadhesive polymer in an acidic condition rather than in the pH 5.5 condition.

4.5 Swelling behavior of CS and 4-CBS-CS conjugates

The swelling behavior indicates the easiness and the speed of liquid able to penetrate into a polymer matrix as an essential step for drug release. The swelling behavior of mucoadhesive polymers also has a great influence on their adhesive properties, water-uptake, drug release and stability. The rapid swelling behavior of mucoadhesive polymers may improve an inter-diffusion process between the polymer and the mucus layer, providing a strong adhesion and then leading to enhance drug delivery rate.

In this experiment, the equilibrium swelling behavior of the 4-CBS-CS at the weight ratio of CS:4-CBS at 1:0.5 and 1:1 could not be measured, because they were completely dissolved within 15 minutes. So only the swelling behavior of CS:4-CBS at the weight ratio of 1:0.05, 1:0.1 and 1:0.2 were studied for 24 hours.

In order to investigate the possibility for using as a drug delivery system in a general condition and in the gastrointestinal tract, the swelling behavior of the different mass ratios of CS to 4-CBS were observed in water, the simulated gastric fluid (pH 1.2) and simulated intestinal fluid (pH 7.4).

4.5.1 The swelling behavior of the CS:4-CBS in water

Figure 4.8 showed the swelling behavior in water of the various mass ratios of CS:4-CBS. The CS gave lower swelling ratio than that of the modified CS. The swelling behavior of CS in water depended mainly on the difference between osmotic pressures inside and outside the CS specimens.

The 1:0.05 CS:4-CBS swelled rapidly in water within 1 hour with the swelling ratio of 1.56 times expect to the CS, and continued to swell gradually to 2.66 times within 24 hours. The modified chitosan can swell more than the CS. This was probably because the 4-CBS prevented the intermolecular interactions between the $–NH_2$ groups of CS, so more water can penetrate into polymeric networks and then increased degree of swell. Furthermore, the swelling ratio increased as the amount of 4-CBS grafted onto CS chains increased. However, when the weight ratios of CS:4-CBS arised to 1:0.5 and 1:1, the modified polymers were completely dissolved in

water within 1 hour. The dissolution mechanism may be related to the higher content of the aromatic sulfonamide groups grafted onto CS, leading to more steric effects that prevented the intermolecular interactions of the $–NH_2$ groups of CS.

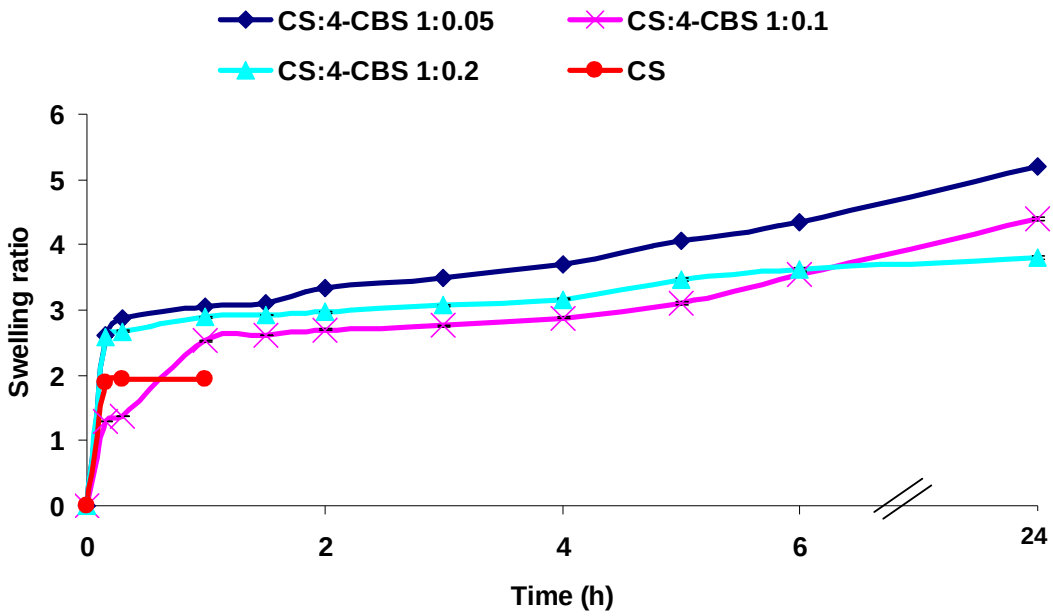

Figure 4.8 Swelling behaviors of the different ratios of CS:4-CBS in water

4.5.2 The swelling behavior of 4-CBS-CS in the simulated gastric fluid (SGF) (pH 1.2)

Figure 4.9 showed the swelling behavior of the different mass ratios of CS:4-CBS in the simulated gastric fluid (pH 1.2).

The first hour, the 1:0.05 CS:4-CBS gave the swelling ratio of 1.77 times of that of the CS. It was continued swelled to reach the swelling ratio of nearly 6 times, based on the dried state. The 1:0.05 CS:4-CBS was more swelled in the SGF than that of the one in water. However, the swelling property decreased with the increased of the degree of substitution.

In acidic medium, the $–NH_2$ groups are protonated to the $-NH_3^+$ groups and hydrogen bonds were dissociated, as induces the network to become loose, leading to increased degree of swelling. This causes the repulsion among polymer chain which

allows more water and simulated intestinal pH 7.4, so at pH 1.2 is more swelling degree than pH 7.4 about 1.2-1.5 times.

The results suggested that the 1:0.05 CS:4-CBS is preferred to use as a drug delivery system in the SIF condition, because the polymer can gradually swell within 24 hours without dissolution.

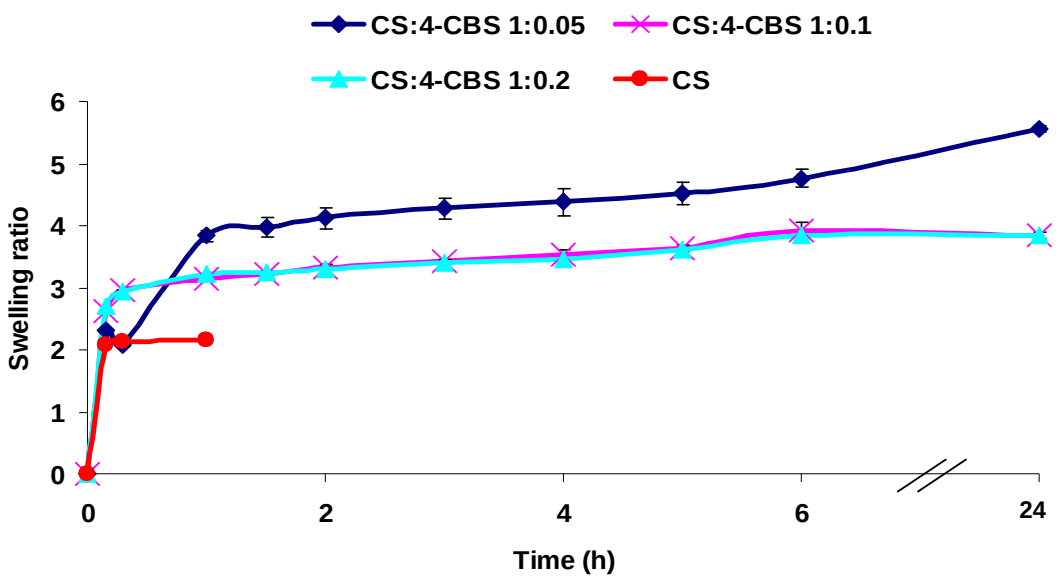

Figure 4.9 Swelling behavior of the different ratios of CS:4-CBS in simulated gastric fluid pH 1.2

4.5.3 The swelling behavior of 4-CBS-CS in simulated intestinal fluid (SIF), pH 7.4

Figure 4.10 showed the swelling behavior of the different ratios of CS:4-CBS in the simulated intestinal fluid (SIF), pH 7.4. The CS gave lower swelling ratio than that of the modified CS and easily dissolved within 1 hour.

The 1:0.05 CS:4-CBS gave the swelling ratio of 1.65 times with respect to the CS at 1 hour and still continued swelled to 2.57 times within 24 hours, based on the CS.

In an alkali medium, the -NH_3^+ was deprotonated to the –NH_2 groups and the hydrogen bonds were re-associated, and consequently causing the degree of swelling were decreased. The results were consistent with the reported behavior of the CS and also consistent with the swelling ratios of CS and the modified 4-CBS-CSs in the SIF pH 7.4 lower than that of in the SGF pH 1.2.

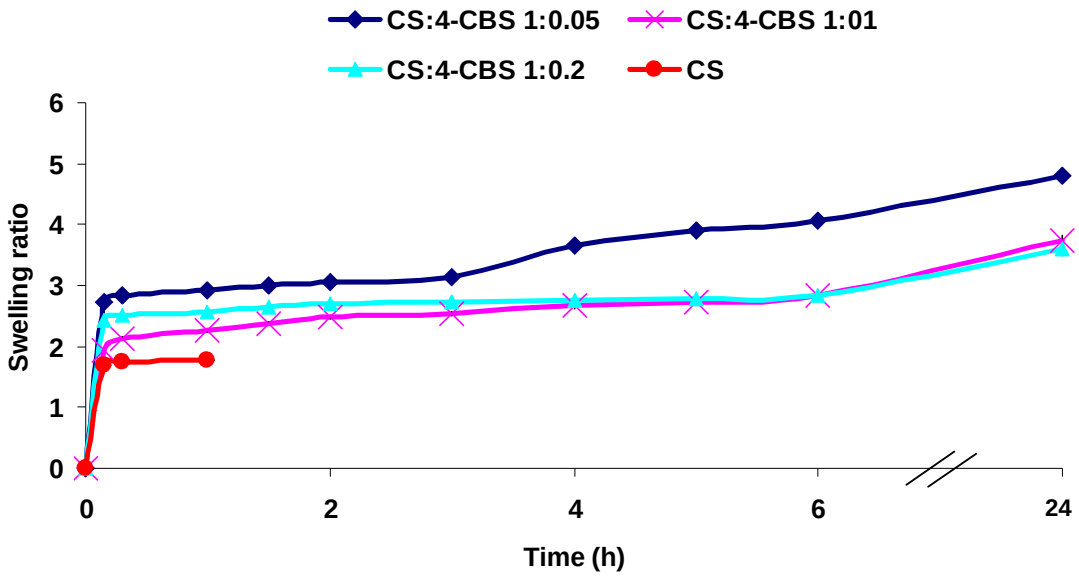

Figure 4.10 Swelling behavior of the different ratios of CS:4-CBS in the simulated intestinal fluid (pH 7.4)

It can be concluded that the swelling behavior of the 4-CBS-CSs depended on the pH of the medium and the compositions of polymeric matrix. Moreover, the pH-dependent variations of the degree of swelling for CS and the 4-CBS-CSs were closely related to the association and dissociation of hydrogen bonds. In lower pH, the swelling degree was maximum because of the protonation of the –NH_2 in the CS polymeric chains to be the –NH_3 groups.

4.6 Cytotoxic activities of the 4-CBS-CS (1:0.05 CS:4-CBS)

In this research, the cytotoxic activities of 4-CBS-CS conjugates were evaluated to investigate the cytotoxicity against the normal primate cell line (Vero cells) and the three anti-cancer cell lines; KB cell line (epidermoid carcinoma of oral cavity), MCF-7 cell line (breast adenocarcinoma) and NCL-H187 (small cell lung carcinoma).

Table 4.4 The cytotoxic activity of 4-CBS-CS conjugates against the Vero, KB, MCF-7 and NCL-H187.

Compound	Cytotoxicity			
	Vero cell	KB	MCF7	NCI-H187
4-CBS-CS (1:0.05)	Non-toxic	Inactive	Inactive	Inactive

The results showed that the 4-CBS-CS conjugate was non-toxic to the Vero cell line and showed inactive cytotoxicity against all the three anti-cancer cell lines. This is implied that the 4-CBS-CS conjugate is biocompatible to human. Furthermore 4-CBS-CS conjugates can to be applied together with anti-cancer drug delivery system.

4.7 Inhibition of 4-CBS-CS conjugates against *E.coli* and *S. aureus* bacteria

The inhibition of 4-CBS-CS conjugates against *E.coli* (Gram-negative) and *S. aureus* (Gram-positive) bacteria by agar diffusion methods were shown in Figure 4.10 and Table 4.5.

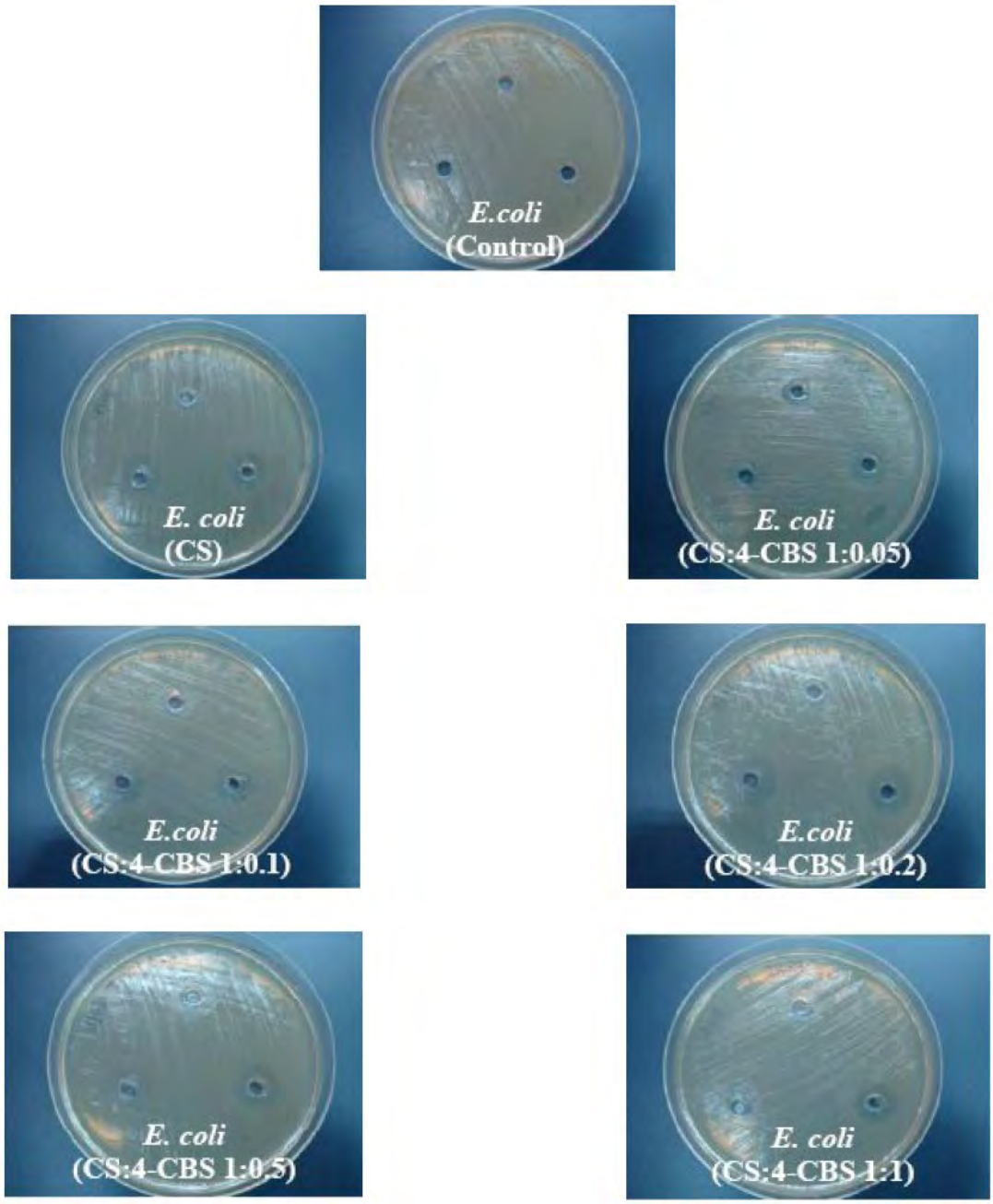

Figure 4.11 Inhibition clear zones of 1:0.05 4-CBS-CS conjugates against *E.coli*

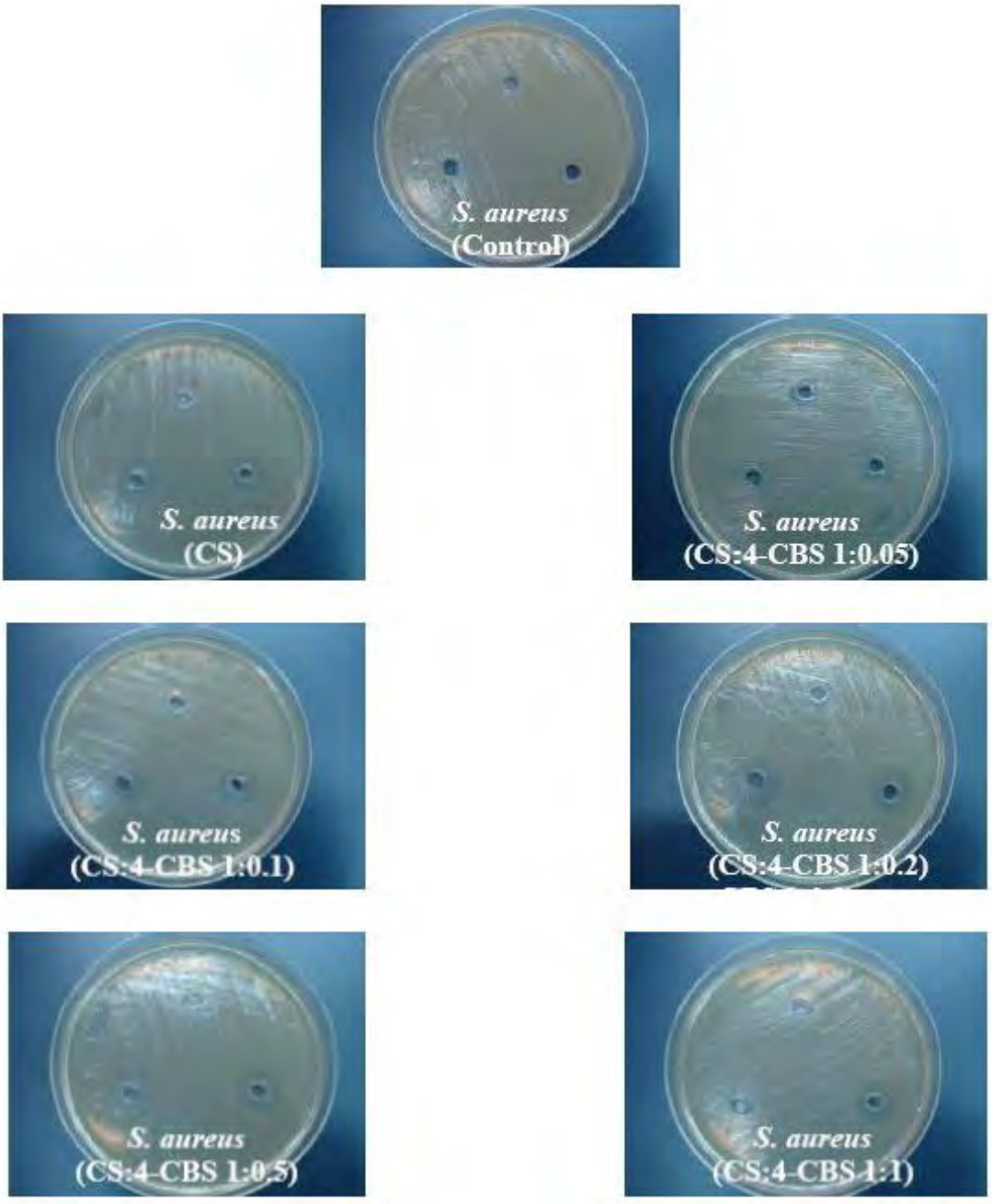

Figure 4.12 Inhibition clear zones of 1:0.05 4-CBS-CS conjugates against *S. aureus*

Table 4.5 Diameters of the wall from the inhibition of 4-CBS-CS conjugates against bacteria

Formulation	*E.coli*	*S. aureus*
Control (1% lactic acid)	0.50 ± 0.00	0.50 ± 0.00
CS	0.60 ± 0.00	0.63 ± 0.06
1:0.05 CS:4-CBS	0.90 ± 0.00	0.90 ± 0.00
1:0.1 CS:4-CBS	0.86 ± 0.06	0.90 ± 0.00
1:0.2 CS:4-CBS	0.90 ± 0.00	0.80 ± 0.00
1:0.5 CS:4-CBS	0.72 ± 0.03	0.77 ± 0.12
1:1 CS:4-CBS	0.70 ± 0.00	0.63 ± 0.06

1% lactic acid as a control can not inhibit both *E.Coli* and *S.aureus* with diameter of well 0.05 cm. The CS can inhibit both *E.Coli* and *S.aureus* with diameter of well 0.060 and 0.63 cm., respectively. The CS:4-CBSs showed the stronger inhibition against both *E.Coli* and *S.aureus* than that of the CS.

Conclusion

The CS:4-CBS 1:0.05 is the optimum ratio for futher studies as a drug delivery system. Because it showed higher mucoadhesive property in pH 1.2, moreover it also had a good swelling property and resistance in an acidic condition. In addition, it is non-toxic to human body and has antibacterial activity against *E.coli* and *S.aureus*.

4.8 Immobilization of ACZ on CS and 4-CBS-CS conjugates

Immobilization of ACZ onto CS and 4-CBS-CS were prepared in the form of microspheres using electrospray technique.

The electrospray parameters used are as follows: needle guage of 26 g, applied voltage of 10 kV, pump flow rate of 2.5 ml/hours and distance between the needle tip and negative electrode of 10 cm.

4.8.1 Characterization ACZ loaded CS microspheres and ACS loaded 4-CBS-CS microspheres

4.8.1.1 Scanning electron microscope (SEM)

The morphology of the CS, 4-CBS-CS, ACZ loaded CS and ACZ loaded 4-CBS-CS microspheres, such as size, shape and surface topography were investigated by scanning electron microscopy (SEM) under the same electrospray condition.

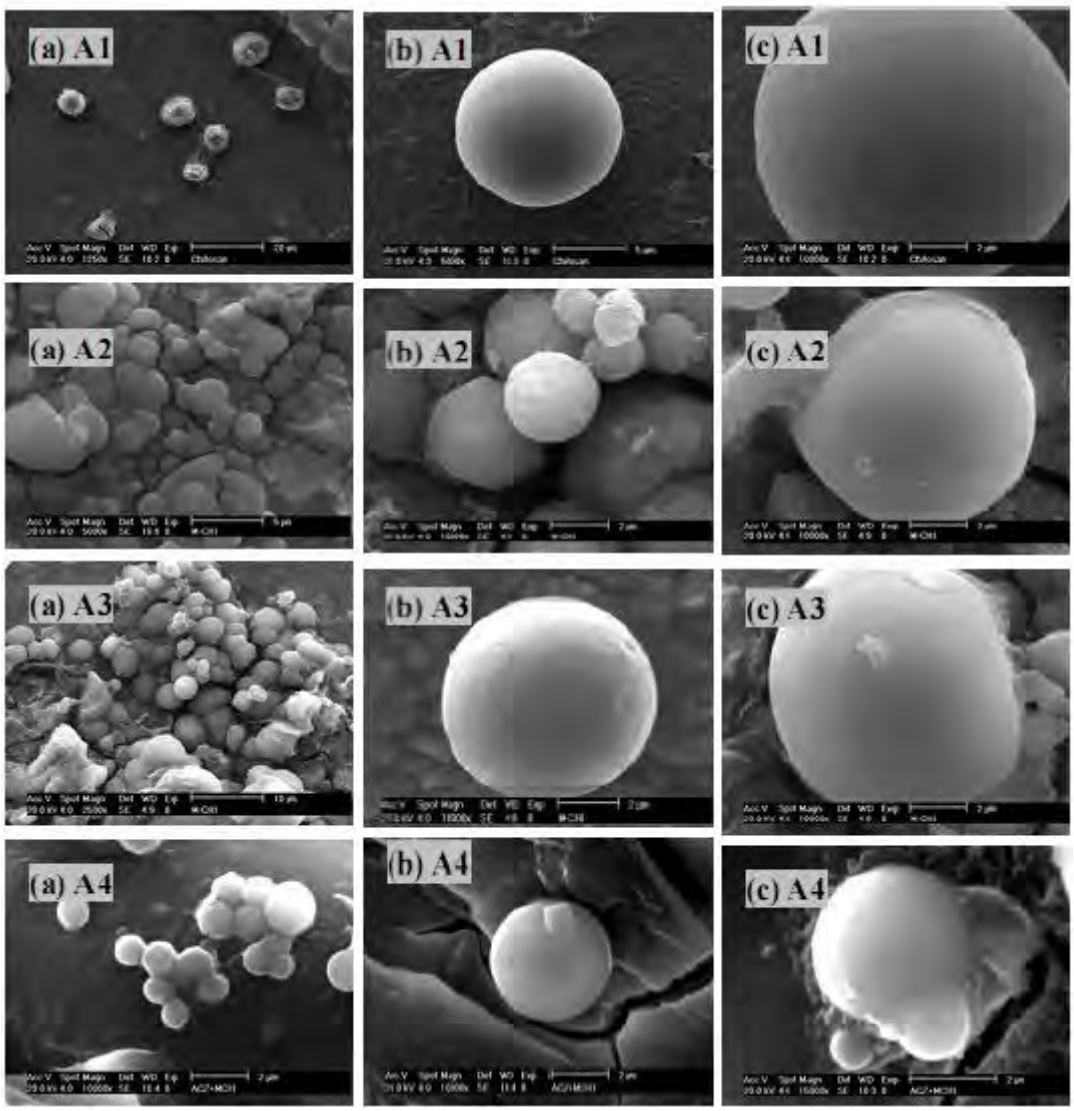

Figure 4.13 Scanning electron micrographs of microsphere CS (A1), 4-CBS-CS conjugates (A2), ACZ loaded CS (1:1 ACZ:polymer) (A3) and ACZ loaded 4-CBS-CS (1:1 ACZ:polymer) (A4): (a) microsphere overviewed (x1000), (b) and (c) surface of microspheres at the magnitude of 10,000x and 15,000x, respectively.

Figure 4.13 showed the surface morphological appearance of CS compared to that of 4-CBS-CS. The diameter sizes of microspheres in TPP/NH_3OH solution were measured by nanosizer and given in Table 4.5. The particle sizes in the dried state of 4-CBS-CS without drug observed from SEM were smaller than that of

CS. The ACZ loaded microspheres showed an increase in particles size. These size increments are mainly affected to viscosity of each microsphere. Incorporation of drug into the polymer becomes higher viscosity which causes a decrease in the microsphere size. In addition, smoothness on the surface could be clearly seen at all formulation expect ACZ loaded CS and 4-CBS-CS. ACZ loaded in CS had rough surface because most of ACZ absorbed onto their surface. Whereas, in case of ACZ containing 4-CBS-CS microsphere, the surface of some exhibited smooth feature that was possibly related to the incorporated ACZ can be absorb into the microsphere completely. Upon detailed observation, it was found that not all possessed this distinct smooth surface.

Table 4.6 Effect of composition on morphology of the microsphere

Formulation	Abbreviations	Shape	Bead size ± SD (μm) by nanosizer	Zetapotential (mV)	Polydispersity (PDI)
A1	CS	Spherical	7.89 ± 0.67	-5.11 ± 0.99	0.53
A2	4-CBS-CS	Spherical	6.87 ± 0.42	-6.57 ± 1.99	0.60
A3	ACZ + CS (1:1)	Spherical	2.43 ± 0.31	-9.52 ± 1.21	0.54
A4	ACZ + 4-CBS-CS (1:1)	Spherical	3.06 ± 0.59	-8.95 ± 2.50	0.46

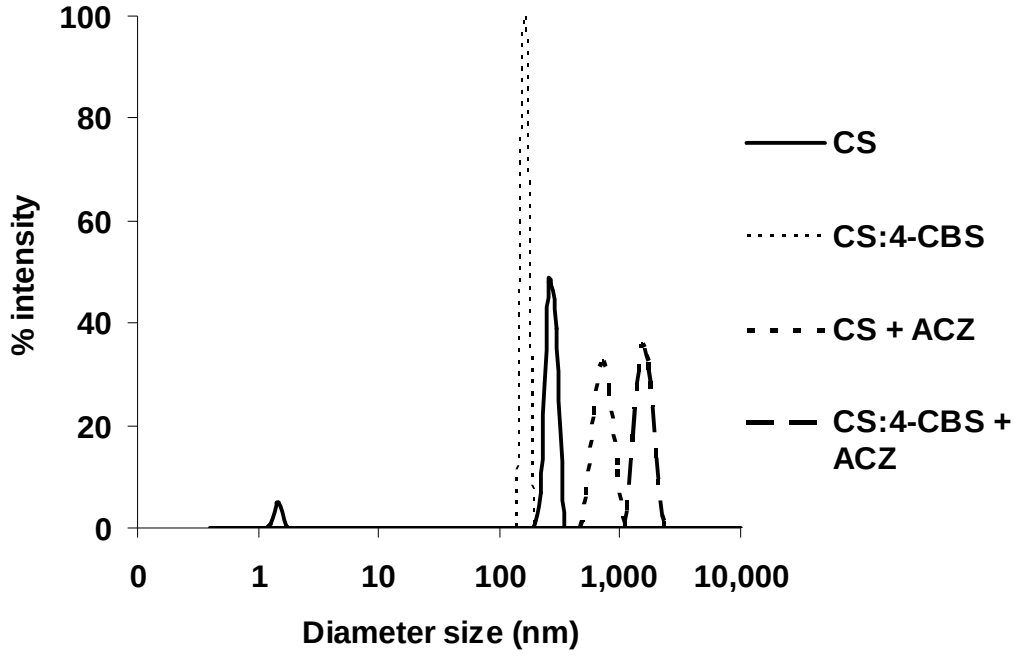

Figure 4.14 Size distributions of microspheres measured by nanosizer

Figure 4.14 showed the size distribution of CS and 4-CBS-CS microspheres both before and after loaded ACZ. The size distributions were narrow for all of formulations. Moreover, it was clearly shown that the size distributions were mono-dispersion for all formulations, excepted for that of the CS. The results can be implied that the 4-CBS-CS may be used for fabricating drug delivery systems due to the monodispersed microsphere form. After the incorporation of the drug into the 4-CBS-CS particles, the obtained microspheres still showed the narrow and monodispersed size distribution. The results suggested that the nanoparticles could be obtained by varying the electrospray parameters, such as concentration of polymer solution, applied voltage or the working distance.

4.8.1.2 Fourier transformed infrared spectroscopy (FT-IR)

FT-IR spectroscopy was used to determine the functional groups of CS, 4-CBS-CS, ACZ and ACZ loaded polymer microspheres were shown the spectrum in Figure 4.15.

The FT-IR spectrum of CS microsphere was displayed in Figure 4.15 (a). The broad absorption band around at 3442 cm^{-1} was shown the stretching vibration of O-H and N-H bonds. The IR absorption at 2925 cm^{-1} was assigned to $–CH_3$ stretching which indicate that the CS not fully deacetylated. The characteristic of CS peaks were observed at 1657 and 1624 cm^{-1}, corresponding to C=O stretching of amide and N–H bending of amine, respectively.

The FT-IR of 4-CBS-CS microsphere was displayed in Figure 4.15 (b). The broad absorption band around at 3446 cm^{-1} was shown the stretching vibration of O-H and N-H bonds. The IR absorption at 2929 cm^{-1} was assigned to $–CH_3$ stretching which indicate that the CS not fully deacetylated. The spectrum of 4-CBS-CS was shown the characteristic C=O stretching of modified unit at 1704 cm^{-1} responding to ACZ loaded 4-CBS-CS (Figure 4.15 (e)), C=O stretching of unmodified CS unit at 1657 cm^{-1} and N–H bending of amine of unmodified CS at 1628 cm^{-1} .

The FT-IR spectrum of CS and 4-CBS-CS conjugates microsphere in Figure 4.15 (a) and (b) were different from CS and 4-CBS-CS conjugates in Figure 4.3 (a) and (c) because they crosslinked with tripolyphosphate (TPP).

The FT-IR spectrum of ACZ was displayed in Figure 4.15 (c). The signals at 3388 and 3337 cm^{-1} related to -N–H stretching of secondary amine. The presence of absorption at 1701 cm^{-1} was attributed to C=O stretching of carboxyl groups. The characteristic peaks of ACZ were observed at 1344 and 1169 cm^{-1} were attributed to S=O stretching of sulfonyl groups.

The FT-IR spectrum of ACZ loaded CS was displayed in Figure 4.15 (d). The spectrum showed the absorption peaks at 1659 cm^{-1} corresponding to the C=O stretching of the CS. A peak showed at 1633 cm^{-1} was attributed to N–H bending of unmodified CS. The characteristic peaks of ACZ were observed at 1171 cm^{-1} were attributed to S=O stretching of sulfonyl groups. These results confirmed that the 4-CBS-CS conjugates were successfully prepared and the spectrum did not show the peak

around 1342 cm^{-1} because the encapsulation efficiency (%EE) was low so the CS shell was appeared only.

The FT-IR spectrum of ACZ loaded 4-CBS-CS conjugates was displayed in Figure 4.15 (e). The spectrum showed the absorption peaks at 1700 cm^{-1} corresponding to the C=O stretching of the modified CS. The characteristic peaks of ACZ were observed at 1340 and 1170 cm^{-1} were attributed to S=O stretching of sulfonyl groups. These results confirmed that the 4-CBS-CS conjugates were successfully prepared and the spectrum showed the peak around 1340 cm^{-1} because the encapsulation efficiency (%EE) was high so ACZ was appeared.

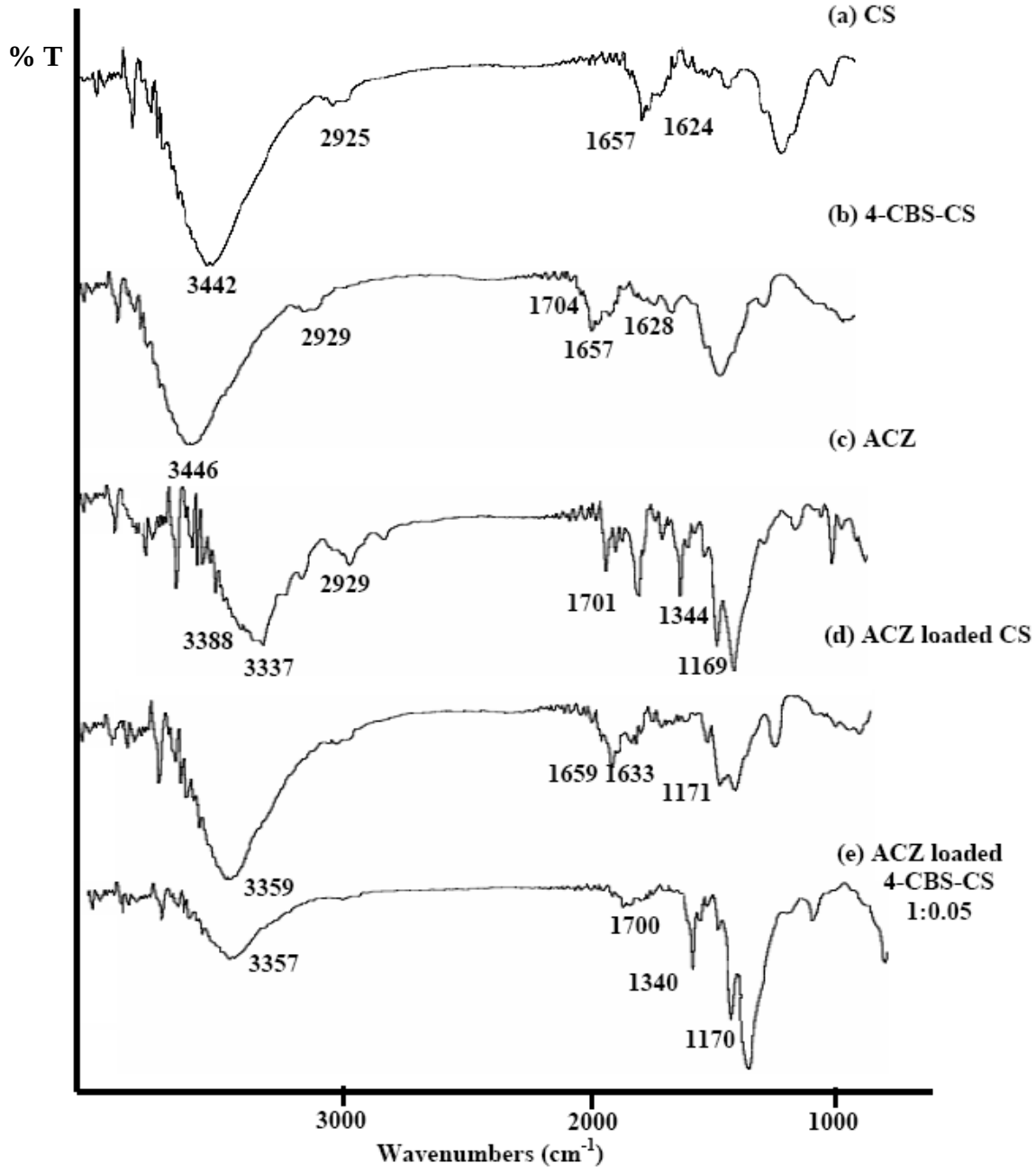

Figure 4.15 IR spectra of microspheres of (a) CS (A1), (b) 4-CBS-CS (A2), (c) ACZ (d) ACZ loaded CS (A3) and (d) ACZ loaded 4-CBS-CS (A4)

4.8.1.3 Differential scanning calorimetry (DSC)

The DSC thermograms of the CS, 4-CBS-CS and ACZ loaded polymer microsphere were shown in Figure 4.16.

The CS microsphere thermogram revealed the endothermic broad peak onset at 149.33^{o}C, Figure 4.16 (a), which represented the melting temperature. Whereas the exothermic peak at about 300 ^{o}C may be related to the decomposition of amine units.

The DSC thermogram of 4-CBS-CS conjugates microsphere, Figure 4.16 (b), showed an endothermic peak at 122.3^{o}C, indicating the melting temperature of 4-CBS. The exothermic peak was shown at 290.0^{o}C, which is a decomposition temperature of 4-CBS.

The DSC thermogram of CS and 4-CBS-CS conjugates microspheres in Figure 4.16 (a) and (b) are different from CS and 4-CBS-CS conjugates in Figure 4.4 (a) and (c) because they can crossliked with tripolyphosphate (TPP) so the melting peaks were shift.

The DSC thermogram of ACZ microsphere, Figure 4.16 (c), showed an endothermic peak at 275.0 ^{o}C, indicating the melting temperature of 4-CBS. The exothermic peak was shown at 290.00 ^{o}C, which is a decomposition temperature of ACZ.

The DSC thermogram of the ACZ loaded CS was displayed in Figure 4.16 (d). The thermogram showed the endothermic peak occurred at 117.00^{o}C which is lower than 149.33^{o}C of the pure CS and higher than 275.00^{o}C of the ACZ. It was seen that the endothermic peaks was shifted temperature from CS because of the ionic interaction between the amine groups of CS and the sulfonamide groups and the carboxylic groups of ACZ.

The DSC thermogram of the ACZ loaded 4-CBS-CS microspheres were displayed in Figure 4.16 (e). The thermogram showed the endothermic occurred at 138.33 ^{o}C which is higher than the endothermic peak of ACZ-CS (117.00^{o}C), resulting from the ionic interaction between the amine groups and the sulphonamide substituent groups of 4-CBS-CS and the sulfonamide groups and the carboxylic groups of ACZ.

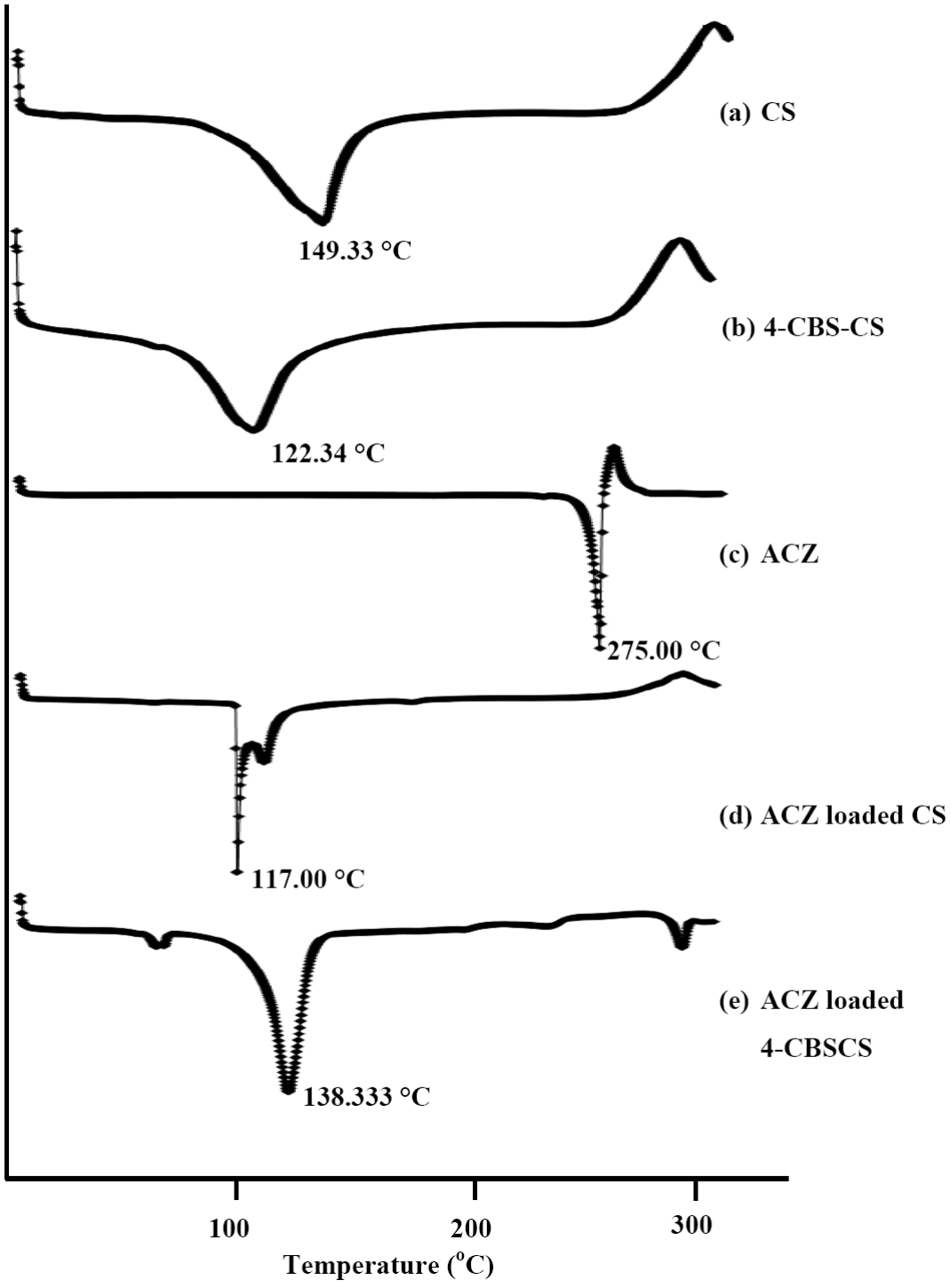

Figure 4.16 DSC thermograms of (a) CS (A1) (b) 4-CBS-CS (A2) (c) ACZ (d) ACZ loaded CS (A3) (e) ACZ loaded 4-CBS-CS (A4)

4.8.2 Evaluation of drug content and drug encapsulation efficiency (%EE)

The percentages of encapsulation efficiency (%EE) and loading efficiency (%LD) of the ACZ-loaded CS and 4-CBS-CS microspheres were given in Table 4.7.

The content of drug within ACZ loaded into CS and 4-CBS-CS microspheres were analyzed using UV-Vis spectroscopy. The ACZ content was determined from the absorption of sulfonamide groups of ACZ at 266 nm.

Table 4.7 ACZ content, the percentages of encapsulation efficiency (%EE) and loading efficiency (%LD)

Formulation	Composition	ACZ content (mg)		%LD	%EE
		Theoretical	Experimental		
A3	1:1 ACZ:CS	1.00	0.47 ± 0.02	17.67 ± 0.12	46.90 ± 1.85
A4	1:1 ACZ:4-CBS-CS	1.00	0.99 ± 0.02	39.06 ± 0.32	98.56 ± 1.69

The ACZ content within 4-CBS-CS microspheres increased with respect to that within the CS microspheres. The percentages of ACZ loading (%LD) in the ACZ-CS and ACZ-4-CBS-CZ microspheres were 17.67±0.12 and 39.06±0.32%, respectively. The encapsulation efficiencies (%EE) were 46.90±1.85 and 98.56±1.69% for the ACZ-CS and ACZ-4-CBS-CZ microspheres, respectively. It was clearly seen that the efficiency of 4-CBS-CS to encapsulate the drug was higher than that of the CS over two fold.

4.8.3 In vitro drug release

Drug release from CS-based particulates systems depends upon the extent of cross-linking, morphology, size and density of the particulated system, physicochemical properties of the drug as well as the presence of adjuvants.

The releases of ACZ can be described as graph to explain the drug released from the microsphere. The release rate of formulations (A2 and A3) was given in Table E (Appendices E).

The release profiles of ACZ loaded CS and 4-CBS-CS were investigated in the simulated gastric fluid (SGF) (pH 1.2) and the simulated intestinal fluid (SIF) (pH 7.4). It had been reported earlier that pure ACZ can be swollen in the simulated gastric fluid (pH1.2) and phosphate buffer solution (pH 7.4) However, ACZ solubilizes faster in neutral environment than the simulated gastric fluid [8]. The fast dissolution of clinically undersiable as it does not promote the contact of the drug with the mucosal membranes over a time sufficient enough to absorbed, so the drug will be washed out of the body. Therefore this sustained release of ACZ is interesting.

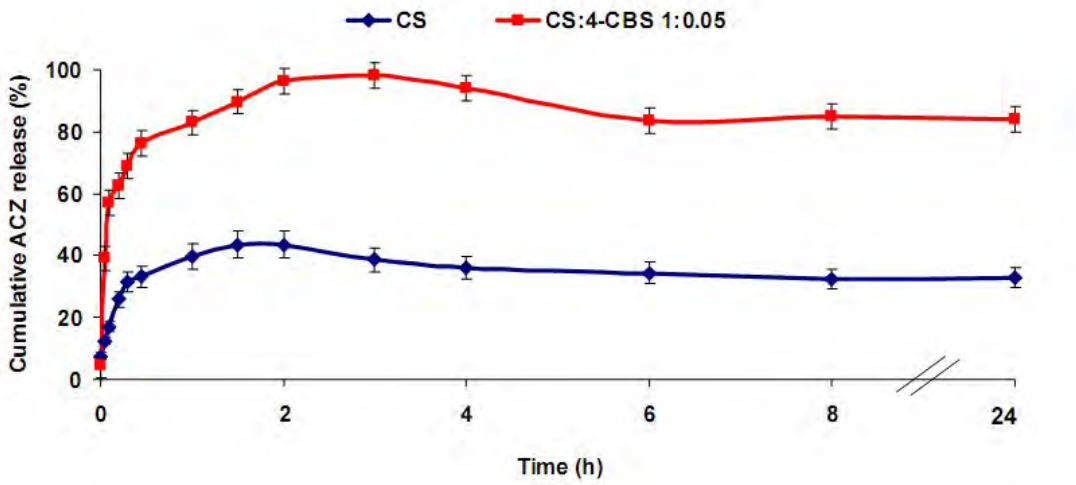

Figure 4.17 The release profiles of ACZ from the ACZ-CS and ACZ-4-CBS-CS microspheres in the simulated gastric fluid (pH 1.2)

The release of ACZ from the 4-CBS-CS microsphere showed the burst effect in the first hour, and then can sustained release of ACZ within 6 hours. The ACZ can be released from 4-CBS-CS microspheres over 80% within 24 hours. In contrast, the ACZ release profile showed that the ACZ can be release from the ACZ-CS microspheres only 40%.

Figure 4.18 illustrated the release profile of the ACZ from the ACZ-CS and ACZ-4-CBS-CS microspheres in the simulated intestinal fluid pH 7.4.

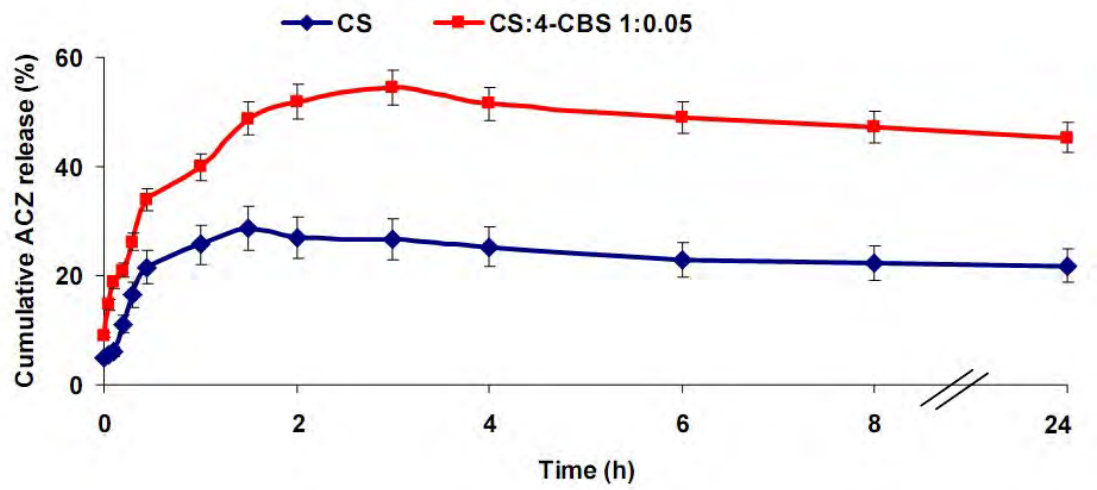

Figure 4.18 The release profiles of ACZ from the CS and 4-CBS-CS microspheres in the simulated intestinal fluid (pH 7.4).

The results showed that the ACZ sustained release from the ACZ-4-CBS-CS microspheres up to 60% within the first three hours. The ACZ-4-CBS-CS microspheres showed a higher released amount of ACZ in comparison to the ACZ-CS in the SIF (pH 7.4). Moreover, the ACZ-4-CBS-CS microspheres exhibited a more sustained release of ACZ in the SGF than that of in the SIF.

The studies of the vitro release behaviors of ACZ from the CS and the 4-CBS-CS microspheres in the simulated gastric acid fluid (pH 1.2) and the simulated intestinal fluid (pH 7.4) found that the ACZ release rate in the SGF (pH 1.2) was higher than that of in the SIF fluid (pH 7.4). Furthermore, the release amount of ACZ from the 4-CBS-CS microspheres was higher than that of released from the CS

microspheres in both SIF and SGF. The reason of the modified CS has a higher encapsulation than that of the native CS, because of the good ionic interactions of ACZ and the modified CS. The more sustained release of ACZ from the ACZ-4-CBS-CS in the SGF condition (pH 1.2) than that of the CS microspheres could be explained by the amino group of the modified CS can be protonated to $–NH_3^+$, given an increase of partial electrostatic interactions between the $–SO_2NH_2$ groups of the ACS and the $–NH_3^+$ groups in the 4-CBS-CS, leading to improve the sustained release of ACZ.

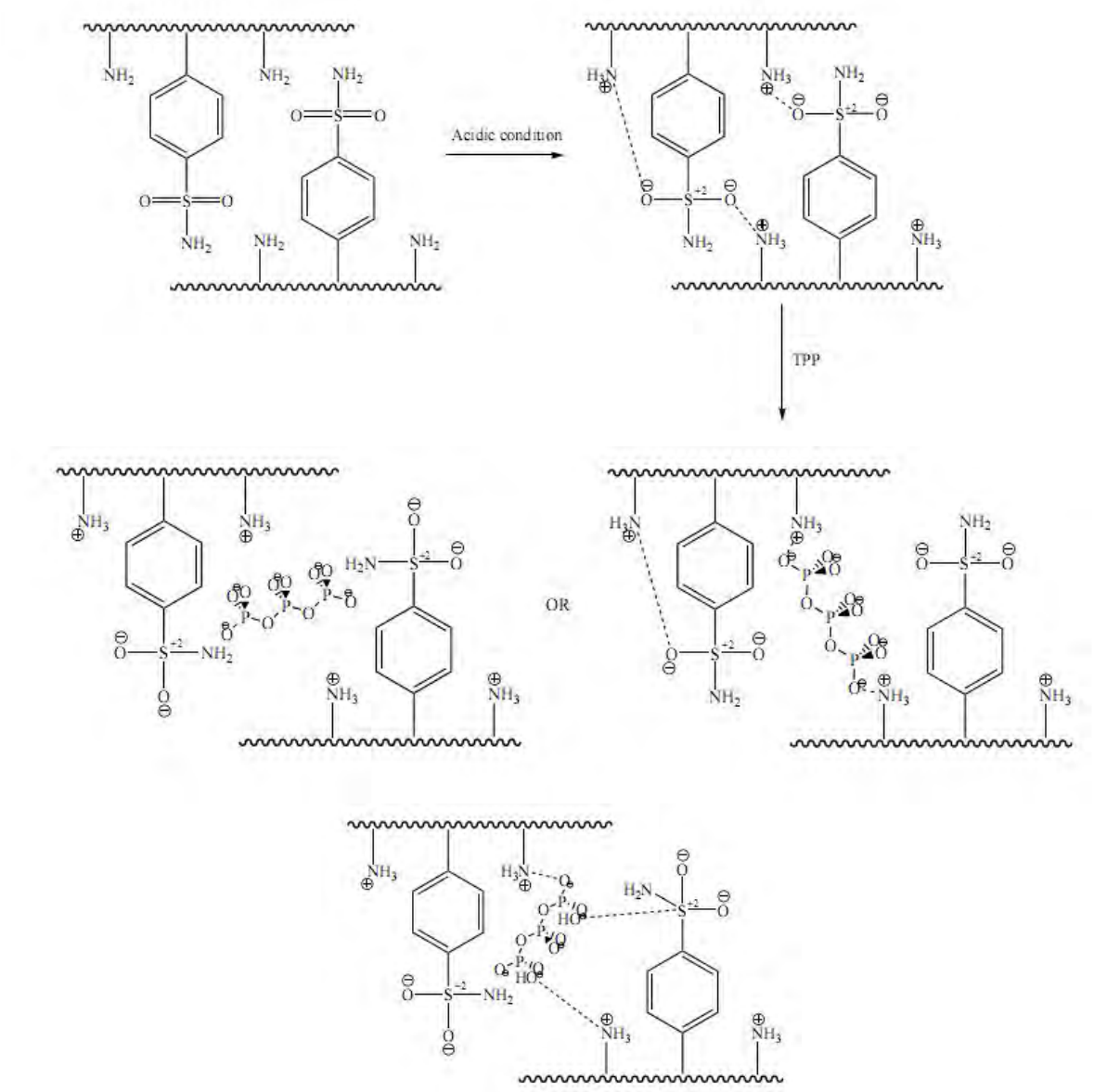

Figure 4.19 Ionic interaction of 4-CBS-CS conjugates and tripolyphosphate (TPP)

However, as the aim of this study is to develop the effective devices for enhance the eradication of *H.pylori* which is the local treatment in the stomach. So the 4-CBS-CS microspheres were preferably concerned.

CHAPTER V

CONCLUSION AND SUGGESTION

5.1 Conclusion

In the present study, the mucoadhesive 4-CBS-CSs were synthesized for drug controlled release application and for enhancing the eradication of *H. pylori* in the stomach. The 4-CBS-CSs can be successfully synthesized via a coupling reaction using EDAC as a coupling reagent. The optimum synthesized conditions are as follows: the mole ratio of 4-CBS to EDAC was 1:1.2, the reactions were carried out at room temperature for 24 hours. The weight ratios of CS to 4-CBS in the range of 1:0.05 to 1:1 were studied. With respect to chitosan, the 4-CBS-CS gave higher mucoadhesive property, has a good swelling property, more resistant in an acidic condition of the stomach. Furthermore, it is non-toxic to Vero cell and inactive against to anticancer cell lines of KB cell line (epidermoid carcinoma of oral cavity), MCF-7 cell line (breast adenocarcinoma) and NCL-H187 (small cell lung carcinoma), which can be implied that the 4-CBS-CS is biocompatible to the human body. It also stronger inhibit *Escherichia coli* (*E.coli*) and *Staphylococcus aureus* (*S.aureus*) than that of chitosan. Therefore, the mucoadhesive polymer of 1:0.05 4-CBS-CS is a suitable polymer for applying as a drug carrier to delivery of acetazolamide for enhancing the eradication of *H. pylori* in the stomach. The ACZ loaded either in CS or 4-CBS-CS microspheres with the 1:1 weight ratio of ACS:polymer were fabricated by electrospray technique using the electrospray parameters as follows: needle guage of 26 g, applied voltage of 10 kV, pump flow rate of 2.5 ml/hours and distance between the needle tip and negative electrode of 10 cm. The obtained CS and 4-CBS-CS microspheres loaded with ACZ were in a spherical shape with smooth surfaces. The particle sizes in the range of about 2 to 8 micrometers. The %EE of ACZ-4-CBS-CS was high up to 98%, only 48% for the ACZ-CS microspheres. The release profiles of ACZ in pH 1.2 and 7.4 showed the prolonged release extended to 4 hours.

5.2 Suggestions for the future work

Generally, when *H. pylori* get into human body, it is immobiliezes in stomach. The bacteria produce at least two enzymes; urease and carbonic anhydrease coated on itself to protect them from the gastric acid. This reason causes pathogenesis of peptic ulcer disease, chronic gastritis, gastric cancer.

To solve these problems, there are several alternatives that we want intend to propose as follows;

- The carbonic anhydrase inhibitor was used in succeeding experiments to reduce the ability of *H. pylori* to survive in an acid environment as presented in to stomach.
- Developing the mucoadhesive polymer for gastroretensive tract in order to have good adhesive with mucosal membrane. In addition at high concentration gradient of drug at the site of adhesive-absorbtion membrane will be good effective treatment.

REFERENCES

[1] Sachs, G., Weeks, D. L., Wen, Y., Marcus, E. A., Scott, D. R. and Melchers, K. Acid acclimation by *Helicobacter pylori.* Physiology 20 (2005): 429-438.

[2] Suerbaum, S. and Michetti, P. *Helicobacter pylori* infection. The New England journal of Medicine. 347 (2002): 1175-1186.

[3] Sahasathian, T., Kerdcholpetch, T., Chanweroch, A., Praphairaksit, N., Suwonjandee, N., and Muangsin, N. Sustained Release of Amoxicillin from Chitosan Tablets. Archives of Pharmacal Research 30 (2007): 526-531.

[4] Wikipedia, the from encyclopedia; *Helicobacter pylori*. Available from: http://en.wikipedia.org/wiki/*Helicobacter pylori*.

[5] Lam, S. K. and Talley, N. J. Report of the 1997 Asia Pacific Consensus Conference on the management of *Helicobacter pylori* infection. Journal of Gastroenterology and Hepatology 13 (1998): 1-12.

[6] Duarte, A. R. C., Roy, C., Vega-Gonzlez, A., Duarte, C. M. M., and Subra-Paternault, P. Preparation of acetazolamide composite microparticles by supercritical anti-solvent techniques. International Journal of Pharmaceutic. 332 (2007): 132-139.

[7] Shahidzadeh, R., Opekun, A., Shiotani, A. and Graham, D. Y., Effect of the carbonic anhydrase inhibitor, acetazolamide, on *Helicobacter pylori* infection in vivo: A Pilot Study. Helicobacter.10 (2005): 136-138.

[8] Marcus, E. A., Moshfegh, A. P., Sachs, G. and Scott, D. R. The Periplasmic α-carbonic anhydrase activity of *Helicobacter pylori* is essential for acid acclimation. Journal of Bacteriology 187 (2005): 729-738.

[9] Wikipedia, the from encyclopedia; acetazolamide. Available from: http://en.wikipedia.org/wiki/Acetazolamide.

[10] Nishimori, I., Minakuchi, T., Kohsaki, T., Onishi, S., Takeuchi, H., Vullo, D., Scozzafava, A. and Supuran, C. T. Carbonic anhydrase inhibitors: The β-carbonic anhydrase from Helicobacter pylori is a new target for sulfona mide and sulfamate inhibitors. Bioorganic & Medicinal Chemistry Letters. 17 (2007): 3585-3594.

[11] Bernkop-Schnurch, A. The use of inhibitory agents to overcome the enzymatic barrier to perorally administered therapeutic peptides and proteins Journal of Controlled Release. 52 (1998): 1-16.

[12] Bernkop-Schnurch, A., and Kast, C. E.. Chemically modified chitosans as enzyme inhibitors. Advanced Drug Delivery Reviews. 52 (2001): 127-137.

[13] Wang, D., Li, W., Pechar, M., Kopeckov, P., Bromme, D. and Kopecek, J. Cathepsin K inhibitor-polymer conjugates: potential drugs for the treatment of osteoporosis and rheumatoid arthritis. International Journal of Pharmaceutics. 277(2004): 73-79.

[14] Bernkop-Shnurch, A., Bratengeyer, I. and Valenta, C. Development and in vitro evaluation of drug delivery system protecting from trypsinic degradation. International Journal of Pharmaceutics. 157 (1997): 17-25

[15] Ray, B. 1997. Specialia. 1439 p.

[16] Crumbliss, A. L. McLachlan, K. L. O'Daly, J. P. and Henkens R. W. Preparation and activity of carbonic anhydrase immobilized on porous silica beads and graphite rods. Biotechnology and Bioengineering 31 (1988): 796-801.

[17] Sogias, I. A., Williams A. C., Khutoryanskiy V. V. Why chitosan is mucoadhesive? Biomacromolecules. 9 (2008): 1837-1842.

[18] Kast, C. E. and Bernkop-Schnurch, A. Thiolated polymers - thiomers: development and in vitro evaluation of chitosan-thioglycolic acid conjugates. Biomaterials. 22 (2001): 2345-2352.

[19] Grabovac, V. and Bernkop-Schnürch, A. Modified poly (lactic-co-glycolide) nanoparticles with chitosan-4-thiobutylamidine. Drug Development and Industrial Pharmacy. 33 (2007): 767-774.

[20] Chowdary K. PR. and Rao Y. S. Preparation and evaluation of mucoadhesive microcapsules of indomethacin. Indian Journal of Pharmaceutical Sciences 65 (2003): 49-52

[21] Kotadiya, R., Patel, V., Patel, H. and Koradiya, H. Effect of cross-linking on physicochemical properties of chitosan mucoadhesive microspheres: A factorial approach. International Journal of Green Pharmacy 3 (2009): 58-62

[22] Yamamoto, H., Kuno, Y., Sugimoto, S., Takeuchi, H., and Kawashima, Y. Surface-modified PLGA nanosphere with chitosan improved pulmonary

delivery of calcitonin by mucoadhesion and opening of the intercellular tight junctions. Journal of Controlled Release. 102 (2005): 373-381.

[23] Bernkop-Schnurch, A. and Krajicek M. E. Mucoadhesive polymers as platforms for peroral peptide delivery and absorption: synthesis and evaluation of different chitosan-EDTA conjugates. Journal of Controlled Release. 50 (1998): 215-223.

[24] Tikhonov, V. E., Radigina, L. A., and Yamskov, Y. A. Metal-chelating chitin derivatives via reaction of chitosan with nitrilotriacetic acid. Carbohydrate Research. 290 (1996): 33-41.

[25] Yuan, X.-b., Li, H., and Yuan, Y.-b. Preparation of cholesterol-modified chitosan self-aggregated nanoparticles for delivery of drugs to ocular surface. Carbohydrate Polymers 65 (2006): 337-345.

[26] Nishimori, I., Vullo, D,. Minakuchi, T., Morimoto, K., Onishi, S., Scozzafava, A. and Supuran, C.T. Carbonic anhydrase inhibitors: Cloning and sulfonamide inhibition studies of a carboxyterminal truncated a-carbonic anhydrase from *Helicobacter pylori*. Bioorganic & Medicinal Chemistry Letters. 16 (2006) 2182–2188.

[27] Martino, P. D., Scoppa, M., Joiris, E., Palmieri, G. F., Andres, C., Pourcelot, Y. and Martelli, S. The spray drying of acetazolamide as method to modify crystal properties and to improve compression behaviour. International Journal of Pharmaceutics. 213 (2001): 209–221.

[28] Shah, S., Qaqish, R., Patal, V. and Amiji, M. Evaluation of the factors influencing stomach-specific delivery of antibacterial agents for *Helicobacter pylori* infection. Journal of Pharmaceutical Pharmacol. 51 (1999): 667-672

[29] Michaela K., Marschutz K., and Bernkop-Schnurch, A. Thiolated polymers: self-crosslinking properties of thiolated 450 kDa poly(acrylic acid) and their influence on mucoadhesion. European Journal of Pharmaceutical Sciences 15 (2002): 387–394.

[30] Prabaharan, M. and Gong, S. Novel thiolated carboxymethyl chitosan-g-b-cyclodextrin as mucoadhesive hydrophobic drug delivery carriers. Carbohydrate Polymers. 73 (2008): 117–125.

[31] Mayol, L., Quaglia, F., Borzacchiello, A., Ambrosio, L. and Rotonda, M.I.L. A novel polosamers/hyaluronic acid in situ forming hydrogel For drug delivery: Dreologican, mucoadhesive and in vitro release properties.European Journal of Pharmaceutics and Biopharmaceutics. 70 (2008): 557-563.

[32] Deacon, M.P,. Mcgurk, S., Roberts, C.J., Williams, P.M., Tendler, S.J.B., Davies, M.C., Davis, S.S., Harding, S.E. Atomic force microscopy of gastric mucin and chitosan mucoadhesive systems. Biochem. J. 348 (2000): 557–563.

[33] Hassan, E. E. and Gallo J. M. A simple rheological method for the *in vitro* assessment of mucin-polymer bioadhesive bond strength. Pharmaceutical Research. 7 (1990): 491-495.

[34] Grabovac,V., Guggi, D.,Schnurch, A.B. Comparison of the mucoadhesive properties of various polymers. Advanced Drug Delivery Reviews. 57 (2005): 1713– 1723.

[35] Agnihotri, S., Mallikarjuna, N. and Aminabhavi T. Recent advances on chitosan-based micro- and nanoparticles in drug delivery. Journal of Controlled Release. 100 (2001): 5-28.

[36] Sinha, V.R. et al. Chitosan microspheres as a potential carrier for drugs. International Journal of Pharmaceutics. 274 (2004): 1–33.

[37] Wikipedia, the form encyclopedia; carbodiimide. Available from http://en.wikipedia.org/wiki/Carbodiimide

[38] Kim, C.J. Controlled Release Dosage Form Design. Technology Publishing Company Book, 2000.

[39] Sunil, A. A., Nadagouda, N. M. and Tejraj, M. A. Recent advances on chitosan-based micro- and nanoparticles in drug delivery. Journal of Controlled Release. 100 (2004): 5-28.

[40] Muzzarelli, R. A. Chitosan-based dietary foods. Carbohydrate Polymer. 29 (1996): 306-316.

[41] Hunt, L., Jordan, M., De Jesus, M. and Wurm, F. M. GTP-expressing mammalian cells for fast, sensitive, noninvasive cell growth assessment in kinetic mode. Biotechnology and Bioengineering. 65 (1999): 201-205.

[42] Brien, J. O., Wilson, I., Orton, T. and Pongnan, F. Investigation of the alamar blue (resazurin) fluorescent dye for the assessment of mammalian cell cytotoxicity. European Journal of Biochemistry. 267 (2000): 5421-5426.

APPENDICES

APPENDIX A

Calibration curve of 4-carboxybenzenesulfonamide

Calibration curve of 4-carboxybenzenesulfonamide

The concentration versus absorbance of 4-carboxybenzenesulfonamide (4-CBS) in 1% (v/v) lactic acid by UV-Vis spectrophotometer as the same conditions described in Chapter III is presented in Table A1 . The plot of calibration curve of 4-CBS is lillustrated in Figure A1.

Table A1 Absorbance of various concentrations of 4-CBS determined by UV-Vis spectrophotometer

Concentration (ppm)	Absorbance (Abs)			
	1	2	3	Average ± SD
1	0.08999	0.09175	0.09126	0.09100
10	0.94105	0.93212	0.92973	0.93430
20	1.76425	1.77422	1.78563	1.77470
30	2.32470	2.45750	2.63020	2.47080

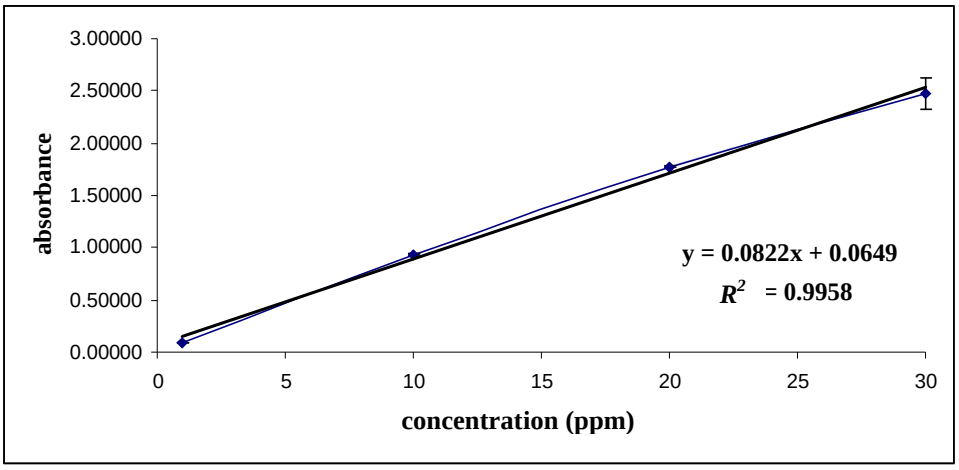

Figure A1 Calibration curve of 4-CBS for determined the degree of substitution of 4-CBS in 4-CBS-CS conjugates

APPENDIX B

Calibration curve of acetazolamide

Calibration curve of acetazolamide

The concentration versus absorbance of acetazolamide (ACZ) in simulated gastric buffer pH 1.2 and simulated intestinal buffer pH 7.4 by UV-Vis spectrophotometer at 266 nm as the same conditions described in Chapter III is presented in Table B1 and B2. The plot of calibration curve of 4-CBS is lillustrated in Figure B1 and B2.

Table B1 Absorbance of various concentrations of ACZ in simulated gastric pH 1.2 determined by UV-Vis spectrophotometer

Concentration (ppm)	Absorbance (Abs)			
	1	2	3	Average ± SD
1	0.00351	0.00367	0.00383	0.00367 ± 0.00
10	0.39752	0.39811	0.39897	0.39820 ± 0.00
20	0.83001	0.84515	0.85069	0.84195 ± 0.01
30	1.22203	1.23115	1.25302	1.23540 ± 0.02
40	1.59117	1.65421	1.74662	1.66400 ± 0.08

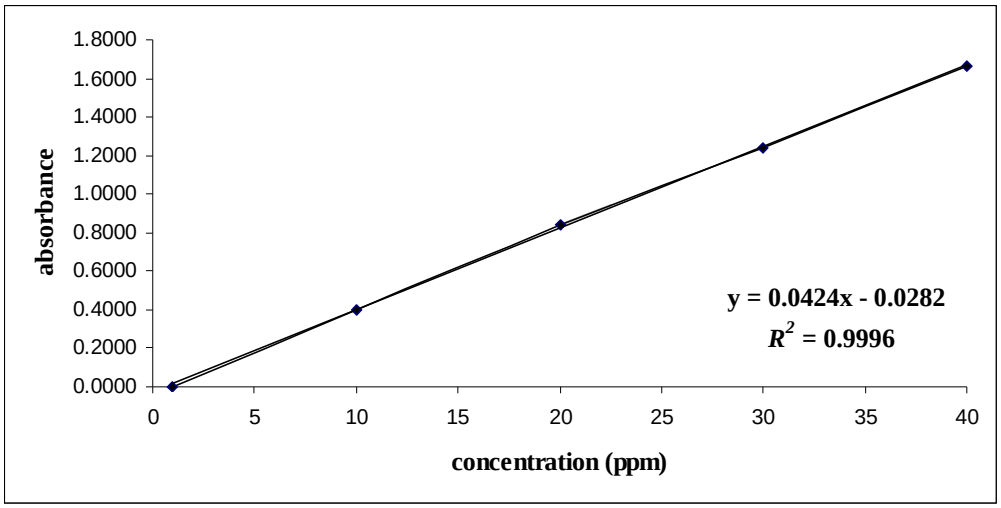

Figure B1 Calibration curve of ACZ for determined ACZ release in simulated gastric pH1.2

Table B2 Absorbance of various concentrations of ACZ in simulated intestinal pH 7.4 determined by UV-Vis spectrophotometer

Concentration (ppm)	Absorbance (Abs)			
	1	2	3	Average ± SD
1	0.00712	0.00765	0.00833	0.00770 ± 0.00
10	0.36945	0.37125	0.37050	0.37040 ± 0.00
20	0.77492	0.77513	0.77495	0.77500 ± 0.00
30	1.12111	1.12311	1.12238	1.12220 ± 0.00
40	1.49321	1.51213	1.50391	1.50310 ± 0.01

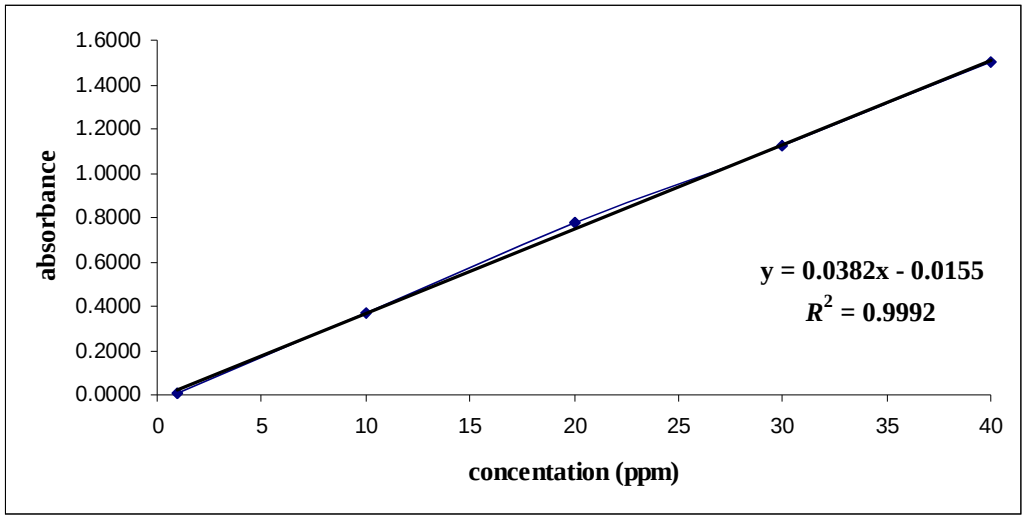

Figure B2 Calibration curve of ACZ for determined ACZ release in simulated gastric pH 7.4

APPENDIX C

Preparation stock solution

Reagents

1 N Hydrochloric Acid

Exactly measured 8.3 ml of 12.1 N HCl was added to 50 ml distilled water in 100 ml volumetric flask and the volume was adjusted with distilled water.

1 N Sodium Hydroxide

Four grams of NaOH were placed in a 100 ml volumetric flask and diluted with distilled water to volume and the solution was mixed.

Simulated Gastric Fluid

Six gram of sodium chloride were placed in a 3-liter round bottom flask, and 2500 ml of distilled water and 21 ml of 1 N HCl were added. The volume was adjusted and the solution pH was adjusted to 1.5 with either 1 N HCl or 0.2 N NaOH. No enzymes were added to the fluid.

Simulated Intestinal Fluid

20.4 g of potassium monobasic phosphate were placed in a 3-liter round bottom volumetric flask, and 570 ml of 0.2 NaOH were added. The volume was adjusted with distilled water. The solution pH was adjusted to 7.4 with either 1 N HCl or 0.2 N NaOH. No enzymes were added to the fluid.

APPENDIX D

Swelling degree

Table D1 The percentage of the swelling degree of the film in water

Time (hour)	Swelling degree															
	Formulation F1				Formulation F2				Formulation F3				Formulation F4			
	1	2	3	mean ± SD	1	2	3	mean ± SD	1	2	3	mean ± SD	1	2	3	mean ± SD
0	0.60	0.60	0.60	0.00 ± 0.00	0.60	0.60	0.60	0.00 ± 0.00	0.60	0.60	0.60	0.00 ± 0.00	0.60	0.60	0.60	0.00 ± 0.00
0.15	1.13	1.12	1.13	1.88 ± 0.01	1.58	1.56	1.57	2.62 ± 0.01	1.30	1.33	1.31	1.30 ± 0.02	1.55	1.56	1.55	2.59 ± 0.01
0.3	1.16	1.16	1.16	1.93 ± 0.00	1.72	1.72	1.71	2.86 ± 0.00	1.37	1.37	1.37	1.37 ± 0.00	1.60	1.61	1.60	2.67 ± 0.01
1	1.17	1.17	1.17	1.95 ± 0.00	1.81	1.84	1.83	3.04 ± 0.01	1.43	1.57	1.54	2.52 ± 0.07	1.73	1.75	1.73	2.89 ± 0.01
1.5					1.86	1.87	1.85	3.10 ± 0.01	1.47	1.62	1.60	2.61 ± 0.08	1.75	1.76	1.75	2.92 ± 0.01
2					1.98	2.03	1.99	3.33 ± 0.02	1.57	1.64	1.65	2.70 ± 0.04	1.78	1.79	1.77	2.97 ± 0.01
3					2.06	2.13	2.08	3.48 ± 0.03	1.63	1.67	1.67	2.76 ± 0.02	1.83	1.86	1.84	3.07 ± 0.02
4					2.20	2.30	2.14	3.69 ± 0.07	1.73	1.76	1.70	2.88 ± 0.03	1.89	1.90	1.91	3.17 ± 0.01
5					2.40	2.55	2.38	4.07 ± 0.08	1.88	1.93	1.78	3.11 ± 0.08	2.07	2.10	2.05	3.46 ± 0.03
6					2.56	2.64	2.60	4.33 ± 0.03	2.04	2.18	2.17	3.55 ± 0.08	2.15	2.18	2.20	3.63 ± 0.03
8					3.12	3.17	3.05	5.19 ± 0.05	2.63	2.73	2.54	4.39 ± 0.10	2.25	2.30	2.29	3.80 ± 0.03
				P = 0.99989 *SS* = 0.68929 *F* = 0.00011				*P* = 0.97645 *SS* = 12.4189 *F* = 0.02385				*P* = 0.95081 *SS* = 7.77841 *F* = 0.05053				P = 0.99493 SS = 5.95202 F = 0.00509

Table D2 The percentage of the swelling degree of the film in simulated gastric fluid pH 1.2

Time (hour)	Swelling degree															
	Formulation F1				Formulation F2				Formulation F3				Formulation F4			
	1	2	3	mean ± SD	1	2	3	mean ± SD	1	2	3	mean ± SD	1	2	3	mean ± SD
0	0.60	0.60	0.60	0.00 ± 0.00	0.60	0.60	0.60	0.00 ± 0.00	0.60	0.60	0.60	0.00 ± 0.00	0.60	0.60	0.60	0.00 ± 0.00
0.15	1.25	1.26	1.25	2.09 ± 0.01	1.38	1.39	1.37	2.30 ± 0.01	1.58	1.57	1.58	2.63 ± 0.01	1.62	1.63	1.60	2.69 ± 0.02
0.3	1.28	1.28	1.28	2.13 ± 0.00	1.85	1.86	1.83	3.08 ± 0.02	1.77	1.77	1.79	2.96 ± 0.01	1.75	1.77	1.75	2.93 ± 0.01
1	1.29	1.30	1.29	2.16 ± 0.01	2.20	2.30	2.40	3.88 ± 0.10	1.87	1.88	1.89	3.13 ± 0.01	1.92	1.94	1.94	3.22 ± 0.01
1.5					2.23	2.40	2.53	3.98 ± 0.15	1.92	1.90	1.99	3.23 ± 0.05	1.94	1.95	1.97	3.26 ± 0.02
2					2.28	2.54	2.60	4.12 ± 0.17	1.96	2.00	2.04	3.33 ± 0.04	1.96	1.97	2.00	3.29 ± 0.02
3					2.38	2.60	2.72	4.28 ± 0.17	2.01	2.05	2.10	3.42 ± 0.05	2.01	2.03	2.09	3.41 ± 0.04
4					2.40	2.65	2.83	4.38 ± 0.22	2.05	2.11	2.19	3.53 ± 0.07	2.05	2.05	2.11	3.45 ± 0.03
5					2.54	2.70	2.89	4.52 ± 0.18	2.13	2.20	2.23	3.64 ± 0.05	2.13	2.16	2.23	3.62 ± 0.05
6					2.74	2.82	3.01	4.76 ± 0.14	2.23	2.40	2.44	3.93 ± 0.11	2.23	2.30	2.40	3.85 ± 0.09
8					3.33	3.29	3.39	5.56 ± 0.05	2.85	2.93	2.94	3.84 ± 0.05	2.64	2.70	2.75	3.85 ± 0.06
				P = 0.99971 *SS* = 1.02947 *F* = 0.00029				*P* = 0.82093 *SS* = 17.4985 *F* = 0.19862				*P* = 0.95312 *SS* = 9.57982 *F* = 0.0481				*P* = 0.97123 *SS* = 8.20247 *F* = 0.02922

Table D3 The percentage of the swelling degree of the film in simulated intestinal fluid pH 7.4

Time (hour)	Swelling degree															
	Formulation F1				Formulation F2				Formulation F3				Formulation F4			
	1	2	3	mean ± SD	1	2	3	mean ± SD	1	2	3	mean ± SD	1	2	3	mean ± SD
0	0.60	0.60	0.60	0.60 ± 0.00	0.60	0.60	0.60	0.60 ± 0.00	0.60	0.60	0.60	0.60 ± 0.00	0.60	0.60	0.60	0.60 ± 0.00
0.15	1.02	1.02	1.01	1.02 ± 0.01	1.65	1.63	1.63	1.64 ± 0.01	1.16	1.16	1.17	1.16 ± 0.01	1.47	1.45	1.46	1.46 ± 0.01
0.3	1.06	1.05	1.05	1.05 ± 0.01	1.70	1.72	1.70	1.71 ± 0.01	1.28	1.29	1.28	1.28 ± 0.01	1.50	1.50	1.51	1.50 ± 0.01
1	1.07	1.06	1.06	1.06 ± 0.01	1.75	1.76	1.74	1.75 ± 0.01	1.35	1.35	1.37	1.36 ± 0.01	1.53	1.54	1.55	1.54 ± 0.01
1.5					1.77	1.79	1.83	1.80 ± 0.03	1.43	1.42	1.44	1.43 ± 0.01	1.57	1.59	1.58	1.58 ± 0.01
2					1.80	1.83	1.87	1.83 ± 0.04	1.47	1.48	1.50	1.48 ± 0.02	1.59	1.63	1.63	1.62 ± 0.02
3					1.86	1.86	1.93	1.88 ± 0.04	1.50	1.54	1.54	1.53 ± 0.02	1.62	1.66	1.65	1.64 ± 0.02
4					2.16	2.19	2.25	2.20 ± 0.05	1.56	1.60	1.63	1.60 ± 0.04	1.64	1.67	1.67	1.66 ± 0.02
5					2.25	2.40	2.37	2.34 ± 0.08	1.60	1.63	1.66	1.63 ± 0.03	1.66	1.68	1.69	1.68 ± 0.02
6					2.38	2.46	2.48	2.44 ± 0.05	1.67	1.70	1.73	1.70 ± 0.03	1.67	1.71	1.73	1.70 ± 0.03
8					2.87	2.94	2.85	2.89 ± 0.05	2.18	2.24	2.32	2.25 ± 0.07	2.03	2.23	2.21	2.16 ± 0.11
				P = 0.99883 *SS* = 0.44827 *F* = 0.00117				*P* = 0.98366 *SS* = 10.177 *F* = 0.01648				*P = 0.7292* *SS = 4.81579* *F = 0.02748*				*P* = 0.96647 *SS* = 4.06749 *F* = 0.03414

APPENDIX E

In vitro drug release

Table E In vitro release of microspheres

Time (hour)	pH 1.2								pH 7.4							
	Formulation A3				Formulation A4				Formulation A3				Formulation A4			
	1	2	3	mean ± SD	1	2	3	mean ± SD	1	2	3	mean ± SD	1	2	3	mean ± SD
0	7.14	7.18	7.43	7.25 ± 0.16	4.48	4.48	4.40	4.45 ± 0.05	6.07	2.07	6.60	4.92 ± 2.47	10.91	7.55	8.87	9.11 ± 1.69
0.05	9.47	16.20	11.67	12.45 ± 3.43	39.28	36.28	41.84	39.13 ± 2.78	6.77	2.79	6.99	5.52 ± 2.37	15.46	13.33	15.13	14.64 ± 1.15
0.1	17.18	19.28	14.53	17.00 ± 2.38	55.83	56.88	58.31	57.01 ± 1.25	7.34	3.07	7.62	6.01 ± 2.55	16.96	19.01	20.90	18.96 ± 1.97
0.2	22.97	26.77	27.96	25.90 ± 2.61	60.48	63.14	64.18	62.60 ± 1.91	13.00	8.10	12.28	11.12 ± 2.65	19.43	20.92	22.61	20.99 ± 1.59
0.3	30.65	33.39	30.30	31.45 ± 1.69	69.87	69.67	67.42	68.99 ± 1.36	18.57	13.38	18.01	16.65 ± 2.85	27.75	26.11	24.62	26.16 ± 1.57
0.45	33.15	33.27	32.91	33.11 ± 0.18	74.57	76.91	77.16	76.22 ± 1.43	23.50	18.85	22.17	21.51 ± 2.39	33.87	34.62	33.44	33.98 ± 0.60
1	41.15	38.80	39.25	39.73 ± 1.25	82.34	82.25	84.22	82.94 ± 1.11	27.40	22.75	27.03	25.73 ± 2.58	39.87	40.90	38.94	39.90 ± 0.98
1.5	42.85	43.71	43.87	43.48 ± 0.55	90.00	90.53	88.60	89.71 ± 1.00	29.43	25.92	30.66	28.67 ± 2.46	47.70	48.67	50.10	48.82 ± 1.21
2	43.07	42.83	44.64	43.51 ± 0.98	97.93	96.09	95.05	96.35 ± 1.46	28.68	24.10	28.44	27.08 ± 2.58	52.34	50.64	52.76	51.91 ± 1.12
3	39.16	39.26	37.95	38.79 ± 0.73	97.81	98.76	98.02	98.20 ± 0.50	28.44	23.70	28.02	26.72 ± 2.63	54.34	53.46	55.75	54.52 ± 1.16
4	36.26	35.96	36.40	36.21 ± 0.23	95.26	92.63	94.62	94.17 ± 1.37	27.24	22.58	26.19	25.33 ± 2.44	51.19	49.93	53.37	51.50 ± 1.74
6	33.22	35.67	34.06	34.31 ± 1.24	83.24	83.72	84.06	83.67 ± 0.41	24.40	19.82	24.33	22.85 ± 2.62	50.14	48.87	47.66	48.89 ± 1.24
8	32.86	32.44	32.39	32.57 ± 0.26	83.91	84.87	85.83	84.87 ± 0.96	23.91	18.90	23.98	22.26 ± 2.91	48.44	47.29	46.10	47.28 ± 1.17
24	32.24	33.99	32.77	33.00 ± 0.90	83.60	84.80	83.45	83.95 ± 0.74	23.14	18.68	23.54	21.79 ± 2.70	45.56	44.17	46.07	45.27 ± 0.98
				P = 0.95565 *SS* = 4946.806 *F* = 0.04542				*P* = 0.99790 *SS* = 25901.28 *F* = 0.0021				*P* = 0.29900 *SS* = 3066.962 *F* = 1.245455				*P* = 0.99057 *SS* = 9611.275 *F* = 0.009474

APPENDIX F

TGA thermogram

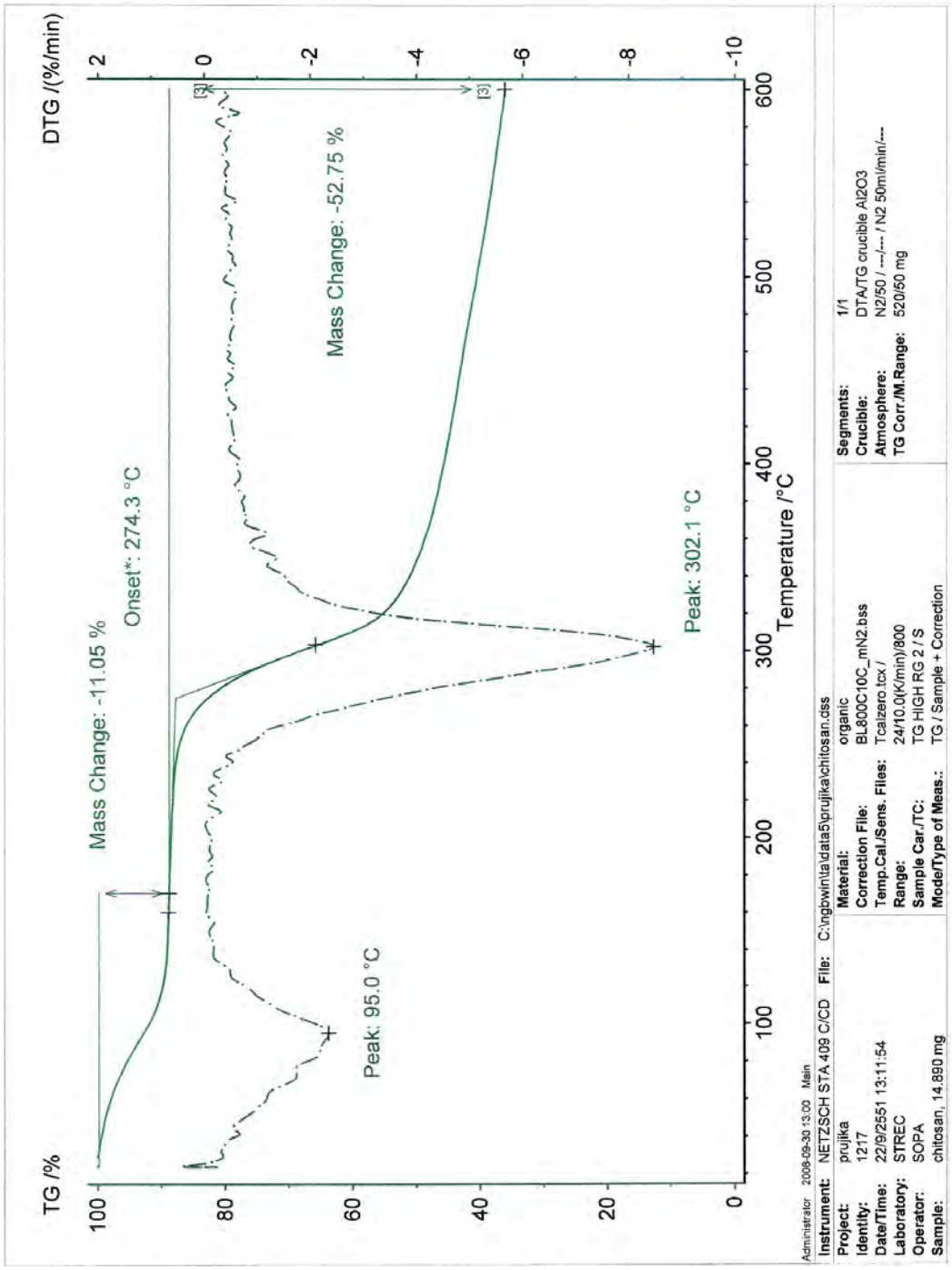
TG /%
DTG /(%/min)
Mass Change: -11.05 %
Onset*: 274.3 °C
Mass Change: -52.75 %
Peak: 95.0 °C
Peak: 302.1 °C
Temperature /°C
Administrator 2008-09-30 13:00 Main
Instrument: NETZSCH STA 409 C/CD File: C:\ngbwin\tadata5\prujika\chitosan.dss
Project: prujika
Identity: 1217
Date/Time: 22/9/2551 13:11:54
Laboratory: STREC
Operator: SOPA
Sample: chitosan, 14.890 mg
Material: organic
Correction File: BL800C10C_mN2.bss
Temp.Cal./Sens. Files: Tcalzero.tcx /
Range: 24/10.0(K/min)/800
Sample Car./TC: TG HIGH RG 2 / S
Mode/Type of Meas.: TG / Sample + Correction
Segments: 1/1
Crucible: DTA/TG crucible Al2O3
Atmosphere: N2/50 / ---/--- / N2 50ml/min/---
TG Corr./M.Range: 520/50 mg

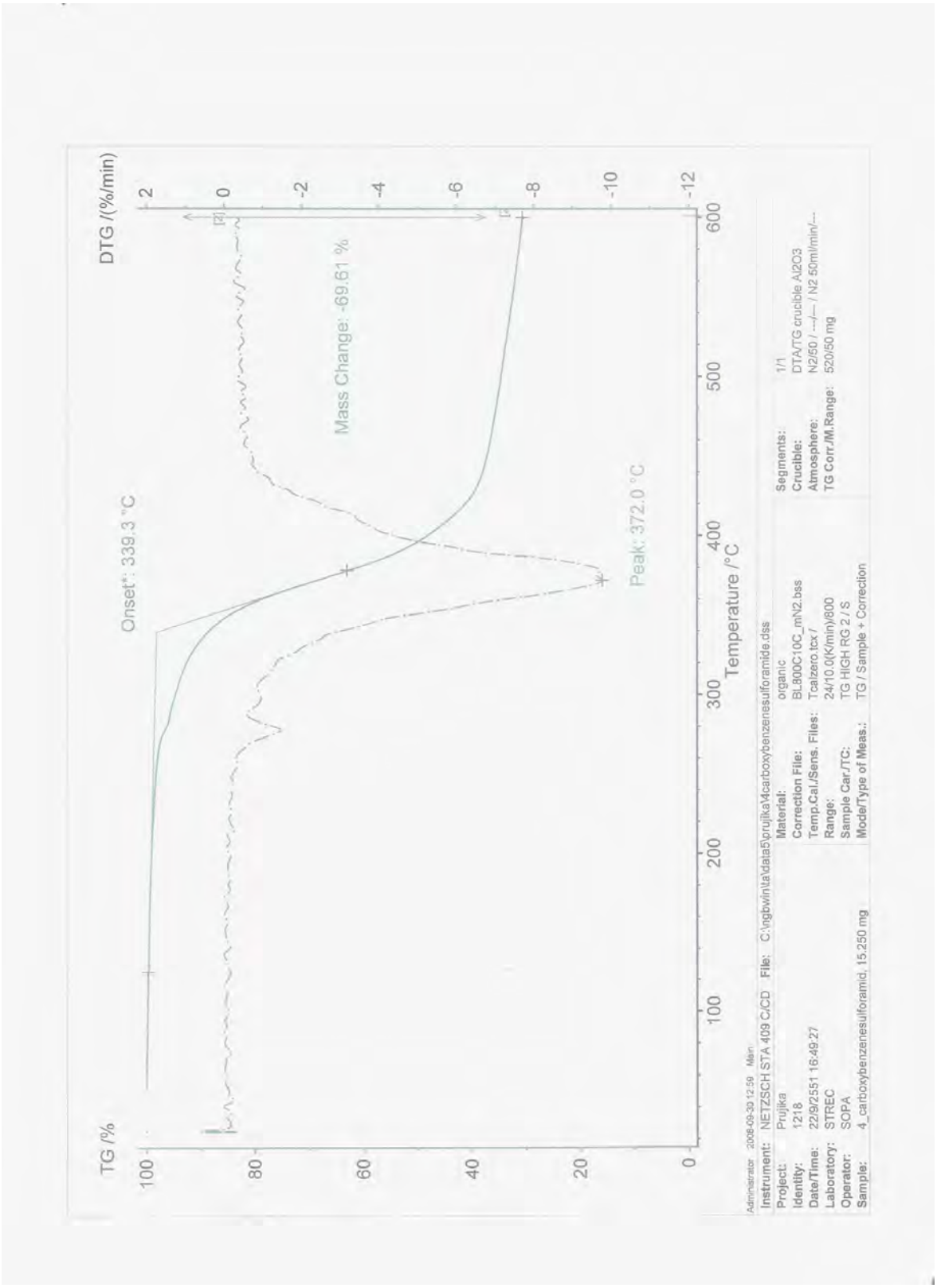
TG /%
DTG /(%/min)
Onset*: 339.3 °C
Mass Change: -69.61 %
Peak: 372.0 °C
Temperature /°C
Administrator 2006-09-30 12:59 Main
Instrument: NETZSCH STA 409 C/CD File: C:\ngbwin\a\data5\prujika\4carboxybenzenesulforamide.dss
Project: Prujika
Identity: 1218
Date/Time: 22/9/2551 16:49:27
Laboratory: STREC
Operator: SOPA
Sample: 4_carboxybenzenesulforamid, 15.250 mg
Material: organic
Correction File: BL800C10C_mN2.bss
Temp.Cal./Sens. Files: Tcalzero.tcx /
Range: 24/10.0(K/min)/800
Sample Car./TC: TG HIGH RG 2 / S
Mode/Type of Meas.: TG / Sample + Correction
Segments: 1/1
Crucible: DTA/TG crucible Al2O3
Atmosphere: N2/50 / ---/--- / N2 50ml/min/---
TG Corr./M.Range: 520/50 mg

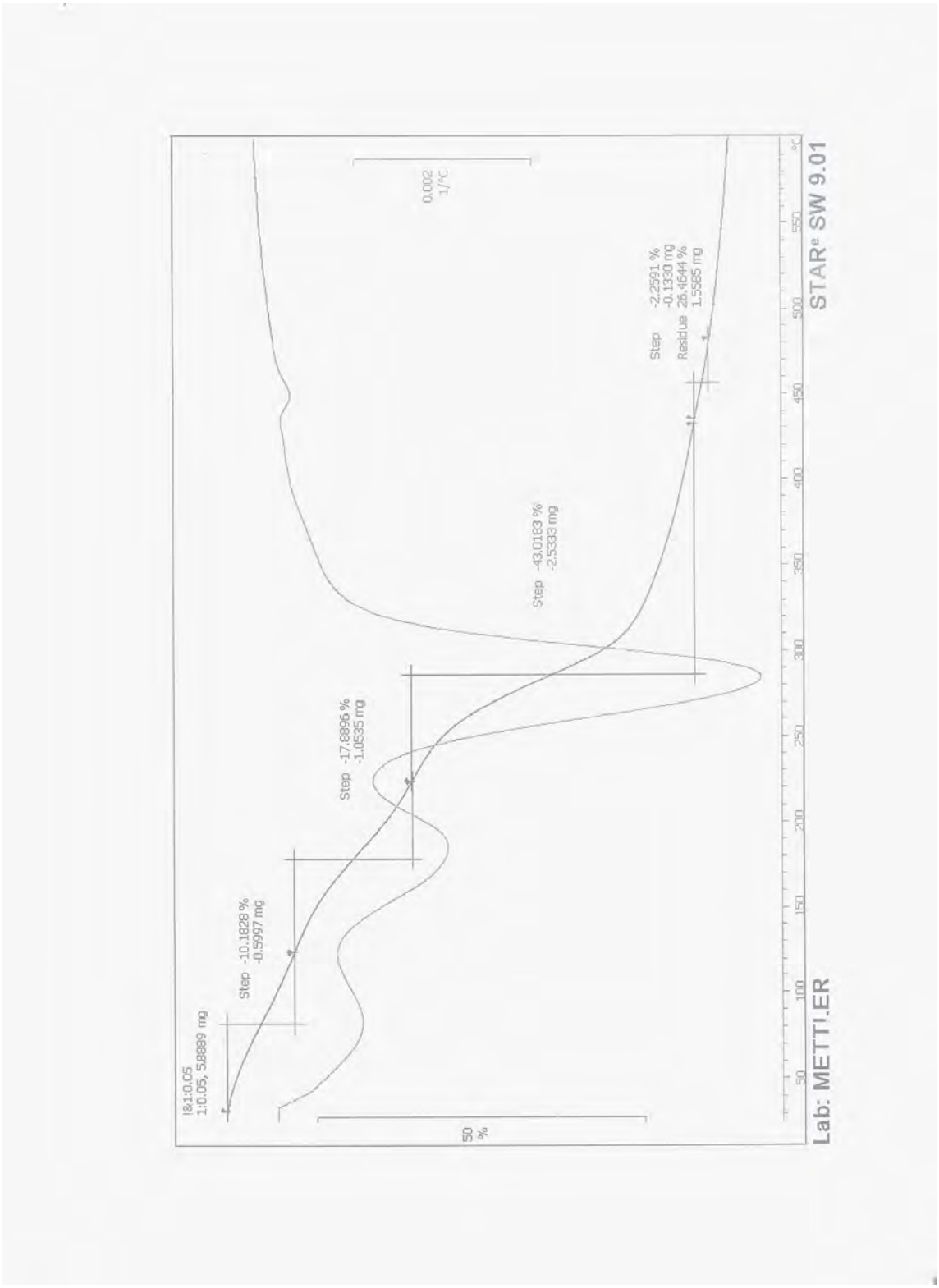
1&1:0.05
1:0.05, 58889 mg
Step -10.1828 %
-0.5997 mg
Step -17.8895 %
-1.0535 mg
Step -43.0183 %
-2.5333 mg
Step -2.2591 %
-0.1330 mg
Residue 26.4644 %
1.5585 mg
0.002
1/°C
50
%
°C
STARe SW 9.01
Lab: METTLER

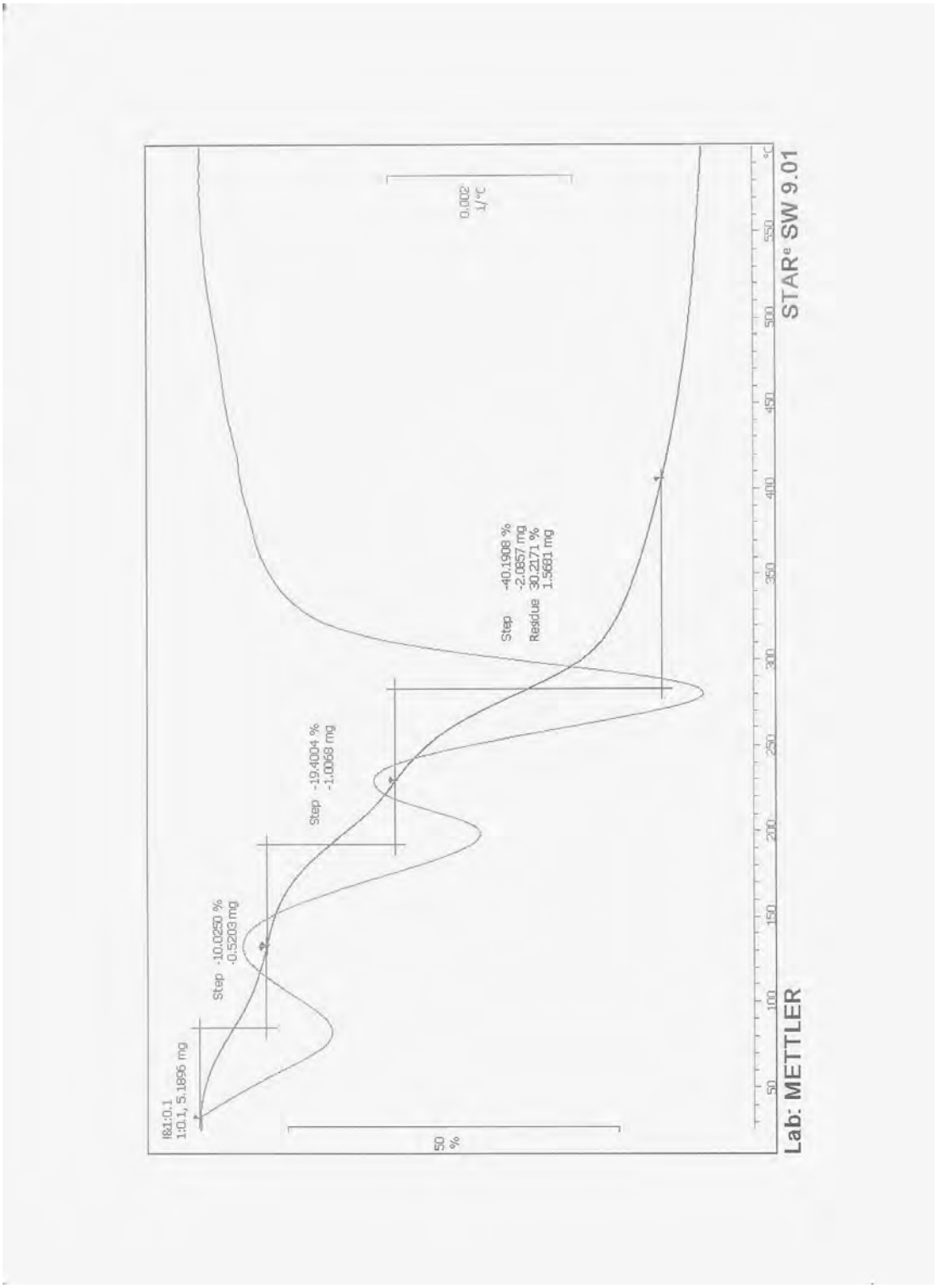
I81:0.1
1:0.1, 5.1896 mg
Step -10.0250 %
-0.5203 mg
Step -19.4004 %
-1.0068 mg
Step -40.1908 %
-2.0857 mg
Residue 30.2171 %
1.5681 mg
0.002
1/°C
50
%
°C
STARe SW 9.01
Lab: METTLER

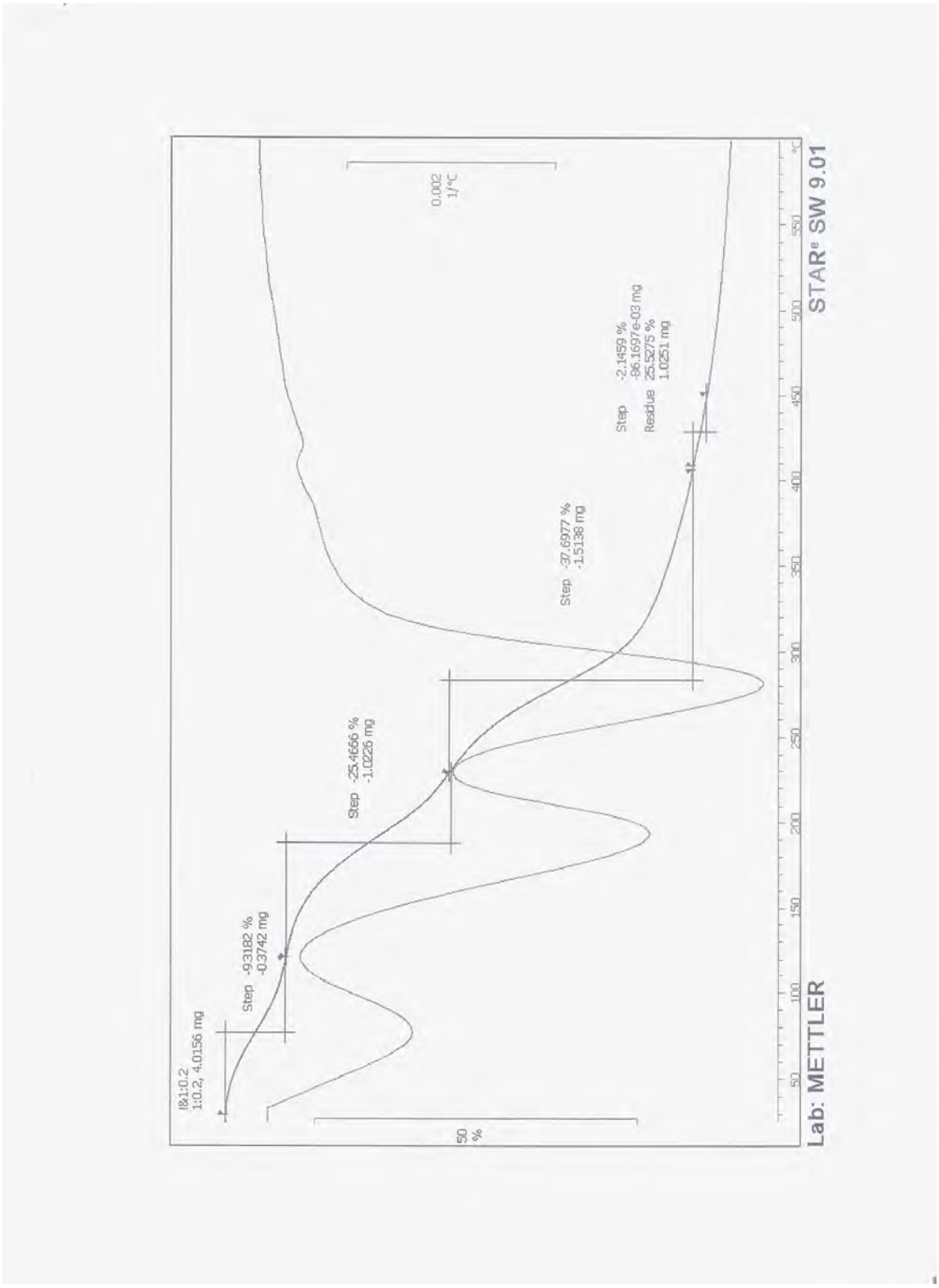
Lab: METTLER
STARe SW 9.01
50 %
0.002 1/°C
Step -9.3182 % -0.3742 mg
Step -25.4666 % -1.0226 mg
Step -37.6977 % -1.5138 mg
Step -2.1459 % -86.1697e-03 mg
Residue 25.5275 % 1.0251 mg
°C

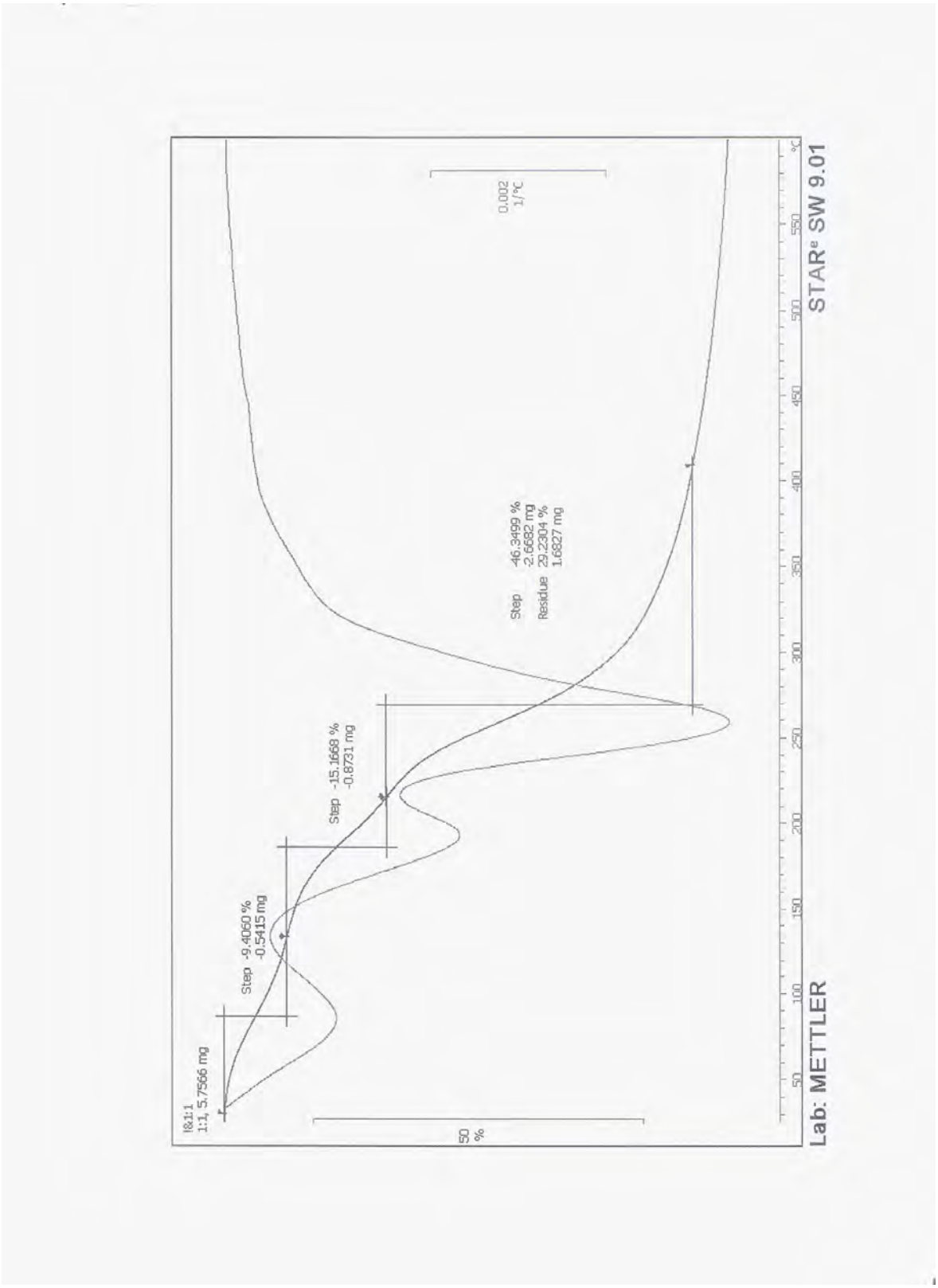
!&1:1
1:1, 5.7566 mg
Step -9.4060 %
-0.5415 mg
Step -15.1668 %
-0.8731 mg
Step -46.3499 %
-2.6682 mg
Residue 29.2304 %
1.6827 mg
0.002
1/°C
50
%
Lab: METTLER
STARe SW 9.01
°C

VITAE

Name	:	Miss Phruetchika Suvannasara
Date of birth	:	October 18, 1985
Nationality	:	Thai
Address	:	205/27, Ngam Wong Wan Rd., Leksi, Bangkok, Thailand 10210
University Education	:	Bacherlor's Degree of Chemistry, Faculty of Science and Technology, Thammasat University, 2004-2007
		Master' s Degree of Science in program of Petrochemistry and Polymer Science, Chulalongkorn University, 2007-2009
Conference attendance	:	Oral presentation "Mucoadhesive polymer for drug delivery systems: synthesis and evaluation of chitosan-4-carboxybenzenesulfonamide conjugates" at The 11th International Conference on Chitin and Chitosan & The 8th Asia-Pacific Chitin and Chitosan Symposium in Taipei, Taiwan